Signaling Pathways Contributing to High-Grade Serous Ovarian Cancer and Metastasis from Fallopian Tube

BY

SUBBULAKSHMI KARTHIKEYAN
B.Sc., Microbiology, University of Madras, India, 2002
M.Sc., Biotechnology, University of Madras, India, 2004

THESIS

Submitted as partial fulfilment of the requirements
for the degree of Doctor of Philosophy in Pharmacognosy
in the Graduate College of the
University of Illinois at Chicago, 2018

Chicago, Illinois 60607

Defense Committee:

Dr. Joanna E. Burdette, Chair and Advisor
Dr. Douglas Thomas
Dr. Leslyn Hanakahi, Biopharmaceutical Sciences
Dr. Carlos Stocco, Physiology and Biophysics
Dr. Hyunyoung (Young) Jeong, Biopharmaceutical Sciences

TO MY FATHER

Daddy - You are my hero; you believed in me, gave me strength, free will and always made me to remember that with learning, hard work, and determination, I can become the person that I meant to be.

ACKNOWLEDGEMENTS

I would like to thank my advisor and mentor, Dr. Joanna E. Burdette for giving me an opportunity to be a part of her lab. She is a very good friend, well-wisher, and an excellent mentor. She is a role model for every woman in the scientific world, and even our research is aiding women's health and wellness. She is a versatile, wise leader and despite her busy schedule, she is able to find quality time with students. I will keep this learning with me as I go through next phases of my career. Working with her helped me to focus on critical topics in our field of research, prepare well for my presentations, deal with critical scientific feedback effectively and mainly to build my self-confidence. Her shrewd nature, in depth scientific knowledge, hardworking personality, and people management skills is always very admiring. I can never find enough words in my dictionary to thank her enough.

I am very happy to be a part of an intellectually strong, fun, loving and caring "Burdette family". Dr. Suzzane Quartuccio, a good teacher, and I thank her for training me during my rotation. I thank Dr. Dimple Modi, for her support within the lab and always been my good friend. I would like to thank Dr. Angela Russo and Dr. Matthew Dean, for teaching me fundamental cancer and reproductive biology, and for motivating me all the time. I thank Dr. Amrita Salvi, for helping me to troubleshoot my experiments and her constant encouragement. I thank Laura Hardy and Alexandria Young for being my sweetest friends, and excellent team members to learn and work with. I also thank Daniel Lantvit for teaching me and performing our animal studies. I thank Jose Colina, Julia Austin, Austin Czarnecki and all the undergraduates of Burdette lab for being awesome team members.

ACKNOWLEDGEMENTS (Continued)

Over the years, I have been very fortunate to work with very talented individuals - Dr. Eoghainín Ó hAinmhire, Dr. Sharon Eddie, Dr. Georgette Heyrman, David Davis, Dr. Wei-Lun Chen and Dr. Michael Endsley. All these people have significantly contributed to my overall development as a scientist. I thank Demi Chae and Hanan Yacoub, for being best mentees.

I extend my sincere gratitude to my thesis committee members, Dr. Carlos Stocco, Dr. Leslyn Hanakahi, Dr. Douglas Thomas, Dr. Hyunyoung (Young) Jeong, my prelim committee members, Dr. Judy Bolton and Dr. Maria Barbolina for their guidance and support. I would like to convey my thanks and sincere gratitude to Dr. Nora C Vasquez-Laslop, Dr. Alexander Mankin, Dr. Michael Federle for their timely advices and career guidance. I whole-heartedly thank the Center for Biomolecular Sciences, for providing a very pleasant work atmosphere.

I thank my mother, Visalatchi Karthikeyan for her unconditional love, care and support. I thank my husband, Raghuraman Ramakrishnan, for his continued love, making me believe, that I can achieve, my dreams, through hard work and dedication and for providing a great moral support. I thank my loving sister, Vijayalakshmi Karthikeyan for her constant care and affection. I thank my brother-in-law (Vivek), niece (Harini), for being the best cheerleaders and my mother-in-law and Late father-in-law for their support. I thank my cousin Arun, who was always there at the time of my need and making things possible. Finally, I cannot end without thanking my well-wishers, Dr. Shalaka Samant and Dr. Rama Mani for their continued encouragement and support.

SK

CONTRIBUTIONS OF AUTHORS

Chapter I is a literature review that provides background information about high-grade serous ovarian cancer, its predicted origins and progression, with specific focus on the fallopian tube as the source. It also summarizes the importance of p53 mutation, requirement of a tissue specific marker, spontaneously derived models, and biological signals that induce disease progression. Chapter II summarizes research methods and reagents utilized to execute experiments. Majority of this chapter has been published previously (1-3). Chapter III is a published manuscript for which I am the primary author (1). Demi Chae contributed to figure. 3A to 3D. Chapter IV contains results that are currently under submission. Dr. Matthew dean contributed to figure. 16A and 16B. Dr. Michael Endlsey generated $MOE^{high}/Wnt7b^{shRNA\#1}$ cell line, and Dr. Angela Russo developed MOE^{high}/Non-$target^{shRNA}$ cells. Chapter V represents a series of experiments that are currently unpublished, which I was the primary person to generate the data that are presented. Chapter VI contains a comprehensive summary of my dissertation and its overall contribution to the field of study, including future implications and exploratory avenues in ovarian cancer research. Daniel Lantvit performed all the animal xenografts. Dr. Joanna E. Burdette participated in the design of all the studies and preparation of the manuscripts.

TABLE OF CONTENTS

TABLE OF CONTENTS (Continued)

LIST OF TABLES

LIST OF FIGURES

LIST OF FIGURES (Continued)

LIST OF FIGURES (Continued)

LIST OF ABBREVIATIONS

AKT	Serine-threonine protein kinase
ARF	Alternate reading frame protein
BCA	Bicinchoninic acid
BRAF	B-Raf protooncogene
BRCA	Breast cancer gene
cDNA	Complementary DNA
CDH6	Cadherin – 6 type 2, K- cadherin
CICs	Cortical inclusion cysts
CK8	Cytokeratin 8
chIP	Chromatin immunoprecipitation
CDK2	Cyclin-dependent kinase 2
Cdkn2a	Cyclin-dependent kinase inhibitor 2A
CRISPR	Clustered regularly interspaced short palindromic repeats
CSIOVDB	Cancer science institute of Singapore data base
CCL2	C-C motif chemokine ligand
DMSO	Dimethylsulfoxide
DCN	Decorin
EOC	Epithelial ovarian cancer
ECM	Extracellular matrix
EGFR	Epidermal growth factor receptor
FDA	Food and drug administration

LIST OF ABBREVIATIONS (Continued)

FTE	Fallopian tube epithelium
FOXM1	Foxhead protein M1
GSK3β	Glycogen Synthase Kinase 3β
GOF	Gain of function
gRNA	guide RNA
HGSOC	High-grade serous ovarian cancer
HER2	Human epidermal growth factor 2
HE4	Human epididymis protein
i.p.	Intraperitoneal
IGF	Insulin like growth factor
IHC	Immunohistochemistry
IGFR	Insulin like growth factor receptor
ITGB2	Integrin, beta 2
JAK	Janus kinase
KRAS	Kristen rat sarcoma viral oncogene homolog
LGSOC	Low-grade serous ovarian cancer
MOE	Murine oviductal epithelium
MOSE	Murine ovarian surface epithelium
MOE^{high}	Murine oviductal epithelium high passage
MOE^{low}	Murine oviductal epithelium low passage
MAPK/MEK/ERK	Mitogen activated protein kinase
MSK	Mitogen- and stress-activated kianses

LIST OF ABBREVIATIONS (Continued)

m-TOR	Mechanistic target of rapamycin
miRNA	MicroRNA
MDM2	Mouse double minute 2 homolog
NOTCH3	Neurogenic locus notch homolog protein 3 precursor
NCI	National cancer institute
OSE	Ovarian surface epithelium
OVCA/OVCAR	Ovarian cancer
PCR	Polymerase chain reaction
PAX8	Paired box gene 8
PAPPA	Pregnancy associated plasma protein
$p53^{WT}$	Wild type p53
PRL2C2	Prolactin family 2, subfamily c, member 2
PRL	Prolactin
PRL-R	Prolactin receptors
PAX2	Paired box gene 2
PIK3CA	Phosphatidylinositol-4,5-Bisphosphate 3-kinase catalytic subunit, alpha
PARP	Poly ADP ribose polymerase
PTEN	Phosphatase and tensin homolog
PBS	Phosphate buffer saline
qPCR	Quantitative reverse transcriptase polymerase chain reaction
STAT5	Signal transducer and activator transcription 5
STAT3	Signal transducer and activator transcription 3

LIST OF ABBREVIATIONS (Continued)

STIC	Serous tubal intraepithelial carcinoma
SCOUT	Secretory cell outgrowths
SRB	Sulforhodamine B
s.c.	Subcutaneous
shRNA	Short hairpin RNA
siRNA	Short interfering RNA
TCA	Trichloroacetic acid
TCGA	The cancer genome atlas
TD	Transactivation domain
VEGF	Vascular endothelial growth factor
WB	Western blotting
WNT4	Wingless-type MMTV integration site family member 4
WNT7B	Wingless-type MMTV integration site family member 7B

SUMMARY

High grade serous ovarian cancer (HGSOC) is the fifth leading cause of cancer related death in American women. One reason for the high mortality rate is due to the uncertainty in its cellular origin, a lack of knowledge in disease etiology, and hence a lack of targeted therapies. Originally, it was thought that HGSOC originated from the ovarian surface epithelium (OSE), but increasing evidence shows that fallopian tube epithelium (FTE) is the predominant progenitor for HGSOC. Fallopian tubes of women who were at high risk of developing HGSOC contained precursor lesions called "p53 signatures", which are areas of stabilized p53, that may be due to mutations in the p53 gene. DNA methylation, transcriptomic, and proteomic analyses all overwhelmingly support that HGSOCs originates from normal FTE.

Mutation in p53 is predicted to be a critical and essential event in development of HGSOC. Almost all (>96-100%) HGSOC have a mutation in p53, and this mutation occurs early in development of the disease, before the tumor is clinically diagnosed. In order to identify if $p53^{R273H}$ (the most common p53 mutation in HGSOC) can result in ovarian cancer and p53 signatures, a tissue specific transgenic mouse model was developed, in which $p53^{R270H}$ ($p53^{R273H}$ in humans) was expressed in the FTE ($PAX8^{cre/+}p53^{R270H/+}$ mice). $PAX8^{cre/+}p53^{R270H/+}$ mice did not develop tumors and this mutation alone did not lead to p53 stabilization, and therefore no p53 signatures. The data obtained using the $PAX8^{cre/+}p53^{R270H/+}$ mice model indicated that additional steps occur between a mutation in p53, and before p53 protein is stabilized, which could potentially be evaluated to identify candidates that may be targeted to prevent the disease. My data also confirms that mutation of p53 is required but not sufficient to form FTE-derived HGSOC.

SUMMARY (continued)

Previously, our lab demonstrated that murine oviductal epithelial (MOE) cells with stable $p53^{R273H}$ displayed significantly increased cellular migration. A cDNA microarray identified migration to be most significantly modified pathway in these cells. However, the same p53 mutation did not increase migration of murine ovarian surface epithelial cells (MOSE), indicating that p53 mutation may have FTE specific pro-migratory targets.

Analysis of a cDNA microarray identified several candidate genes that could be responsible for increased migration, including CDH6 (cadherin – 6 type 2, K- cadherin, cell adhesion proteoglycan), DCN (decorin, small proteoglycan associated with collagen), PAPPA (pregnancy-associated plasma protein A, secreted metalloprotease), and WNT4 (wingless-type MMTV integration site family, member 4, local signaling molecule). qPCR and western blotting analyses identified that MOSE cells did not express CDH6, while $p53^{R270H}$ decreased CDH6 levels in MOE cells. Expression of $p53^{R270H}$ increased DCN levels in MOE, with no change in MOSE cells. Oviducts from $PAX8^{cre/+}p53^{R270H/+}$ mice showed decreased levels of CDH6. Confirming these results in human tissues, human FTE stained positive for CDH6, while human OSE cells lacked expression.

Analysis with MOE $p53^{R248W}$ (the second most common p53 mutation in HGSOC) cells found that $p53^{R248W}$ repressed CDH6 and increased DCN expression. Expression of $p53^{R248W}$ also increased migration of MOE cells, but to a lesser extent than R273H. Chromatin immunoprecipitation (ChIP), showed that both R273 and R248 bound to the CDH6 promoter. Experiments in the human OVCAR5 cells, which are $p53^{null}$, confirmed that both R273 and R248W p53 mutations suppressed CDH6 expression, while $p53^{WT}$ did not change its expression, suggesting a gain of function activity by mutant p53.

NSC59984 (small molecule), that degraded mutant p53 (R273 and R175) in colorectal cancer cells, degraded $p53^{R273H}$, reduced CDH6 expression, and decreased the cell migration in $MOEp53^{R273H}$ cells. Therefore, CDH6 expression is specific to the FTE and mutations in p53 increase migration through, in part, suppression of CDH6.

To help further define the pathogenesis of FTE-derived ovarian cancer, the Burdette lab developed the first spontaneous model of FTE-derived ovarian cancer by serial passaging MOE cells (MOE^{high}). In vitro, MOE^{high} proliferated more than control, but migration was unchanged. MOE^{high} formed highly proliferative, non-metastatic tumors after subcutaneous xenograft. MOE^{high} cells lacked a p53 DNA binding mutation, but instead contained a p53 splice variant. RNA sequencing analysis identified >1000 genes and critical pathways modified in MOE^{high} cells, which were concordant with HGSOC.

Two novel transcripts with an unknown role in ovarian cancer that were highly upregulated included prolactin (PRL) like murine homolog (*Prl2c2*) and *Wnt7*b. Therefore, the objective was to determine if *Prl2c2* and *Wnt7b* were critical mediators of MOE^{high} ovarian tumor proliferation, to test if human homologs of *Prl2c2* (prolactin) and *Wnt7b* (same in humans) are the key drivers of human HGSOC tumors, and if expression of $p53^{R273H}$ would increase the metastatic phenotype of MOE^{High} cells.

A stable knockdown of *Prl2c2* and *Wnt7b* significantly reduced cell proliferation, 2D foci formation and anchorage independent growth of MOE^{high} cells. Reduction of *Prl2c2* completely blocked MOE^{high} tumor formation in nude mice, however, *Wnt7b* suppression did not alter the tumor burden. Genetic deletion of WNT7B was generated in human HGSOC cell (OVCAR8),

using CRISPR/Cas9, to identify if WNT7B homozygous knockout will reduce tumor formation in human ovarian cancer.

As observed with *Wnt7b* knockdown in MOE^{high} model, WNT7B deletion did not alter OVCAR8 tumor formation in mice models, suggesting that WNT7B deletion, although reduced the cell proliferation, may not be a critical mediator of HGSOC tumor formation. While *Prl2c2* does not have a direct human homolog, it belongs to prolactin family of proteins. Evidencing a role for PRL in serous ovarian cancer, serum PRL levels are higher in patients with serous ovarian cancer and PRL was a component of an ovarian screening kit (Ovasure).

Therefore, the ability of prolactin to stimulate proliferation and tumor growth was analyzed. PRL significantly increased the cell proliferation of human fallopian tube cell line (FT33-Tag-Myc) and the HGSOC cell line, OVCAR3.

A CRISPR/Cas9 mediated knockout of PRL receptor (PRL-R), significantly reduced the proliferation of FT33-Tag-Myc and OVCAR3 cells and inhibited the tumor formation after xenograft of OVCAR3. A human phosphokinase array identified that PRL treatment, resulted in the phosphorylation of multiple proteins including STAT5, AKT, m-TOR and MEK. Interestingly, PRL phosphorylated ß-catenin (activates canonical WNT signaling) and p53 at multiple serine residues, which are reported to increase p53 stability. Using small molecule inhibitors, it was confirmed that, STAT5, AKT, m-TOR and MEK mediated, PRL-simulated proliferation. These results identified, PRL as an important regulator of ovarian tumor growth.

Overall, CDH6 could be a marker to differentiate FTE derived tumors and to monitor the efficacy of treatment involving p53 modulators. p53 DNA binding mutations are distinct and may require different molecules to trigger mutant p53 clearance. A mutant p53 marker would add to the existing tools for identifying the cell of origin and to provide a tissue specific biomarker for efficacy of therapies for HGSOC patients. PRL accumulation may result in malignant transformation of FTE cells, and blocking its receptor, reduces ovarian tumor burden. Bioneutralizing antibodies to block PRL-R exist that could be used to attenuate PRL signaling. PRL elevation is reported in multiple ovarian cancer histotypes and was even previously included as a biomarker for early detection of ovarian cancer. Hence these results will illuminate the role of key early mutations and drivers of HGSOC tumors from the fallopian tube.

I. INTRODUCTION

High grade serous ovarian cancer (HGSOC), the most lethal histotype of epithelial ovarian cancer (EOC), originates from fallopian tube epithelium (FTE). The high mortality rate of the disease is primarily due to the absence of targeted therapies, which are limited in part due to the relatively recent appreciation for the FTE as a source of the tumor. Patient genetic profiles and the overall survival were significantly different between serous tumors originating from FTE vs ovarian surface epithelium (OSE), the previous cell type thought to give rise to ovarian cancer. Mutations in the tumor suppressor gene p53 are reported in 96% of HGSOC, and is also predicted to be an early precursor for HGSOC. Mutations in p53 can exert both dominant negative functions and gain-of-function activity. Studies from our lab found that the most common DNA mutation ($p53^{R273H}$) increased FTE cell migration mainly by inducing SLUG (a pro-migratory protein), but did not alter the OSE migration, indicating a tissue specific role of mutant p53. Small molecule inhibitors and modulators are being investigated to inhibit the function of mutant p53. Hence, identifying a p53 tissue specific marker to discern the FTE derived tumors from OSE derived, would help to decide the nature of treatment and may help monitor the treatment efficacy of mutant p53 inhibitors. The American Cancer Society (ACS) identified the 5-year survival rate to be >80%, if ovarian cancer is detected before metastasis, but sadly >60% of the tumors are diagnosed after the disease had spread in the peritoneal cavity. Identifying the biological signals that mediate ovarian tumor initiation and progression would broaden the field of drug discovery to develop new agents that block HGSOC tumor growth and prevent its metastasis.

A. Epithelial ovarian cancer and its histotypes

Ovarian cancer is a heterogeneous disease, which is sometimes referred to as the "silent killer" and encompasses distinct groups of pathologies affecting the ovary (4). Ovarian cancer is the fifth leading cause of cancer related death in women. The ACS predicts 22,440 new cases in 2017, and >50% of women may die of the disease. The three major classifications of ovarian tumors based on their predictive origins are: sex cord-stromal tumors, germ cell tumors and epithelial tumors (5). The non-epithelial tumor (sex cord stromal and germ cell tumors) contribute to only 10% of ovarian tumors, and they mostly do not progress to malignant disease (4,5). About 90% of the epithelial ovarian carcinomas are malignant and overall account for >70% of all ovarian tumors (5). Staging of EOC is determined based on metastasis beyond the ovary, where stage I is defined as having lesions that are benign within the ovary, stage II is invasion to the pelvic regions including the fallopian tube and uterus, stage III is metastatic tumors to the peritoneum (abdominal canvity) and lymph nodes, and stage IV indicates tumors that have metastasized beyond the peritoneum (6).

Among all histotypes of EOC, the three most predominant subtypes are serous, mucinous and endometrioid (4,7). Serous carcinomas morphologically resemble FTE, and they account for 70% of EOC, whereas endometrioid (resembles endometrial glands) and mucinous (resembles endocervical epithelium) account for only 7% and <3% respectively (4,7,8). Each subtype is further classified as benign or malignant, and, based on the tumor subtype, they are divided into low - or high - grade (9). The two-tier grading system (i.e., low grade vs. high grade) is primarily based on the mitotic rate and the pathologist's assessment of nuclear atypia (9). Within the serous histotype, the low-grade serous ovarian carcinomas (LGSOC) consist of uniform cells with mild to moderate nuclear atypia and have a low mitotic index. HGSOC contains pleomorphic cells with marked nuclear atypia (10). The LGSOC, also called serous borderline tumors, arise in a stepwise

manner from a precursor lesion and contain cells of low malignant potential. In contrast, the precursor lesions are yet debatable for the HGSOC (*de novo* development) (11,12). HGSOC is more aggressive, and rapidly spread to the entire pelvis, and peritoneum, whereas mucinous and endometrioid are usually low-grade and limited to the ovary (13,14).

B. Molecular profiling of serous carcinomas

Genetic profiling and microRNA (miRNA) profiling of EOC determined that each subtype possesses a unique molecular signature (4). The mitogen-activated protein kinase (MAPK) signaling pathway, which is activated by mutations in KRAS (Kirsten Rat Sarcoma Viral Oncogene homolog), is critical for a variety of cellular responses. In more than half of LGSOC, constitutive activation of MAPK signaling is reported (15-17). In 9% of LGSOC an insertion mutation in HER2, is detected that regulates KRAS upstream. HER2 amplified tumors lack KRAS and BRAF (B-Raf proto-oncogene) mutations (18,19). Multiple reports have identified that KRAS and BRAF mutations occur at the early stages of development of LGSOC (20). Only some LGSOC are reported to contain a mutation in p53 (21). A step-wise progression for the LGSOC was derived based on their genomic profiles, i.e., the cystadenofibroma develops into atypical serous tumor, then acquires mutations in KRAS, BRAF leading to activated MAPK signaling and eventual LGSOC (22).

HGSOC, which have a high mortality rate and spread rapidly throughout the peritoneum, possess dramatically different gene signatures compared to other EOC (23). HGSOC harbors p53 mutations in >96% of cases, often contains KRAS amplifications, and rarely acquires BRAF mutations (23). Only familial HGSOC possess mutations in the tumor suppressors, BRCA1 and BRCA2. Hypermethylation of the BRCA1 promoter leading to BRCA1 inhibition is reported in

another 10% of HGSOC (21). Some significant differences between HGSOC and other EOCs include cyclin E1 amplification, high DNA copy numbers of AKT2, NOTCH3, RSF1 and the PIK3CA loci (24). Recent integrated genomic analyses of messenger RNA (mRNA) expression, miRNA expression, promoter methylation and DNA copy number alterations in 489 HGSOC samples revealed more critical genetic alterations in known cancer–associated pathways (25). The retinoblastoma pathway was altered in 67% of cases. Mutations in CSMD3, CDK12, deletion of PTEN (tumor suppressor gene involved in PI3K/PTEN signaling), deletion of NF1, and decreased expression of CDKN2A was detected in >30% of the samples (25). The FOXM1 pathway was amplified in more than half of the HGSOC tumors evaluated (25). HGSOC loses PAX2 and contains enriched expression of PAX8 (PAX2 and PAX8 - transcription factors). Although gene signatures vary between LGSOC and HGSOC, rare instances of clonal relationships between LGSOC and HGSOC in an individual patient have been reported, indicating progression of LGSOC to HGSOC may occur (26). Overall, LGSOC and HGSOC contain distinct abnormalities in cell signaling mechanism, where all LGSOC share the same precursor lesions, reiterating their stepwise progression, which usually involves activation of MAPK pathway. In contrast, HGSOC have a high frequency of p53 mutations and BRCA1/2 mutations, but lack other mutations that are seen in LGSOC.

C. Progenitors of HGSOC

Many hypotheses exist describing how the HGSOC may originate from either the human FTE and OSE (4), but the overwhelming evidence suggests that the majority of HGSOC come from FTE. The first hypothesis involves inflammation associated with cyclic ovulation. OSE are PAX8 negative, flat to cuboidal, non-ciliated and mesothelial cells lining the ovarian surface. In

cycling women, during ovulation, follicular rupture creates a wound in the OSE, that gets repaired and re-modelled multiple times over the course of a women's reproductive life (27). The OSE is frequently exposed to ovulation-induced inflammatory cytokines, and constant DNA damage occurs due to reactive oxygen species, that may increase their susceptibility for transformation (28).

A second hypothesis involves an involution of the OSE within the connective tissue of the ovary. Due to aging, the OSE may invade the cortical stroma, and these invaginations later becomes trapped within the ovary forming "cortical inclusion cysts" (CIC), thereby OSE is exposed to new ovarian microenvironment, and that is predicted to trigger metaplasia into cells resembling Müllerian epithelia (4). However, a third hypothesis indicates that the CIC are primarily due to shedding of FTE. The majority of CICs exhibited tubal phenotype with PAX8 positivity, and given that fimbriae is at such close proximity to ovarian surface, the tubal mucosa may implant on the ovary due to ovulation inflammations and becomes CIC, rather than being due to OSE invaginations (29). These FTE cells covering the CIC, are now exposed to hormone rich ovarian microenvironment and that is predicted to induce their proliferation, differentiation, that may lead to ovarian carcinomas (30). However, all these hypothetical origins of HGSOC from the OSE have limitations.

The presence CICs does not explain why HGSOCs are not associated with precursor lesions in the ovary. Careful evaluation of the FTE from prophylactically removed fallopian tubes, of women who are predisposed to get ovarian cancer contained precursor lesions leading to the hypothesis that HGSOC arise outside of the ovary (31). Germline mutations in BRCA1 or BRCA2 are associated with increased risk of breast and ovarian cancer. FTE consists of columnar cells, which are made up of both secretory and ciliated types. The fallopian tubes from BRCA mutated

patients contained patches of proliferative epithelial dysplasia, and a complete shift to the secretory phenotype, that presented with areas of cells that expressed mutant p53 protein (31). Another study specifically examining the prophylactically removed fallopian tubes of BRCA positive women, revealed >30% of the samples had serous tubal intraepithelial carcinomas (STICs) in the fallopian tube, but not in the ovaries, and 80% of the STICs were in the fimbriated end (32). Kindelberger et al. examined 55 cases of ovarian, tubal and peritoneal serous cancer without BRCA mutation and found predominant STICs in >90% of the cases in the fimbrial region (33). Later, multiple studies confirmed the presence of STIC lesions in the FTE, supporting the hypothesis that many HGSOC may originate from the distal end of the fallopian tube (4).

A tissue specific (PAX8) driven BRCA1/2 mutation, p53 mutation, and deletion of PTEN in the murine fallopian tube (oviduct) secretory epithelium established STIC, developed HGSOC and peritoneal metastasis (34). Both STICs and the tumors contained high Ki67 (measures proliferative tumors) and stabilized p53 signatures as observed with human HGSOC. This model was subjected to hysterectomy (removal of uterus), oophorectomy (removal of one or both the ovaries), and salpingectomy (removal of the fallopian tube). Hysterectomy and oophorectomy still resulted in STICs and tubal transformation, however, oophorectomy blocked peritoneal metastases. Salpingectomy, resulted in the absence of HGSOC lesions and metastases (34). These results provided a stronger evidence that the fallopian tube could be the origin for HGSOC, and that the ovarian microenvironment is critical for early metastatic disease. These tumors had genetic alterations that correlated with the TCGA (The Cancer Genome Atlas, a web source for exploring, visualizing, and analyzing multidimensional cancer genomics data) indicating that this murine model effectively recapitulated the HGSOC profile (34).

Two retrospective studies demonstrated a high correlation in the transcriptomic profiles between HGSOC and FTE. First, Marquez et al. evaluated the gene expression profile of 50 ovarian cancers with normal OSE and FTE using > 50,000 probe sets and found a significant correlation ($p = 0.0013$) between serous ovarian cancers and normal FTE (35). In 2013, another study performed a microarray analysis on cultured normal ovarian, fallopian tube cells, and primary ovarian cancers. The results identified that the gene profile of serous cancer was 94% identical to normal fallopian tube cells, and a significant decrease in the overall survival of fallopian tube-like ovarian cancer vs. ovarian-like ovarian cancer (36). The DNA methylome pattern was analyzed in 10 HGSOC samples and compared matched normal FTE and OSE controls, and it was determined that the HGSOC methylation profiles were more identical to FTE than OSE (37). Our lab made multiple pathway alterations in the murine oviductal epithelial cells (MOE, analogue of human fallopian tube epithelium) including PTEN silencing, mutation in p53, mutation in KRAS, and activation of AKT alone and in combination and determined that some of these combinations were capable of generating tumors in nude mice (38). These analyses provide great support that most HGSOC originate from the FTE. However, it is still possible that some percentage of tumors arise from the OSE, or that other histotypes of ovarian cancer come from the OSE. Since these data indicate that the FTE-derived ovarian cancer has a very distinct transcriptome compared to OSE–derived ovarian cancer, a tissue specific marker to distinguish where the tumors arise would be helpful and could be used to develop targeted therapies and monitor treatment responses.

D. Hypothetical progression and metastasis of serous ovarian cancer

Two different hypothetical models were derived for serous ovarian cancer origin and progression. The first model is through ovarian inclusion cysts, the trapped OSE within the ovary, undergoes defined genetic alterations and transformations, which may lead to LGSOC (39). The second model is that the fimbria gets exposed to genotoxic stress triggered by ovulation-related cytokines and reactive oxygen species that lead to p53 mutation. The combination of mutation in p53 and genotoxic stress may lead to a precursor lesion that contains mostly secretory phenotype cells. Additional genetic alterations like loss of a transcription factor PAX2, PTEN deletion, or other unidentified modifications may facilitate the secretory cells to transform into STICs and further become invasive serous carcinoma (39,40). This new model, while describing the step wise progression of HGSOC, is completely based on pathological evidences and needs further mechanistic validations. Ovarian cancers are predicted to metastasizes in multiple different ways: 1) direct exfoliation off the fallopian tube into the peritoneal cavity 2) through ascitic fluid, 3) through lymph nodes, 4) the transformed FTE cells may implant onto the ovary during ovulation induced stress, and, 5) hematogenous spread (41). Cancer–derived extracellular vesicles that contain bioactive molecules including miRNAs, mRNA and proteins have also been shown to be a significant mediators of ovarian tumor metastasis (42). A recent evaluation of ovarian cancer metastatic trajectories using integrative whole – exome sequencing stated that STICs also are a representation of intraepithelial metastases (43). Despite the remaining controversies in the field, the strongest evidence suggests that p53 signatures are early precursors for HGSOC. By studying the role of p53 mutation in the FTE may provide significant mechanistic insight that can be targeted to block ovarian tumor formation.

E. Role of p53 in ovarian cancer

The *TP53* gene encodes for the p53 protein, which is a transcription factor and is the most frequently mutated tumor suppressor gene in all tumors. Wild type p53 ($p53^{WT}$) protein is activated by many external stressors like hypoxia and reactive oxygen species. Following activation, it protects the cells from propagating DNA damage by inducing cell cycle arrest and apoptosis (44). p53 signaling is therefore a critical pathway for tumor suppressive function. The functional domains of p53 are the N-terminal transactivation domain, a proline rich domain, a DNA-binding domain in the center, a tetramerization domain, and, a c-terminal regulatory domain (45). p53 binds to its responsive element, composed of approximately 14 nucleotides, to transactivate its targets. MDM2, a p53-specific ubiquitin ligase, regulates the p53 protein in cells. Under non-stressful conditions, MDM2 constantly ubiquitinates the p53 protein and directs it for proteasomal degradation. The interaction of MDM2 and p53 is tightly regulated based on cellular stress, and disruption of this interaction may lead to constant p53 expression (46). Many tumors carry abundant levels of mutant p53 protein, which can alter its function to that of a cellular oncogene. Unlike most tumor suppressor genes, mutations in p53 are mostly missense, single amino acid alteration. The vast majority of mutations in p53 are detected in the DNA-binding domain in hotspot regions (nucleotide positions that are highly susceptible for mutations). Mutant p53 can exert a dominant negative (DN) effect or through gain-of-function (GOF) action, which surprisingly converts the p53 protein from a tumor suppressor to a proto-oncogene (47). There are multiple proposed mechanism for p53 gain of function: through physical interaction with other p53 family proteins that block its activity, through recruitment of transcription factors to their cognate binding sites that leads to the enrichment of their targets, or through activating the targets that are not usually transcribed by $p53^{WT}$ that promotes oncogenic functions (47).

Mutation of p53 is reported in 96% of HGSOC. The most common p53 mutations in ovarian cancer is R273 followed by R248, R175 and Y220. These mutations induces cell migration, survival, angiogenesis, proliferation, and chemoresistance (48). In R273 mutation, arginine is changed to histidine or cysteine. The R273 mutation does not alter the structure of the p53 protein, however it significantly modifies the transcriptional activity (49). When the murine version of human $p53^{R273H}$ ($p53^{R270H}$) was introduced into mice, they developed a distinct tumor phenotype including carcinomas when compared to p53 null ($p53^{-/-}$) mice, which did not form tumors. The tumors expressed stable p53 protein (p53 signatures), which could be due to the mutation in p53, but the non-tumorigenic cells expressing mutant p53 did not show p53 stabilization(50). The overexpression of $p53^{R273H}$ in $p53^{-/-}$ lung cancer cells resulted in increased resistance to cisplatin. However, this resistance was found to be selective to a few drugs, since these tumors were still sensitive to topoisomerase II poison (51). Novel interacting partners of $p53^{R273}$ included NF-Y, p63 and SP1 that could mediate cell cycle arrest. A study found that after DNA damage, $p53^{R273H}$ forms a complex with the transcription factor NF-Y and activates the expression of cyclins including cyclin A, cyclin B, cdc25c and cdk1, which could lead to enriched cell cycle progression (52). It had been previously characterized that $p53^{R273}$ inhibited the tumor suppressive function of p63, and promoted tumor metastases through TGF-β induction and enriched recirculation of EGFR and integrins (53). When $p53^{R273H}$ was deleted in breast cancer cell lines, it reduced tumor invasion. Both $p53^{WT}$ and mutant p53 efficiently bound to MRE11, which is essential for repairing DNA double strand breaks, however $p53^{R273H}$ prevented its recruitment to the damage complex, indicating the opposite effects of $p53^{WT}$ and $p53^{R273H}$ (54). Together, all these findings demonstrated that $p53^{R273}$ mutation may have a significant role in tumor invasion and survival.

The second most common p53 mutation in ovarian cancer is R248 (R245 in mice), where arginine is replaced with tryptophan or glutamine. Similar to R273 mutation, the R248 mutation does not modify the structure of the protein; however, it changes its interaction with DNA (55). Although this mutation did not alter the proliferation rate of lung cancer cells, it potentiated their resistance to chemotherapeutics. The $p53^{R248}$ mutation-mediated resistance effect was mainly through the enrichment of multidrug resistance 1 (MDR1) (56). The $p53^{R248W}$ knock-in mice model had accelerated development of sarcomas and lymphomas, and the cells cultured from these tumors demonstrated a complete abolishment of the G2/M checkpoint of the cell cycle that may potentially lead to genomic instability (57). $p53^{R248}$ was found to activate the transcription of genes that encode for chemoresistance, including c-myc, CXCL1, MDR1 and IGFR (58). In addition, $p53^{R248}$ also interacts with p73, thereby inhibiting the apoptosis. Blocking this interaction may sensitize the tumors to platinum drugs (59). Overall, these data demonstrate that $p53^{R248}$ mutation increases the therapeutic resistance of tumors, but has little involvement in tumor proliferation and invasion.

The third most common p53 mutation observed in many cancers including ovarian cancer is R175H (R172 in mice), which distorts the conformation of p53 protein (47). The $p53^{R172H}$ knock-in transgenic mice model established more carcinomas compared to $p53^{-/-}$ mice and was a model of Li-Fraumeni syndrome which is a genetic disorder that greatly increases the risk of developing many cancers (50). Forced expression of $p53^{R175H}$ enhanced resistance to cisplatin and etoposide in $p53^{-/-}$ lung cancer cells and mediated paclitaxel resistance that involved G2/M checkpoint maintenance in endometrial cancer cell lines (60). Hence, R175H also acts similar to R248 by increasing chemoresistance. Overall, these analyses confirm that p53 mutations can amplify oncogenic potential beyond the loss of heterozygosity or complete loss of p53 function (48).

The hypothetical HGSOC progression suggests that p53 signatures are the putative precursor lesions and they are considered to be the earliest mutation (39). Since $p53^{WT}$ expression is constantly regulated by MDM2, p53 signatures were predicted to be a result of a mutation in p53 (46). In the mutant p53 (R270H and R172H) knock-in murine Li-Fraumeni models, the stabilized p53 protein was detected only in the tumors but not in the adjacent normal tissues (50). $p53^{R175}$ mice were crossed with either MDM2 loss or $p16^{INK4a}$ loss, this combination stabilized the mutant p53 levels and displayed an earlier tumor onset (61). Our lab had also earlier generated murine cellular models with a $p53^{R273H}$ mutation, PTEN deletion, alone and in combination. The PTEN deletion model alone and in combination with $p53^{R273H}$ had stable p53 expression, but the $p53^{R273H}$ mutation cell model had unstable p53 protein (38). Analysis of ovarian cancer tumors with p53 missense mutations identified no change in the levels of MDM2 indicating there could be other mechanisms that could potentiate the p53 protein stabilization. For example, elevated levels of β-catenin, PTEN deletion or complete loss of MDM2 combined with a mutation in p53 may trigger its stabilization (62).

F. Current mutant p53 modulators and inhibitors

When p53's significant contribution to pathogenesis of HGSOC was accepted, multiple researchers focused on identifying small molecules and peptides to degrade the mutant p53 protein and/or stabilize $p53^{WT}$ function. NSC319726, a compound from the thiosemicarbazone family from the National Cancer Institute (NCI), was identified to induce a conformational change in mutant $p53^{R175}$ to $p53^{WT}$ and quenched the tumor growth by inducing apoptosis in the human ovarian cancer cellular models. The compound activity was determined to be dependent on its zinc ion chelating properties and redox modifications (63).

Another strategy to develop drugs was to restore p73 signaling in mutant p53 cancer cells. p73 is a transcription factor and a tumor suppressor that belongs to p53 family and possesses sequence homology with p53. p73 can transactivate most of p53's downstream targets and exhibit similar activity by inducing apoptosis and chemosensitivity (64). Most of the platinum drugs are known to enhance the expression of p73, indicating its critical involvement in tumor suppressive function. But when p53 is mutated, it forms an aberrant complex with p73 and abrogates its activity (47). NSC59984, also from NCI, was tested on colorectal cancer cell lines containing $p53^{R273H}$ mutation. NSC59984 was identified to degrade mutant p53 by MDM2-mediated ubiquitination and restored $p53^{WT}$ signaling through p73 activation (65). NSC59984 induced p73-dependent cell death in cancer cells at therapeutic index with minimal genotoxicity and it did not have any toxic effect on normal cells. This compound also suppressed the tumor growth when injected into tumor xenograft models, indicating that NSC59984 could be a promising lead compound for its anti-cancer effects (65).

Most segments in the DNA binding domain (252-258) of p53 are likely to form amyloid adhesive segments, which result in mutant p53 aggregates in HGSOC patients that appear as puncta in the cytosol. These aggregates can increase the tumor invasion and resistance to many drugs. A cell-penetrating peptide called ReACp53 was validated on human HGSOC primary cell cultures that possessed the most common p53 mutations R175 and R248 (66). The ReACp53 peptide was modeled on the 252-258 regions of p53 that encodes for p53 aggregation and found to efficiently inhibit the p53 aggregation in HGSOC cell lines and organoids. Intraperitoneal administration of this peptide resulted in reduced proliferation and ovarian xenografts. ReACp53 rescued $p53^{WT}$ activity thereby inducing apoptosis-mediated cell death in HGSOC primary cell cultures, indicating its potential applicability in treating HGSOC (66). Hence, all these studies

demonstrated that quenching mutant p53 function and stimulating $p53^{WT}$ activity would be a valid therapeutic approach. The challenges with these approaches are: 1) the genetic differences between distinct origins of HGSOC, 2) p53 functions in each tissue differ, 3) a p53 tissue specific marker is required to monitor the p53 therapeutic responses because $p53^{WT}$ is constantly degraded by the cells.

G. Screening of ovarian cancer

HGSOC is especially difficult to detect because it does not usually present with any unique symptoms (67). Most symptoms are similar to those experienced during the normal menstrual cycle and with minor gastrointestinal issues, including abdominal pain, nausea, and frequent urination (68,69). Although a non-invasive technique, called transvaginal sonography (TVS), and the presence of some serum biomarkers can be used to screen ovarian cancer, they do not exhibit adequate sensitivity (70). TVS can only detect tumors if they cause a significant increase in ovarian size, which is very challenging in case of HGSOC, because tumors can spread rapidly to other sites in the pelvis before ovarian enlargement (71,72). For example, a diagnostic evaluation of four women revealed late stage ovarian cancer within a year of negative TVS scan results (73). Additionally, TVS scan can also provide false-positive results due to its inefficiency at distinguishing malignant tumors from the benign cysts that are commonly seen in postmenopausal women (74,75), but still the technique is a useful tool for secondary screening (76,77).

Serum biomarkers are another tool for screening for ovarian cancer. The most commonly used biomarker is CA-125, discovered in 1981, which is a membrane glycoprotein expressed by Müllerian epithelium including fallopian tube (78). The normal CA-125 level is <35 U/mL, but its levels are elevated in >50% of HGSOC patients (79,80). A study was done on prediagnostic serum

samples and found that CA-125 levels were higher in >25% of ovarian cancer patients before they were diagnosed with the disease (81). However, later studies identified that CA-125 levels can rise even with non-malignant conditions like pelvic inflammation, ovarian cysts and fibroids. Despite these caveats, CA-125 is still considered to be a reliable marker for monitoring ovarian cancer recurrence (82). A recent study reported that the effect of CA-125 in cell proliferation and migration could be inhibited using a WNT inhibitor (83), however WNT signaling can still be induced by other alterations, including local accumulation of the lactation hormone, prolactin (84). Later, in an attempt to increase the screening sensitivity, another tumor marker called human epididymis protein 4 (HE4), a glycoprotein secreted by Müllerian epithelia, was included in combination with CA-125 (85). The combination of CA-125 and HE4 produced more reliable results in ovarian cancer screening compared to either of the marker alone (86). Although, US Food and Drug Administration (FDA) approved the use of HE4 in combination with CA-125 to screen ovarian cancer, a prospective study demonstrated that HE4 levels were not significantly changed in postmenopausal women with ovarian cancer which pose a challenge in using HE4 levels as a diagnosis of ovarian cancer (87).

Another screening option was a kit called Ovasure that was developed by the Laboratory Corporation of America. Ovasure was an immunoassay kit that measured the levels of prolactin, CA-125, leptin, osteopontin, insulin growth factor and macrophage inhibitory factor. The combination of 6 biomarkers was claimed to have better screening capability compared to CA-125 alone (88). A local increase in levels of serum prolactin levels significantly correlated with peritoneal cancers, including serous cancer and breast cancer (84,89). Similar to prolactin signaling, leptin receptor dysregulation modulates PI3K/AKT3/ERK signaling predominantly through JAK/STAT pathways in gynecological cancers (90). Due to inadequate data to support its

use, the Ovasure kit was removed from the commercial market. The other main challenge in detecting HGSOC has been the uncertain tissue of origin as most of the biomarkers are proteins that are expressed in fallopian tube cells. Therefore, HGSOC biomarkers may reflect the cell of origin, the fallopian tube, or they may play important roles in disease. This study examined the role of prolactin as both a biomarker and tumor driver.

H. Current therapies for ovarian cancer

The gold standard treatment for all ovarian cancer is a combination of carboplatin, a platinum-based DNA alkylating agent, and paclitaxel, a mitotic spindle disruptor (91,92). Angiogenesis, which is mainly mediated through vascular endothelial growth factor (VEGF) receptors, is a critical factor for HGSOC lethality (93). Thus, a humanized monoclonal antibody (bevacizumab) that can block VEGF-mediated angiogenesis was also developed. The European Medicines Agency (EMA) approved the use of bevacizumab with the combination of carboplatin and paclitaxel as a first line treatment for ovarian cancer (94). Molecular profiling revealed the activation of P13K/AKT/mTOR in HGSOC. Hence, inhibitors for m-TOR or AKT are currently in phase II clinical trials for HGSOC (94). Other therapies in the pipeline are immunotherapies that include dendritic cell-based vaccines, and pressurized intraperitoneal aerosol chemotherapy (94). Poly-ADP ribose polymerases (PARP) are a family of proteins involved in DNA base excision repair and inhibiting PARP activity results in cell death. PARP inhibitors are a very promising new class of agents that are potent and tested against many cancers (95). Normal cells will survive the PARP inhibition using homologous recombination repair, and, hence PARP inhibitors may exhibit specific activity on tumor cells (96). The most well studied PARP inhibitor is olaparib, which, in Aug. 2017, the FDA approved for treating EOC (97). Although, many

approaches are being evaluated for treating HGSOC, the key challenge in cestablishing a therapeutic approach or diagnostic marker, is that the etiology of the disease remains unknown.

I. Importance of spontaneous models of HGSOC

While xenograft models are significantly useful for advanced human ovarian cancers, cellular models would be helpful to study the step wise progression of the disease. A concurrent inactivation of p53 and Rb using a cre-lox system in the OSE of female mice was sufficient to establish EOC. The progression of the disease started with ovarian neoplasms, that spread to the peritoneum through the ascites and metastasized to the lung and liver, which was similar to what is seen in women (98). Recently, to support the evidence that the ovary is not the source of HGSOC, a transgenic fallopian tube mouse model was generated. $p53^{R172H}$ was introduced into inducible *Dicer-Pten* KO mice and identified that these models formed HGSOC (99). Perets et al. made a triple variant transgenic mouse model to prove that fallopian tube is the origin for HGSOC. A deletion of PTEN, mutations in p53 and BRCA in mice demonstrated STICs and HGSOC from the fallopian tube secretory epithelium. These mice failed to form tumors when the oviduct was removed (34). Our lab made cellular models, murine oviductal epithelium (MOE) with combinations of PTEN silencing, p53 mutation, KRAS mutation, and amplified AKT and showed that few of these in combination formed high grade cancer (38). Although, many models with tissue specific modifications or targeted genetic alterations provided critical clues about which tissues are capable of malignant transformation, they could not explain the stepwise progression of the disease or find novel new players responsible for tumor initiation. A spontaneous model of ovarian cancer was needed to resolve this issue.

Originally, it was thought that all ovarian cancer originated from the OSE, hence multiple spontaneous models of OSE derived ovarian cancer were created. Rat ovarian surface epithelial cells (ROSE) were isolated from 10 adult mice and passaged for >20 passages to generate a passage-dependent spontaneously transformed ovarian cancer model (100). Anchorage independent growth, a characteristic that is closely related to cell transformation, was significantly increased in serially passaged cells compared to its control cells. ROSE had alterations in chromosomes 21- 24, which is commonly observed in ovarian cancer, and formed tumors when injected into subcutaneous and intraperitoneal spaces. This model was widely used to study the role of repeated ovulations in ovarian cancer (100). The only non-primate species that can naturally and spontaneously develop ovarian cancer is laying hen, which is predicted due to extraordinary number of ovulations they undergo. Many chemoprevention strategies have been analyzed using this hen model. The histology and metastatic trajectories of ovarian tumors in hen highly resembled the human disease. While the laying hen tumor model contained identical transcriptome as seen in ovarian cancer, they predominantly developed endometrial tumors. Additionally, the oviduct primarily functions as a shell gland in the laying hen, which is different from its function in humans, making this model challenging to study HGSOC that is derived from FTE (101).

Later, OSE from various mouse strains, such as murine ovarian surface epithelial cells (MOSEC) from C57 black mice (C57BL6) and the spontaneously transformed ovarian surface epithelial cells (STOSE) from FVB mice, were isolated and cultured long term (102,103). MOSEC obtained a cobblestone morphology, established anchorage independent growth and formed both subcutaneous and intraperitoneal tumors in athymic nude mice and syngenic C57BL6 mice. Histopathologic analysis on these tumors revealed malignant carcinoma and sarcoma and the presence of ascitic fluid (102). STOSE cells were highly proliferative and formed tumors when

injected into subcutaneous and intrabursal spaces, making them a realistic model to study ovarian cancer origin and metastatic pattern. Transcriptome profiling revealed that >1500 genes were altered, and the significant pathways were Wnt/β-catenin and Nf-κB signaling, which supported the stem-like properties in STOSE (103). STOSE cells were the first spontaneous murine model of OSE-derived HGSOC and are a tool to monitor the transformation of the normal OSE cells to transformed stem-like cells (103).

These models recapitulated the OSE origin of HGSOC; however, since FTE is thought to be the most common progenitor for HGSOC, spontaneous FTE-derived models were required. Our lab made the first spontaneous model of FTE-derived ovarian cancer. The MOE cells, called MOE high passage (MOE^{high}), were isolated from outbred CD1 mice and cultured for extended time (3). These high passaged cells exhibited a high proliferative capacity, and formed solid spindle-like benign tumors with moderate nuclear atypia and abundant mitosis. RNA sequencing on these cells identified pathways that are known to significantly promote the pathogenesis of many cancers, and were concordant with human HGSOC (3). MOE^{high} cells had a splice variant of p53, but did not acquire a DNA contact mutation, which is very common in HGSOC. The p53 splice variant had an elimination of the regulatory domains that are required for MDM2-mediated ubiquitination. The p53 splice variant exhibited mutant p53-like functions, such as amplifying FOXM1, and reducing p21, but also increased IGFBP3 levels, indicating $p53^{WT}$ activity (3). The MOE^{high} cells had a significant enrichment in a prolactin like murine homolog (*Prl2c2)* and *Wnt7b* (a conical WNT target, expressed in humans) (3).

Prolactin is enriched in many ovarian cancer types, including serous ovarian cancer (84). A recent study demonstrated that accumulation of prolactin altered mammary epithelial cells leading to breast cancer in transgenic mouse models (89). Prolactin can activate JAK/STAT

signaling by acting through prolactin receptors, which are a critical mediator of tumor formation and invasion. Blocking antibodies for prolactin do exist (104). Hence, investigating the molecular mechanism behind the role of prolactin in mediating ovarian tumor formation would facilitate drug discovery. WNT7B levels increase in invasive ovarian carcinomas compared to benign ovarian tumors (105). MOE^{high} cells did not form peritoneal disease which could possibly due to absence of p53 mutation. Hence, our objective is to induce $p53^{R273H}$ mutation, to observe if the MOE^{high} model can be converted to one that can form peritoneal disease. This will reveal the critical role of p53 DNA contact mutation in FTE derived ovarian cancer metastasis.

Overall, this study aimed to identify a p53 tissue specific marker to distinguish FTE derived HGSOC and to identify potential targets that can be targeted, to block ovarian tumor formation and metastases.

II. MATERIALS AND METHODS

A. Cell culture

Murine oviductal epithelial (MOE) cells were obtained from Dr. Barbara Vanderhyden at the University of Ottawa and were maintained in media as previously described (2). MOE^{Neo}, MOE^{floxed}, $MOEp53^{R273H}$, $MOEp53^{R270H}$, $MOSE^{floxed}$ and $MOSEp53^{R270H}$ cell lines were made as previously described (2). OVCAR3 and OVCAR8 (from ATCC) and OVCAR4 cells (from National Cancer Institute), were maintained in media as described previously and HGSOC cell lines were recently verified by STR analysis (106). OVCAR5 cells (gifts from Dr. Gustavo Rodriguez and Dr. Teresa Woodruff at Northwestern University) and are available through NCI as part of the NCI60 tumor cell line anticancer drug screen and maintained in media as described previously (107). The molecular profiles and *in vivo* tumor growth capabilities of OVCAR3, OVCAR4, OVCAR5 and OVCAR8 cell lines, have been previously characterized (106). Small molecule NSC59984 was available through National Cancer Institute (NCI) as part of NCI/DTP Open Chemicals Repository. High passage MOE cells (MOE^{high}) were established by serially passing MOE^{low} cells for at least >85 passages as previously described (3). The human FT33 cells were immortalized with SV40 to derive FT33-Tag cells, later transduced using retrovirus to express c-Myc (FT33-Tag-Myc); a generous gift from Dr. Ronny Drapkin, at the University of Pennsylvania, PA, and were maintained in the media as described earlier (108).

B. Transient Transfection and Generation of stable Cell Lines

OVCAR5 cells were transiently transfected with antibiotic resistant plasmids containing gene of interests which includes pCMV6-Myc-Neo (Origene, donated by Dr. Kwong Wong, M.D.

Anderson Cancer Center, Houston, TX, pCMV-Neo-BAM p53 R273H, pCMV-Neo-BAM p53 wt were a gift from Bert Vogelstein (Addgene plasmid # 16439) (109), and pCMV-Neo-BAM p53 R248W. MOE cells were transiently transfected with pCDNA-Wnt7b (gift from Dr. Marian Waterman, University of California, CA; Addgene plasmid # 35915) (110). All transfections were performed using TransIT LT1^{TM} (Mirus Bio, Madison, WI) according to the manufacturer's instructions.

For stable cell lines, MOEp53^{R248W} stable cell lines were generated using a construct pCMV-Neo-BAM p53 R248W was a gift from Bert Vogelstein (Addgene plasmid # 16437) (109). MOE^{high} cells stably expressing shRNA targeting *Prl2c2*, *Wnt7b*, or a non-target shRNA control were produced by transfecting MOE^{high} cells with shRNA targeting each gene (**Table I**). MOE^{high} cells with stable knockdown of p19^{ARF} or empty vector control or with constitutive expression of p53^{R273H} were produced by transfecting MOE^{high} cells with pSIRIP-puro-p19^{ARFshRNA} and pSIRIP-puro; gift from Dr. Pradeep Raychaudhri, at the University of Illinois at Chicago (111), pCMV6-Myc-Neo and pCMV-Neo-BAM p53 R273H. Stable clones were selected using Neomycin and puromycin resistance and were verified with Western blot and qPCR analysis.

TABLE I - shRNA USED FOR MAKING MOE^{high} STABLE KNOCKDOWNS

Gene/Exon	shRNA sequence	Manufacturer/Cat no
Prl2c2 / Exon2	GAACAGCTCGTTATTGTGGAA	Sigma-Aldrich, MO / TRCN0000109931
Prl2c2 / Exon5	CGTCCTGAAGTGTTACATGTT	Sigma-Aldrich, MO / TRCN0000109933
Wnt7b / Exon 2	GCTACCTAAGTTCCGCGAGGT	Sigma-Aldrich, MO / TRCN0000071779
Wnt7b / Exon 3	GCAGCTACGCAGCTACCAGAA	Sigma-Aldrich, MO / TRCN0000071781

FT33-Tag-Myc cells stably expressing a constitutively active PRL-R or empty vector control were produced by transfecting FT33-Tag-Myc cells with pCDNA-PRL-R_{CA} (gift from Dr. Geula Gibori and Dr. Carlos Stocco, at the University of Illinois at Chicago, IL) and pCMV6-Myc-Neo (donated by Dr. Kwong Wong, M.D. Anderson Cancer Center, Houston, TX). Cell lines were produced by treatment with selection antibiotic and colonial selection. Guide RNA (gRNA) for CRISPR/Cas9 were designed using CRISPOR (http://crispor.tefor.net/; **Table II**) (112).

TABLE II - LIST OF gRNA AND PRIMERS USED FOR GENERATING CRISPR/CAS9 KNOCKOUTS

Gene/Exon	Sequence (5'-3')	gRNA/primer
PRL-R / Exon2	TAAATGTCGTTCTCCCAATA	gRNA
PRL-R / Exon2	GAGCAATGCCAACATCAGGGCA	PCR primer forward
PRL-R / Exon2	CTAGGAGATGGTGGCTCTTGGATG	PCR primer reverse
PRL-R / Exon2	GGTCCATCAATCTGTTTCTGTCACCA	Sequencing primer forward
WNT7B / Exon2	TCGGCGAGAAGACCGTCT	gRNA
WNT7B / Exon2	GTCACGCATGTGAGTTGATGGGA	PCR primer forward
WNT7B / Exon2	GTCCATCAAACCACTCCCCACA	PCR primer reverse
WNT7B / Exon2	GCTGAGTGGGGGAAAGGTGTT	Sequencing primer forward
Pax2 / Exon2	TACCCGACGTGGTGAGGCAG	gRNA
Pax2 / Exon2	GATAATCCTCTATCCGGACCGCC	PCR primer forward
Pax2 / Exon2	CTTGACTAGGGTGGGAAACAGGC	PCR primer reverse
Pax2 / Exon2	GCCTCGGACCCTGACTAATGG	Sequencing primer forward
Pax2 / Exon3	GAACCCGACTATGTTCGCCT	gRNA
Pax2 / Exon3	GCAGCTCTGGAGCTTGCAGC	PCR primer forward
Pax2 / Exon3	CCAGACCCCAGATTGGAGTGAC	PCR primer reverse
Pax2 / Exon3	GTACTACGAGACTGGCAGCATCA	Sequencing primer forward

The gRNAs are bought from Integrated DNA Technologies (IDT), IA, and cloned into pX330-U6-Chimeric_BB-CBh-hSpCas9 plasmid (gift from Dr. Feng Zhang, Massachusetts Institute of Technology, MA; Addgene plasmid # 42230) (113) . The PX330 plasmid with gRNA was co-transfected with pPGKpuro plasmid (gift from Dr. Rudolf Jaenisch, Massachusetts Institute of Technology, MA; Addgene plasmid # 11349) (114). Cells were treated with puromycin and single cell clones were isolated. Genomic DNA was extracted from cells using genomic DNA extraction kit (#G170, Sigma-Aldrich, MO) as per the manufacturer's instructions, the targeted exon was amplified and sequenced (primers in **Table II**).

C. Quantitative Reverse transcriptase PCR (qPCR) and standard PCR

RNA extraction was performed using Trizol (Life Technologies, Grand Island, NY) and chloroform with isopropanol precipitation followed by ethanol washes and DNAse step. RNA concentrations were determined using NanoVue plus spectrophotometer (GE healthcare, product code 28-9569-62). 1μg of RNA was reverse transcribed using iScript cDNA synthesis kit (Biorad, Hercules, CA) according to manufacturer's instructions. All qPCR measurements were performed using the ABI ViiA7 (Life Technologies, San Diego, CA) and SYBR green (Roche, Madison, WI). Samples are normalized to the internal control 18srRNA. The test values are normalized relative to the respective controls ($\Delta\Delta C_t$ expressions) All primers were validated for efficiency through serial dilutions and generation of a standard curve and visual inspection of the melt curve. Standard PCR was done on the mouse models for genotyping and to demonstrate cre-mediated expression of the mutant p53 allele in PAX8-cre expressing tissues. The primers and the protocol are as described previously (34). Primers used in qPCR are listed in **Table III**.

TABLE III - TABLE SHOWING THE LIST OF PRIMERS USED FOR QPCR

Gene	Forward primer (5' - 3')	Reverse primer (5' - 3')
Ccl2	GTCCCTGTCATGCTTCTGG	GCTCTCCAGCCTACTCATTG
Dcn	CTGGCCAATGTTCCTCATC	GGTAGACGACCTGGATATACTT
Pappa	CTTTGCCTAGAAGGGAGAATC	ACATCTGGGTGACCTTCT
Wnt4	CAGGAAGGCCATCTTGAC	ACCGTCAAACTTCTCCTTTAG
Cdh6	GATCCGATTATCAGTACGTGGG	TGTATGTCGCCTGTGTTCTC
Prl2c2	CAGGCTCACACACTATTCAG	CTGTGGCTTTGGAGATGATTA
Wnt7b	GAACTCCGAGTAGGGAGTC	TTCCGCCTGGTTGTAGTA
Mdm2	GAAGGTGGGAGTGATCTGAAG	CAGGTAGCTCATCTGTGTTCTC
Slug	CTGGACACACACACAGTTATTA	AGGTGAGGATCTCTGGTTT

D. Western blot analyses

Cells were lysed using RIPA buffer (50mM Tris, pH 7.6, 150 mM NaCl, 1% Triton X-100, 0.1% SDS) with protease and phosphatase inhibitors (Sigma-Aldrich, St. Louis, MO). Protein concentration was determined by BCA assay (Pierce, Rockford, IL). Protein (25 to 30 μg) was electrophoresed in 10% SDS – PAGE gel and transferred to nitrocellulose membrane (Thermo Fisher Scientific, Waltham, MA). Blots were then blocked with 5% milk in TBS-T or 5% BSA in TBS-T and probed at 4°C overnight with primary antibodies (**Table IV**). Membranes were then washed and incubated with anti-rabbit and anti-mouse, HRP-conjugated secondary antibodies. for 30 min in blocking buffer. After washing, membranes were incubated in SuperSignal West Femto substrate ((#34095, Thermo Scientific, Rockford, IL) before imaging on a FlourChem™ E system (ProteinSimple, Santa Clara, CA). Densitometric analysis was performed using ImageJ (imagej.nih.gov).

TABLE IV - LIST OF ANTIBODIES USED FOR WESTERN BLOTTING (WB) AND IMMUNOHISTOCHEMISTRY (IHC)

Primary antibody	Manufacturer/Cat no	WB Dilution	IHC Dilution
CDH6	Abcam, Cambridge, MA / #197845	1:500	1:50
DCN	ThermoFisher scientific, Rockford, IL / # PA5-13538	1:1000	1:50
p53	Santa Cruz Biotechnology, Dallas, TX / # SC6243	1:500	1:50
PAX2	Life technologies, MA / #71-6000	1:500	-
Proliferin	Santa Cruz Biotechnology, TX / #135167	1:1000	-
WNT7a/b	Santa Cruz Biotechnology, TX / #32865	1:500	1:50
PRL	Santa Cruz Biotechnology, TX / #271773	1:1000	-
PRL-R	Cell Signaling, MA / # 13552	1:1000	-
Actin	Sigma-Aldrich, MO / #A2066	1:1000	-
α - tubulin	Cell Signaling, MA / # 2144	1:1000	-

CK8	Developmental Studies Hybridoma Bank, IA	-	1:200
Ki-67	Abcam, Cambridge, MA / #15580	-	1:100
p-AKT	Cell Signaling, MA / #4060	1:1000	-
p-Stat5	R&D systems, MN / MAB4190	1:50	-
p-mTOR	ThermoFisher Scientific, MA / 44-1125G	1:1000	-
SLUG	Abcam, Cambridge, MA / #38551	1:1000	-
FOXM1	Santa Cruz Biotechnology, TX / SC500	1:500	-
ARF	Abcam, Cambridge, MA / #80	1:1000	-

E. Animals

All animals were treated in accordance with the National Institutes of Health Guidelines for the Care and Use of Laboratory Animals and the established Institutional Animal Use and Care protocol at the University of Illinois at Chicago (UIC). In addition, the Animal Care Committee approved the protocol 14-163. Animals were housed in a temperature and light controlled environment (12 hours' light, 12 hours dark) and were provided food and water *ad libitum*. The Lox-stop-Lox regulating $p53^{R270H}$ mice (from Mouse models of Human cancer consortium) were bred with mice that express Cre- Recombinase (from Research institute of molecular pathology, Vienna, Dr. Bohr-Gasse (115) under the control of *Pax8* promoter to generate $p53^{R270H/+}$ mice. Genotyping was done as previously described (Jackson Laboratory, Bar Harbor, ME) to identify $p53^{R270H/+}$ mice from $p53^{Cre/+}$ mice. All mice were euthanized by CO_2 inhalation followed by cervical dislocation. Reproductive tract was extracted and used for immunohistochemistry and qPCR analysis. For all the subcutaneous xenografts, 1×10^6 cells were injected subcutaneously into athymic female nude mice. At humane endpoints, all mice were euthanized by CO_2 inhalation followed by cervical dislocation. Tumors were extracted and used for immunohistochemistry analysis.

F. Immunohistochemistry (IHC)

Reproductive tract and tumors were fixed with 4% paraformaldehyde, dehydrated, and embedded in paraffin. Immunohistochemistry or hematoxylin and eosin stain was performed as described previously (116). The tissues were deparaffinized, and probed with primary antibodies for overnight at 4°C (**Table IV**). The next day the slides were washed, incubated in secondary

antibody conjugated to biotin and developed with horseradish peroxidase (HRP) and DAB to enable the chromogenic detection of HRP. In all experiments, tissues without the primary antibody treatment were used as a negative control. Images were acquired on a Nikon Eclipse E600 microscope using a DS-Ri1 digital camera and NIS Elements software (Nikon Instruments).

G. Migration assay

Cells were plated to confluence (1.5 x 10^5 cells/well) in a 24- well plate. A uniform wound was created through the cell monolayer. Cells were washed with 1X phosphate buffer saline (PBS) and replenished with new media. Pictures were taken at 0 and 8 hrs after scratching using an AmScope MU900 with Toupview software (AmScope, Irvine, CA). The area of the scratch was analyzed with ImageJ NIH software. Percentage of closure was determined by measuring the final volume of the wound relative to the initial volume of the scratch.

H. Chromatin Immunoprecipitation (chIP analysis)

30 µl Dynabeads protein G (Life technologies, Cat no. 10003D) were used per pull down assay. Bead washing and antibody binding was performed as described previously (117). A magnetic separation rack (Cell signaling – 7017) was used to pull the beads off between washes. Normal rabbit IgG 1:100 (Cat No: 2729, Cell signaling, Beverly, MA) was used as control and p53 1:100 (Cat No: SC6243, Santa Cruz Biotechnology, Dallas, TX) as test antibody. MOEp53^{WT} and MOEp53^{R273H} and MOEp53^{R248W} cells in 10cm dish were fixed with 1% formaldehyde. MOEp53^{WT} were treated with 10 µM proteasome inhibitor MG132 (Sigma - M7449) for 4 hours prior to fixing. Cell lysis and cross-linking was done as described previously (117). Sonication was done with 20 second pulse “on”, 40 second pulse “off” for a total of 4 minutes, with 50%

amplitude using a Sonic Dismembrator (Branson, Model 500). Cross-linking was achieved by mixing 250 µl sonicated supernatant and 100ul of Protein G bead slurry attached to IgG and p53 antibodies separately. De-crosslinking and dissociation of chromatin-antibody complexes from the beads was done as described previously (117). Phenol chloroform extraction was performed using UltraPure™ Phenol: Chloroform: Isoamyl Alcohol (25:24:1 v/v) as described by manufacturer's protocol (Thermo Fisher Scientific, Waltham, MA). Combining 3.6 µl dH_2O, 0.5 µM primer pair, 5 µl SYBR green mix and 1 µl sample qPCR analysis was done using the ABI ViiA7 (Life Technologies, San Diego, CA). The relative occupancy of the immunoprecipitated protein (IgG and p53) on the target gene promoter was estimated using the following equation: $2^{(\text{Mean Ct}^{\text{Input-log100}_2} - \text{Mean Ct}^{\text{IgG or p53}})}$. Primers used are listed in **Table V**.

TABLE V - LIST OF PRIMERS USED IN chIP ANALYSIS

Gene	Forward primer (5' -3')	Reverse primer (5' -3')
Mdm2	GTCCCTGTCATGCTTCTGG	GCTCTCCAGCCTACTCATTG
Atf	GCAGGTAAACCCCAGGCGT	GGCAGGTAGGAGGAGATCCCA
Cdh6	GCAAGTGAATGAAGTGGGAGGGA	CTGTCAAGGGGAGGGGGC
Mdm2 negative control	GTGCACCGTGTGCAAACAGTG	GATAAGGTGGCTCAGCCCTCTTG
Atf negative control	GCTTGATCCGATTCCTTCGCTTC	CAGCCTCACTCGCTGTTGTGA
Cdh6 negative control	GAGAGGGTGAGACACAGTTGTTCT	CATGGAGAGGGCAAAGGGTACA

I. SRB Proliferation Assay

The sulforhodamine B (SRB) assay was used to measure cell proliferation as previously described (118). Cells (500 - 25000, depending on cell line) were plated in 96 well plates and incubated for 0, 1, 3, 5 and 7 days. Cell were treated with PRL, small molecule inhibitors, or siRNA. The media was changed on day 1 to media with 2% FBS before the addition of PRL, inhibitors (**Table VI**), or PRL-R siRNA (#EHU095011, Sigma-Aldrich, MO) to each well as indicated. Dose response curves to cisplatin were generated by plating MOE^{High} cells and treating with indicated concentrations of cisplatin for 4 days. Plates were collected, fixed with 20% TCA, and stored at 4C. Plates were developed by staining cells with SRB, re-suspending SRB in 10 mM TrisOH, and reading absorbance at 505 nm. Absorbance was normalized to its corresponding control (day 0 or vehicle control treatment) to determine relative cell proliferation.

TABLE VI - LIST OF RECOMBINANT PROTEIN AND INHIBITORS

Inhibitor/Protein	Concentration used	Supplier / Cat no
Prolactin	0.1 to 10 ng/ml	Peprotech Inc, NJ / # 100-07
MEK	10 μM	Cayman chemical, MI / # 70970
AKT	1 μM	Cayman chemical, MI / # 11593
Stat5	10 μM	Cayman chemical, MI / # 15784
mTOR	1 μM	Sigma-Aldrich, MO / # R8781
β-cat	10 μM	Medkoo Biosciences, NC / #205865
EGFR	100 nM	Cayman chemical, MI / # 15363
RAS	10 μM	Sigma-Aldrich, MO / # SML1166

J. 2D foci assay

The 2D foci assay was used to measure cell proliferation (3). Cells were plated (200 – 500 cells per 60 mm plate), based on cell lines and incubated for 7 – 15 days according to the growth of cells. After incubation, the cells were fixed with 4% (w/v) paraformaldehyde and then stained

with 0.05% crystal violet. Images were taken using FlourChem™ E system (ProteinSimple, Santa Clara, CA). Colonies were counted using ImageJ (imagej.nih.gov).

K. Soft agar colony formation or anchorage independent growth assay

All cells subjected to the soft agar colony formation assay was plated at a density of 15,000 cells/well in a 24-well plate as elucidated previously and cultured for 14 days by replacing fresh media every 5 days (3). The colonies were imaged using Nikon Eclipse TS100 microscope and counted using ImageJ. Average number of colonies was determined for each well and normalized to control.

L. Cell cycle assay

Cells (2 x 10^6) were seeded in a 10cm dish and treated as indicated. The cells were collected, centrifuged, fixed with 100% ethanol and PBS, stained with propidium iodide, and analyzed using a K2 Cellometer (Nexcelom Biosciences, MA) as per the manufacturer's protocol. Percentage of cells at each stage of the cell cycle was analyzed with FCS Express program (De Novo Software, Nexcelom Biosciences, MA).

M. Phosphokinase array

The human phospho-kinase array kit (#ARY003B, R&D systems, MN) was used to identify the proteins that were phosphorylated in response to PRL in OVCAR3 cells. Cell lysis, protein purification and the assay was performed as per the manufacturer's protocol. Before lysis, the cells, were incubated with 10 ng/ml of PRL and 0.1% BSA in PBS (control) for 30 minutes. Protein (>500 μg) was used for the analysis and the membranes were imaged on x-ray films (Konica

Minolta model: SRX-101A). The mean pixel density of the positive signals that were visually distinct between the control and the PRL treatment were analyzed using ImageJ (imagej.nih.gov).

N. xCELLigence

Migration was also measured with the xCELLigence® DP system as previously described (119) with the help of Dr. Douglas Thomas's lab. 4 x 10^4 cells were suspended in serum-free media and plated in the upper chamber of the CIM plate. 10% FBS media was used as an attractant. Cells were allowed to settle for 30 minutes before measurements were taken every 15 min for 50 hours.

O. Statistical analyses

Data are presented as the mean ± standard error of the mean and represent at least 3 independent biological replicates. Statistical analysis was carried out using GraphPad Prism software (GraphPad, La Jolla, CA). Statistical significance was determined by Student's unpaired t -test or one-way ANOVA or two-way ANOVA. ANOVAs were followed by with Dunnett's multiple comparison or Tukey's posthoc test. $p<0.05$ considered significant.

III. CADHERIN – 6 TYPE 2, K- CADHERIN (CDH6) IS REGULATED BY MUTANT P53 IN THE FALLOPIAN TUBE BUT IS NOT EXPRESSED IN THE OVARIAN SURFACE

(Reprinted with permission from *Oncotarget 2016 Oct 25;7(43):69871-69882. doi: 10.18632/oncotarget.11499*).

A. INTRODUCTION

Epithelial ovarian cancer (EOC) constitutes the most predominant form of the disease with high grade serous ovarian cancer (HGSOC) being the most common and lethal histotype (4). One of the obstacles in developing treatments for HGSOC is the lack of understanding of the pathogenesis of HGSOC due to an uncertain site of origin (120). Traditionally, it was thought that HGSOC arises from the ovarian surface epithelium (OSE), but over the last decade it has become apparent that the fallopian tube epithelium (FTE) is also a likely source for HGSOC (121). Mutations in p53 occur in 96% of HGSOC, and the identification of p53 mutations in putative benign lesions suggests that mutation of this gene is critically important and occurs early in fallopian-tube derived HGSOC (122).

In HGSOC, the most frequent p53 mutations occur in the DNA binding domain at codons R273, R248 and R175 (47). Some DNA binding mutations are termed gain of function (GOF) mutations, which refers to the enhanced biological activity that facilitates tumor growth and metastasis (48). Mouse models with $p53^{R270H}$ and $p53^{R172H}$ develop more carcinomas, with increased capacity for metastasis (50). Mice expressing a knock-in $p53^{R248W}$ have accelerated formation of lymphomas and sarcomas with increased chemoresistance (57). Ovarian carcinoma patients harboring a R248W mutation have a poor overall survival compared to R273H with selective chemoresistance to microtubule stabilizers (123). Currently, small molecules are being

identified that can reverse the mutant p53 configuration to wild-type or can degrade mutant p53 protein. Treatment with NSC59984 in $p53^{R273H}$ mutant colorectal cancer cell lines demonstrated an increase in mutant p53 degradation and stabilization of $p53^{WT}$ signaling through activation of p73 (65). Given the evidence that mutation in p53 impacts tissues differently, the response of HGSOC derived from OSE and fallopian tube to small molecules that alter mutant p53 may differ.

Murine oviductal epithelial cells (MOE), the equivalent of human fallopian tube, harboring the $p53^{R273H}$ mutation migrated more than control cells (2). Microarray data confirmed expression changes of pro-migratory genes in $p53^{R273H}$ transfected MOE cells compared to parental cells (2) (Figure 1). The tissue specificity of the pro-migratory genes remains unknown. However, the same mutation did not show any phenotypic changes in murine ovarian surface epithelial cells (MOSE) (2) largely due to a lack of SLUG induction. SLUG is a p53 transcriptional target and a migratory protein (124). The hypothesis is that mutant p53 may exhibit tissue specific functions, which can be further validated to identify a mutant p53 tissue specific marker to differentiate OSE vs FTE derived ovarian tumors. The tissue specific activity of p53 mutations have been reported earlier by multiple studies in many other cancers. For example, a study in pediatric adrenal cortical carcinoma found that $p53^{R337H}$ did not form sarcoma in soft tissues or bone which is frequently found in case of Li-Fraumeni families (125). Another study found tissue specific regulation of p53 targets in liver and spleen cells (126). Liver cells had induced p21 induction with no expression of apoptotic genes, but spleen cells had the inverse, specific induction of apoptotic gene PUMA occurred without changes in p21 (126).

The objective of this study was to identify a mutant p53 FTE target gene to determine if markers might be present that can facilitate determination of the cell of origin (Figure 1). Two frequently reported p53 DNA contact mutants (R273H and R248W) in HGSOC were chosen and

a panel of pro-migratory genes from our previously published cDNA microarray data in FTE vs OSE was mined to determine if they are differentially regulated by mutant p53 in the OSE compared to oviductal cells. In addition, NSC59984 treatment in MOE cells harboring $p53^{R273H}$ and $p53^{R248W}$ suggests that p53 DNA binding mutants may differ and may require different small molecules to inhibit their activity.

B. RESULTS

CDH6 is decreased by p53 mutation in MOE cells not MOSE cells.

A microarray analysis in MOE cells expressing the $p53^{R273H}$ revealed a significantly altered pro-migratory gene signature compared to the MOE vector control cells (2). Based on those results, several candidate genes (**Table VII**) were chosen based on their expression in the fallopian tube, their role in migration, and their association with cancer (127-131). The selected candidate genes were cadherin – 6 type 2, K- cadherin (*Cdh6,* cell adhesion proteoglycan), pregnancy-associated plasma protein A (*Pappa,* secreted metalloprotease), wingless-type MMTV integration site family, member 4 (*Wnt4,* local signaling molecule) and decorin (*Dcn,* small proteoglycan associated with collagen). A quantitative PCR (qPCR) was used to validate the microarray using MOE cells expressing $p53^{R270H}$ mutation (the murine equivalent of R273H). *Ccl2* expression was repressed by mutant p53 (132) and this was confirmed as a positive control (**Fig. 1A**). Increased *Dcn,* decreased *Pappa* and *Wnt4* expression levels were measured in MOE $p53^{R270H}$ (**Fig. 1A**) cells compared to control cells. Next, CDH6 and DCN protein levels were examined. A reduced CDH6 and increased DCN protein was seen in MOE cells with $p53^{R270H}$ (**Fig. 1B and 1C**).

To test if human p53 mutations (R273H and R248W) alter the pro-migratory gene expression in MOE cells, qPCR was performed. MOE cells harboring human p53 mutation R273H exhibited induced *Dcn* expression and reduced *Cdh6*, *Pappa*, *Wnt4* and *Ccl2 mRNA* levels

compared to control cells (**Fig. 1D**). Western blot analysis confirmed that $p53^{R273H}$ repressed CDH6 expression and induced DCN expression in MOE cells (**Fig. 1E and 1F**) similar to the murine $p53^{R270H}$. To further determine if any of these targets are uniquely regulated in fallopian tube cells compared to the OSE, MOSE cells expressing $p53^{R270H}$ mutation (the murine equivalent of R273H) were used. qPCR revealed increased *Dcn* and reduced *Ccl2*, *Pappa* and *Wnt4* in MOSE$p53^{R270H}$ cells compared to control cells (**Fig. 1G**). Interestingly, *Cdh6* expression was not detected in MOSE cells. Consistent with qPCR analysis, CDH6 protein was not detected and DCN expression was not altered in MOSE cells with $p53^{R270H}$ (**Fig. 1H**). These analyses revealed that CDH6 is repressed in MOE cells by p53 mutation, but its expression and regulation in MOSE cells was not detectable.

TABLE VII - TABLE SHOWING THE LIST OF GENES CHOSEN FOR THE STUDY

Genes	**Log_{10} Fold change**	**p value**
Ccl2	-1.50314	< 0.0001
Dcn	1.4153	< 0.0001
Cdh6	-0.62727	< 0.0001
Pappa	-0.2883	< 0.01
Wnt4	-0.9896	< 0.0001

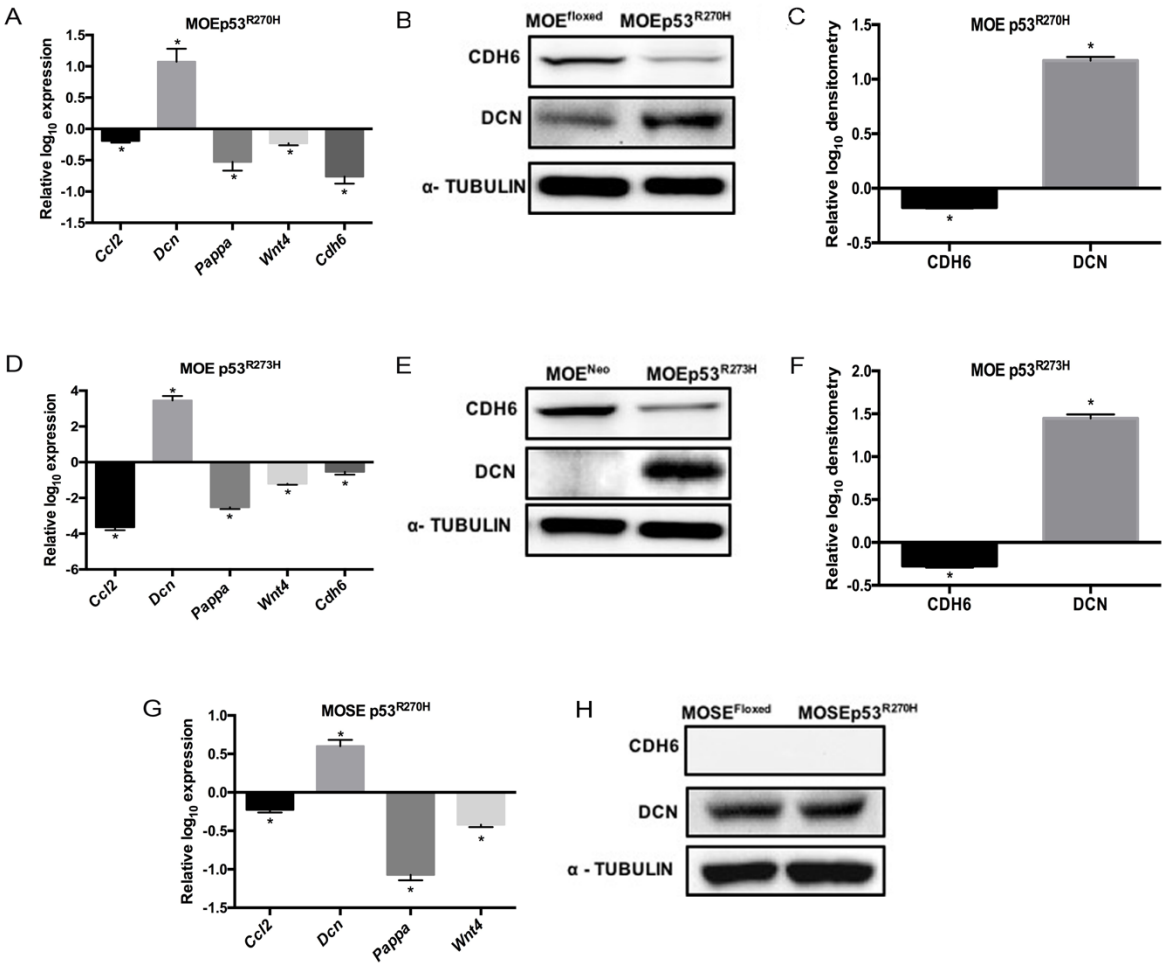

Figure 1 - Comparative pro-migratory gene expression levels in MOE and MOSE cells.

A. qPCR data of MOEp53^{R270H} relative to MOE^{Floxed} control cells. B. Representative western blot. C. Densitometry analysis of MOEp53^{R270H} relative to MOE^{Floxed} control cells. D. qPCR of MOEp53^{R273H} relative to MOE^{Neo} control cells. E. Representative western blot. F. Densitometry analysis of MOEp53^{R273H} relative to MOE^{Neo} control cells. G. qPCR data of MOSEp53^{R270H} relative to MOSE^{Floxed} control cells. H. Representative western blot. Data represent mean ± SEM (N ≥ 3). Student *t*-test was used to determine significance, (*$p < 0.05$) relative to control. α - Tubulin is used as a loading control.

MOE cells with stable $p53^{R248W}$ expression were next investigated. A MOE$p53^{R248W}$ clone was confirmed for human p53 mRNA (**Fig. 2A**) and p53 protein expression (**Fig. 2B and 2C**). $p53^{R248W}$ increased *Dcn* and reduced *Ccl2*, *Cdh6*, *Pappa* and *Wnt4* as compared to control (**Fig. 3A**). CDH6 protein levels were decreased and DCN was induced due to $p53^{R248W}$ in MOE cells (**Fig. 3B and 3C**) similar to $p53^{R273H}$. Because $p53^{R273H}$ and $p53^{R248W}$ are the two most frequently mutated sites in ovarian cancer, and our previous data indicated that $p53^{R273H}$ mutation enhanced migration (2), we tested the effect of stable $p53^{R248W}$ on migration. MOE$p53^{R248W}$ cells migrated ~20% faster than the vector control (MOE^{Neo} cells), but not as rapidly as MOE $p53^{R273H}$ cells (**Fig. 3D**). FOXM1 is induced by mutant p53 and can increase tumor metastases (133). Our previous data indicated that SLUG was a key downstream target of R273H that mediated motility (133). FOXM1 expression levels in MOE $p53^{R248W}$ cells were lower than the levels in MOE $p53^{R273H}$ cells (**Fig. 3E and 3F**). SLUG expression was not detected in MOE $p53^{R248W}$ cells (**Fig. 4E and 4F**). These data suggest that $p53^{R273H}$ and $p53^{R248W}$ do not equally induce SLUG and FOXM1 expression in the fallopian tube and this modified migration.

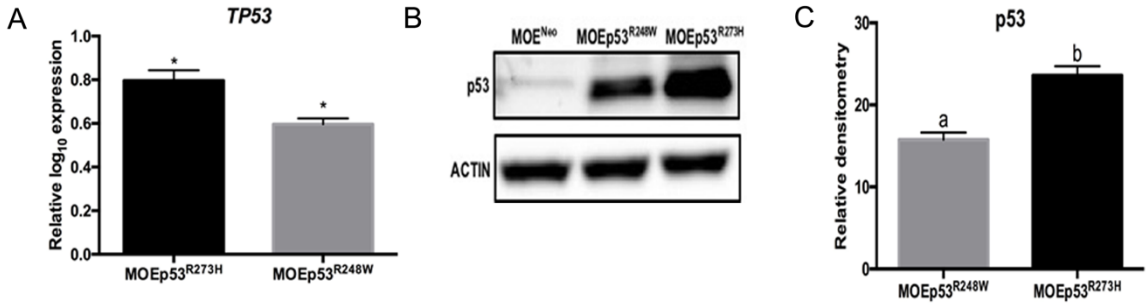

Figure 2 – p53 mRNA and protein levels in MOEp53^{R248W} cells to validate the stable transfections.

A. qPCR showing p53 mRNA levels in MOE cells stably transfected with p53^{R248W} relative to MOE^{Neo} control cells. MOEp53^{R273H} cells were used as a positive control. B. p53 western blot image. C. Densitometry analysis on p53 levels in MOE cells with p53^{R273H} and p53^{R248W}. Data represent mean ± SEM (N ≥ 3). Student *t*-test was used to determine significance, (*$p < 0.05$) relative to control. One-way ANOVA was used to determine, a – b ($p < 0.05$) bars without common letter differ.

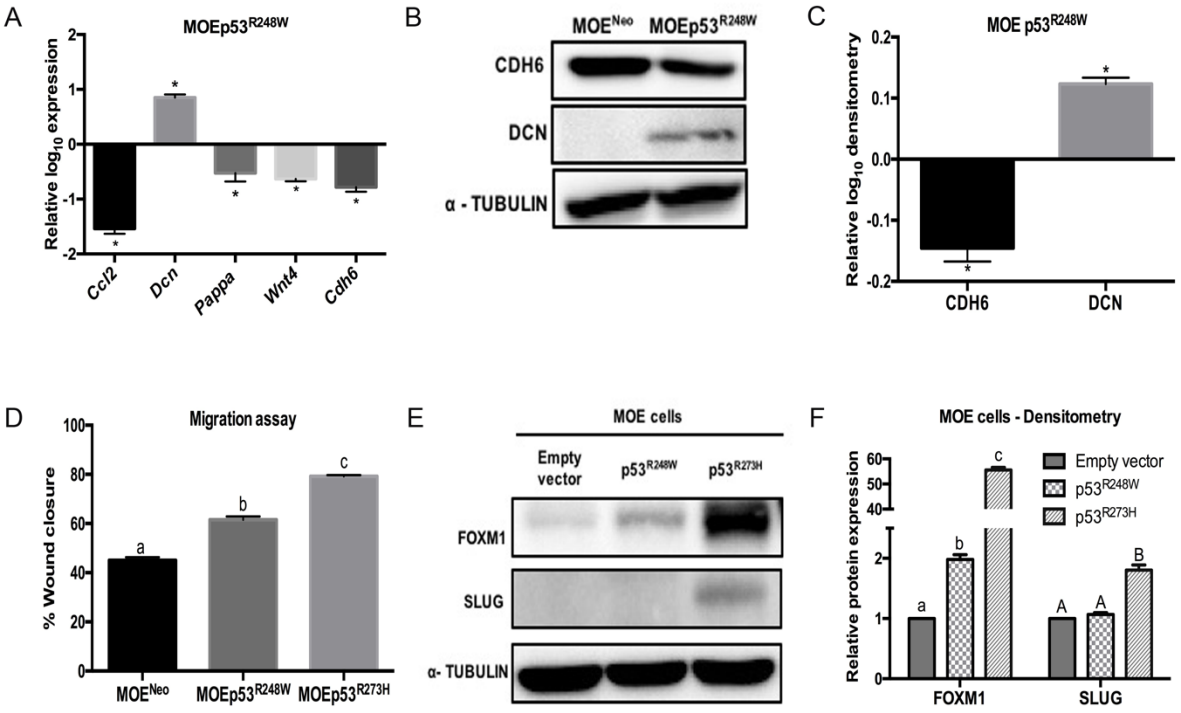

Figure 3 – p53^{R248W} reduces CDH6 expression and increases migration in MOE cells.

A. qPCR analysis on MOEp53^{R248W} cells relative to MOE^{Neo} control cells. Cell lysates were probed with CDH6 and DCN antibodies. α - Tubulin is used as a loading control. B. Western blot on MOE^{Neo} and MOEp53^{R248W} cells. C. Densitometry analysis of MOEp53^{R248W} relative to MOE^{Neo} control cells. D. Migration assay of MOE^{Neo}, MOEp53^{R273H}, and MOEp53^{R248W} cells 8 hours after wounding. E. FOXM1 and SLUG western blot. α - Tubulin is used as loading control. F. Densitometry analysis on relative FOXM1 and SLUG protein levels compared to empty vector cells. Data represent mean ± SEM (N ≥ 3). Data was analyzed with a student *t*-test (*$p < 0.05$ relative to control) or one-way ANOVA (a–c or A-B bar without common letter differ, $p < 0.05$).

The PAX8$^{cre/+}$p53$^{R270H/+}$ mouse model confirms CDH6 is regulated in the oviducts and not the ovaries.

In order to verify whether CDH6 is regulated by mutant p53 *in vivo*, a transgenic mouse model was developed. A tissue specific transgenic mouse model was generated by crossing mice with a Lox-stop-Lox site regulating expression of the R270H mutation with mice expressing cre-recombinase driven by the *Pax8* promoter (**Fig. 4**). Using this model, p53^{R270H} remains floxed and only p53^{WT} is expressed except in PAX8 expressing tissues, such as the oviduct, uterus, and kidney (**Fig. 4**). PCR confirmed that the p53^{R270H} had recombined in the oviduct and uterus, but not in the ovaries, which do not express PAX8 and therefore would lack cre-recombinase (**Fig. 5A**). Mice were sacrificed after 9 months, tissues were dissected and mRNA was extracted for qPCR. *Cdh6, Pappa, Wnt4,* and *Ccl2* mRNA levels were decreased and *Dcn* mRNA was increased in PAX8$^{cre/+}$p53$^{R270H/+}$ compared to control PAX8$^{cre/+}$ oviducts (**Fig. 6A**). *Cdh6, Pappa, Wnt4,* and *Ccl2* were not significantly altered in the PAX8$^{cre/+}$p53$^{R270H/+}$ ovaries (**Fig. 5B**). Consistent with the cellular models, *Cdh6* mRNA levels were not detected in ovaries. Immunohistochemistry (IHC) analysis was used to identify the protein levels in PAX8$^{cre/+}$p53$^{R270H/+}$ and PAX8$^{cre/+}$ oviducts and ovaries. CDH6 staining was high in PAX8$^{cre/+}$ oviducts and the staining intensity decreased in PAX8$^{cre/+}$p53$^{R270H/+}$ oviducts as predicted based on repression from p53^{R270H} (**Fig. 6B**). DCN was detected in PAX8$^{cre/+}$ and was induced in PAX8$^{cre/+}$p53$^{R270H/+}$ oviducts (**Fig. 6B**). p53 stabilization was not detected in PAX8$^{cre/+}$p53$^{R270H/+}$ oviducts (**Fig. 6B**). Negative CDH6 and p53 staining was seen in the ovaries (**Fig. 5C**). Both PAX8$^{cre/+}$p53$^{R270H/+}$ and PAX8$^{cre/+}$ ovaries stained positive for DCN with no change at the protein level by R270H (**Fig. 5C**). Normal human fallopian tube fimbriae also expressed CDH6 (**Fig. 6C**). DCN expression and p53 stabilization was

not observed in normal human fallopian tube fimbriae (**Fig. 6C**). CDH6 staining was not detected in normal human ovarian surface epithelium by IHC (**Fig. 6D**). CK8 positive staining confirmed the presence of OSE (**Fig. 6D**). Additionally, CDH6 protein was not detected in immortalized ovarian surface epithelial cell lysate (IOSE80) (**Fig. 6E**). These *in vivo* analyses demonstrate that CDH6 is specifically repressed by mutant p53 in the oviducts.

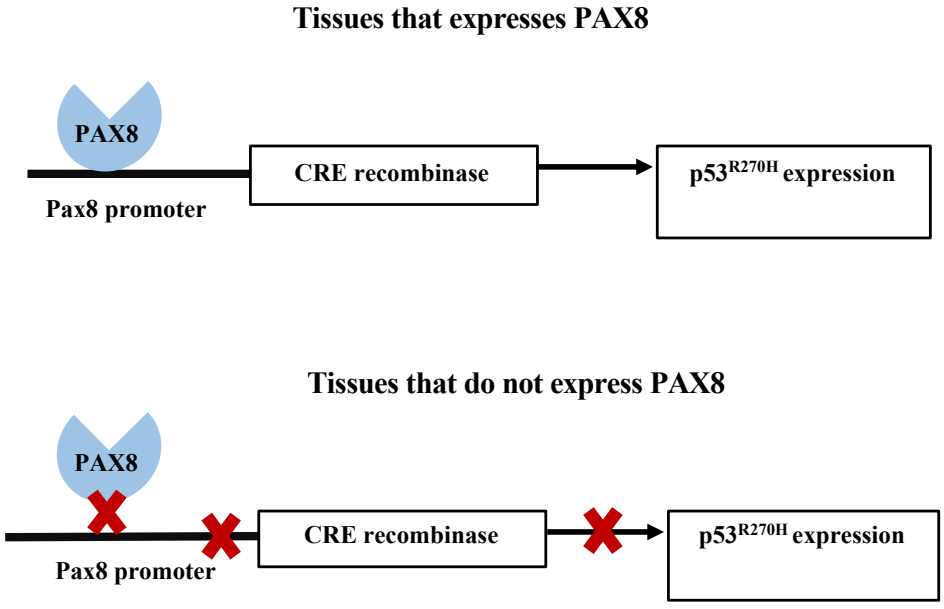

Figure 4 - Schematic representation of PAX8 driven tissue specific expression of $p53^{R270H}$. Mice expressing the cre – recombinase was crossed with mice expressing Lox-stop-Lox regulating $p53^{R270H}$. In tissues that expresses PAX8, the cre-recombinase enzyme is expressed, thereby cleaving the Lox site flanking the stop codon in the $p53^{R270H}$, resulting in activating its expression. In tissues, that do not express PAX8 will lack cre– recombinase and $p53^{R270H}$ expression.

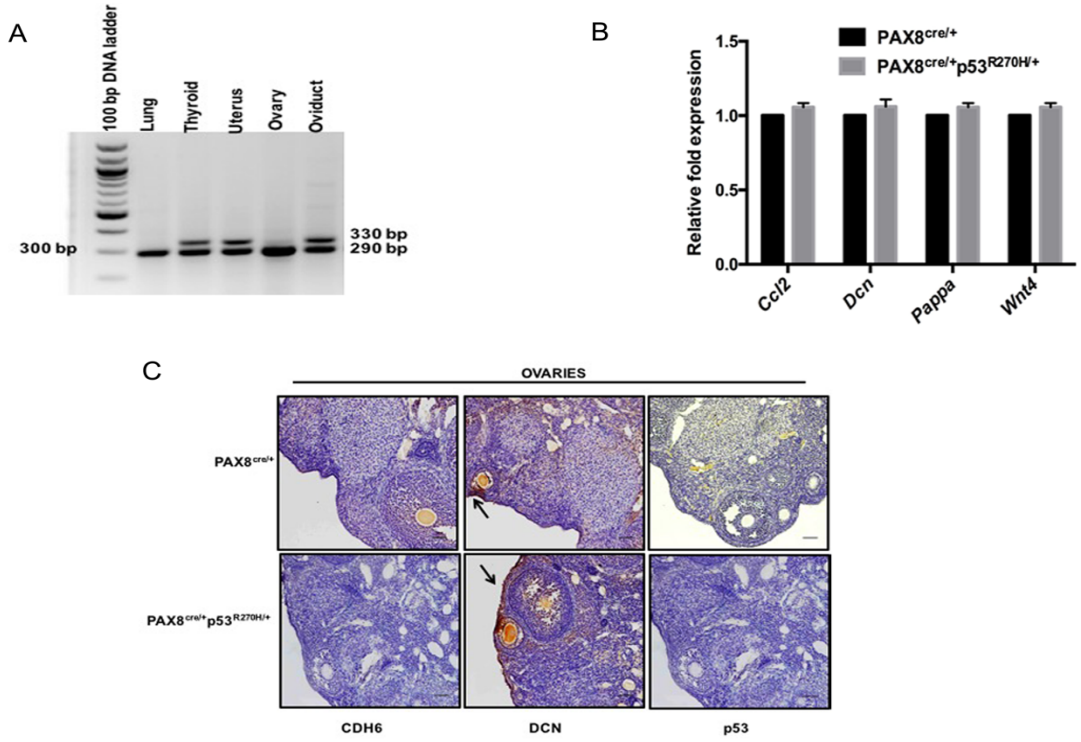

Figure 5 – CDH6 is not detected in MOSE cells and murine ovaries.

A. Standard PCR was performed on the genomic DNA extracted from tissues of $PAX8^{cre/+}p53^{R270H/+}$ mice using primers specific to *loxP* sites. Agarose gel image showing recombined mutant p53 band at 330 bp in PAX8 expressing tissues and $p53^{WT}$ positive band at 290 bp in all tissues tested. B. qPCR showing no significant change in pro-migratory gene expression in $PAX8^{cre/+}p53^{R270H/+}$ ovaries compared to $Pax8^{cre/+}$ ovaries. C. Immunohistochemistry analysis on $Pax8^{cre/+}$ and $PAX8^{cre/+}p53^{R270H/+}$ ovaries with absence of CDH6 and no change in DCN expression. p53 staining is used as negative control. Black arrow indicates positive staining. Data represent mean ± SEM ($N \geq 3$). Scale bars = 50 μm.

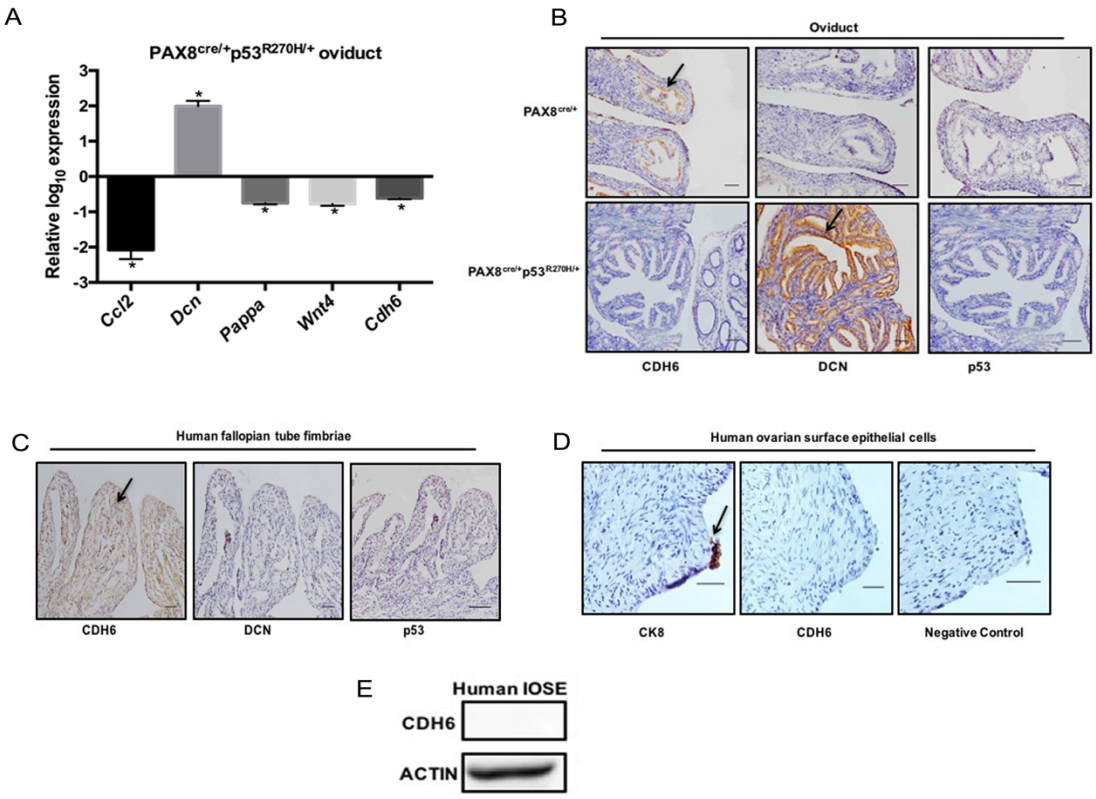

Figure 6 – CDH6 is repressed by mutant p53 in murine oviducts.

A. qPCR data on the pro-migratory genes from PAX8$^{cre/+}$p53$^{R270H/+}$ oviducts relative to Pax8$^{cre/+}$ oviducts. B. IHC analysis of CDH6, DCN and p53 staining in Pax8$^{cre/+}$ and PAX8$^{cre/+}$p53$^{R270H/+}$ oviducts C. IHC on human fallopian tube for CDH6, DCN and p53. Black arrow indicates positive staining. Scale bars = 100 μm. D. Immunohistochemistry on human ovaries for CDH6 and CK8. Black arrow indicates positive staining. Scale bars = 20 μm. E. CDH6 western blot in normal human IOSE cells. Actin is used as loading control. Data represent mean ± SEM (N ≥ 3). Student *t*-test was used to determine significance, (*$p < 0.05$) relative to control.

Mutant p53 reduces CDH6 expression independently and through SLUG induction in HGSOC.

Mutations in p53 may directly or indirectly repress *Cdh6* promoter activity. To determine if mutant p53 regulates CDH6 through direct transcriptional repression, MOE cells harboring $p53^{WT}$, $p53^{R273H}$, and $p53^{R248W}$ were cultured and ChIP analysis was performed using p53 and Non–specific IgG antibodies. *Mdm2* and *Atf* were used as positive controls in ChIP analysis (**Fig. 7A and 7B**) (134). Increased $p53^{WT}$ occupancy was observed on the *Cdh6* promoter when compared to control IgG (**Fig. 8A**). The $p53^{R273H}$ and $p53^{R248W}$ demonstrated a significantly higher occupancy on the *Cdh6* promoter compared to $p53^{WT}$ (**Fig. 8A**). These findings suggest that p53 mutation decreases *Cdh6* expression in oviductal epithelium through direct repression of the promoter.

A panel of human HGSOC cell lines including OVCAR3, OVCAR5, OVKATE, OVSAHO and OVCAR8 were tested for the presence of CDH6. CDH6 protein was detected in OVCAR5, OVKATE, OVSAHO and OVCAR8 cells (**Fig. 7C**). A weak expression of CDH6 was observed in OVCAR3 cells (**Fig. 7C**). In order to decipher the regulation of CDH6 by mutant p53 in the absence of $p53^{WT}$, a $p53^{null}$ human HGSOC cell line (OVCAR5 cells) was transfected to express $p53^{WT}$, $p53^{R273H}$ or $p53^{R248W}$. Endogenous CDH6 protein expression did not change in $p53^{WT}$ compared to empty vector control transfected cells (**Fig. 8B and 8C**). CDH6 expression was decreased by $p53^{R273H}$ and $p53^{R248W}$ in OVCAR5 cells (**Fig. 8B and 8C**). These results suggest that CDH6 was repressed by mutant p53 and that its repression was not dependent on blocking $p53^{WT}$ protein. To identify if SLUG, a mutant p53 induced pro-migratory protein can reduce CDH6, MOE cells with stable $p53^{R273H}$ expression and *Snai2* (encodes SLUG) knock down were

used. MOEp53^{R273H} cells had increased SLUG expression and stable SLUG knock down significantly decreased cell migration compared to control cells (2). SLUG can repress cadherin expression by binding to the E-box motifs on their promoters (135). Knockdown of SLUG restored CDH6 protein compared to MOEp53^{R273H} cells (**Fig. 8D & 8E**). Therefore, both SLUG and mutant p53 regulate CDH6 (**Fig. 8F**).

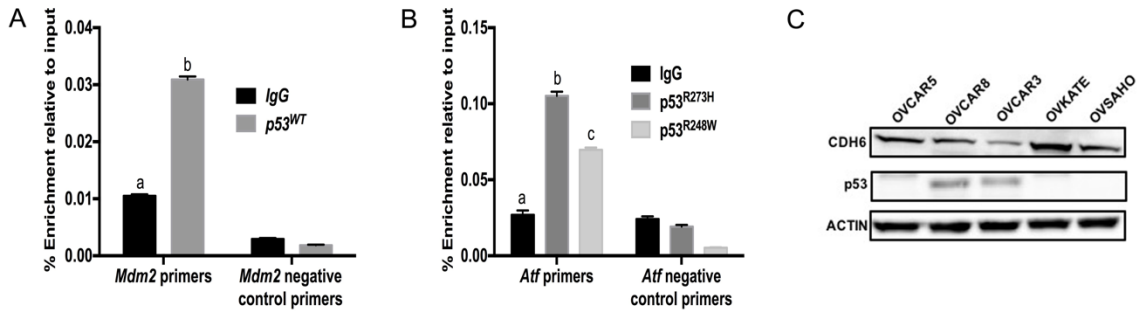

Figure 7 – chIP analysis positive controls and CDH6 expression in human HGSOC cell lines.

Mdm2 and *Atf* are used as positive controls for $p53^{WT}$ and mutant p53 occupancy respectively. A. ChIP analysis showing increased $p53^{WT}$ occupancy on *Mdm2* promoter compared to IgG. B. ChIP analysis showing high $p53^{R273H}$ and $p53^{R248W}$ occupancy on *Atf* promoter compared to IgG. Primers designed on non-p53-binding site in the promoters is used as controls. C. CDH6 and p53 western blot in human HGSOC cell lines. Data represent mean ± SEM (N ≥ 3). One-way ANOVA was used to determine, a – c ($p < 0.05$) bars without common letter differ.

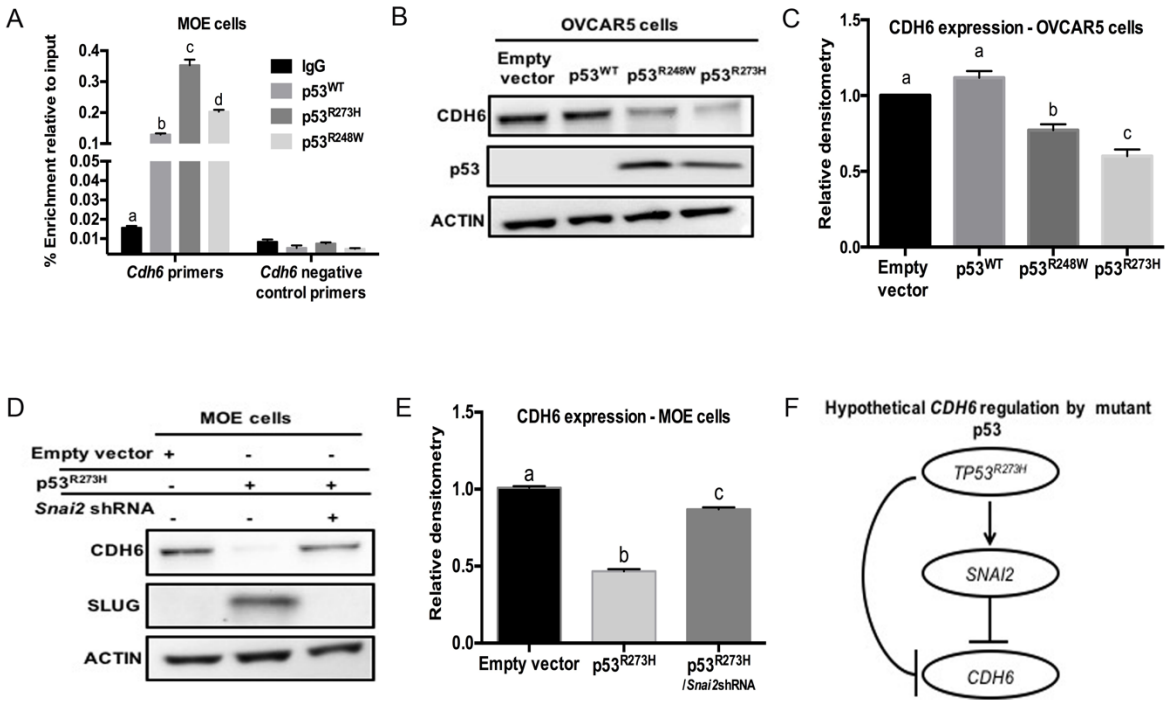

Figure 8 – Mutant p53 repress CDH6 independent of p53^{WT} in human HGSOC cell lines.

A. ChIP analysis on MOE cells for non-specific IgG, p53^{WT}, p53^{R273H} and p53^{R248W} occupancy on *Cdh6* promoter. Primers designed on non - p53-binding site used as negative control primers. B. OVCAR5 cells were transiently transfected with empty vector, p53^{WT}, p53^{R273H} and p53^{R248W}. Western blot analysis for CDH6 and p53 levels. Actin is used as loading control. C. Densitometry analysis for CDH6 expression levels on transiently transfected OVCAR5 cells relative to actin. D. Western blot image for CDH6 and SLUG levels in MOE cells. E. Densitometry data obtained on CDH6 expression levels in MOE cells with empty vector, p53^{R273H} and p53$^{R273H/Snai2shRNA}$ stable expression. F. Hypothetical pathway for CDH6 regulation by p53^{R273H} in HGSOC. Data represent mean ± SEM (N ≥ 3). One-way ANOVA was used to determine, a – d ($p < 0.05$) bars without common letter differ.

NSC59984 rescues CDH6 expression and inhibits cell migration in MOE cells.

In order to study if inhibition of mutant p53 activity can rescue CDH6 repression, MOE cells with $p53^{R273H}$ and $p53^{R248W}$ were treated with NSC59984. NSC59984 is a small molecule that stabilizes wild type p53 signaling and increases the degradation of mutant p53 (65). NSC59984 degraded mutant p53 protein and rescued CDH6 repression in MOE cells with $p53^{R273H}$ (**Fig. 9A and 9B**). NSC59984 also reduced the cell migration in $MOEp53^{R273H}$ with no change in migration in $MOEp53^{WT}$ cells compared to DMSO treated cells (**Fig. 9C and 9D**). HGSOC cell lines OVCAR3 cells was selected to test the activity of NSC59984 because it expresses the $p53^{R248W}$ mutation and is considered a viable model of high grade serous cancer (136). NSC59984 did not have an effect on OVCAR3 cells (**Fig. 10**). Our results demonstrate that NSC59984 reduces $p53^{R273H}$ activity, but not R248W, and can revive CDH6 repression and reduces cell migration.

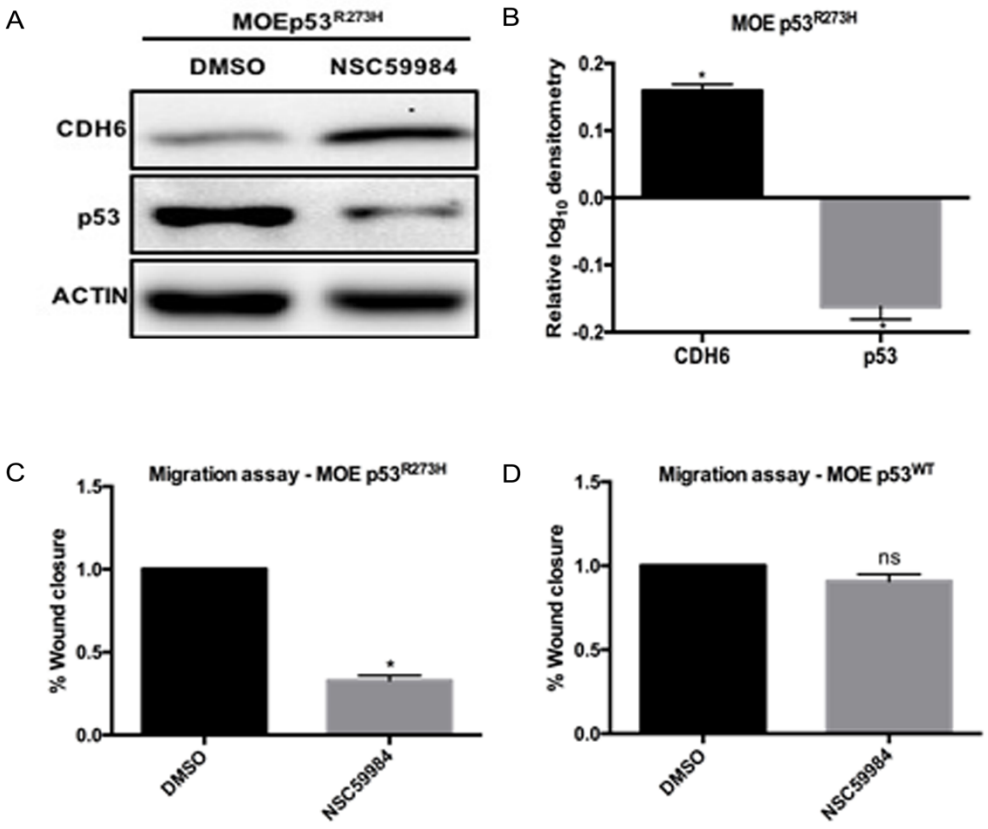

Figure 9 – NSC59984 degrades p53R273H, restores CDH6 and inhibits cell migration in MOE cells.

A. MOE cells with $p53^{R273H}$ and $p53^{R248W}$ cells were treated with 25 μM/L NSC59984 for 8 hours. Cells lysates were probed for CDH6 and p53. Western blot image is represented, and Actin is used as loading control. B. Densitometry analysis on CDH6 and p53 expression levels with NSC59984 treatment in $MOEp53^{R273H}$ cells relative to DMSO treated cells. C. Migration assay after 8 hours of scratch in $MOEp53^{R273H}$ cells with 25 μM/L NSC59984. D. Migration assay after 8 hours of scratch in $MOEp53^{WT}$ cells with 25 μM/L NSC59984. Data represent mean ± SEM ($N \geq 3$). Student *t*-test was used to determine significance, (*$p < 0.05$) relative to control. n.s – not significant.

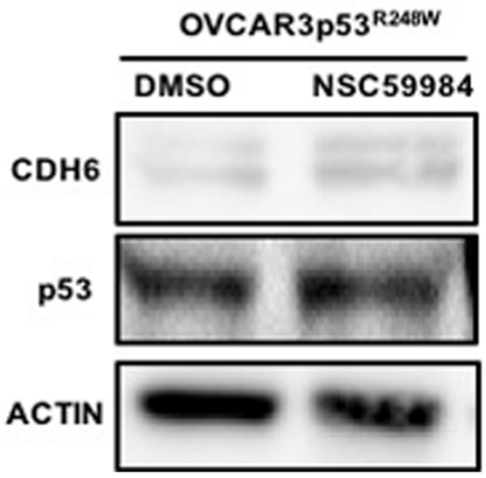

Figure 10 – NSC59984 did not degrade $p53^{R248W}$ in OVCAR3 cells. CDH6 and p53.

Western blot image of OVCAR3$p53^{R248W}$ cells treated with 25 μM/L NSC59984 for 8 hours. Actin is used as loading control.

C. DISCUSSION

Mounting evidence suggests that the FTE is a likely progenitor cell for HGSOC with p53 mutation almost being essential in HGSOC (31,35,36,122). However, the ovarian surface may still give rise to some serous tumors (99). While almost all tumors have a p53 mutation, the two most frequent mutations are the DNA binding missense mutations, R273H and R248W (48,137). One potential route to improving personalized therapy for ovarian cancer is to understand the accumulating steps in tumor formation that might be targeted, which could be specific to the tissue from where the tumors originate. Thus, if a tissue specific target of mutant p53 exists, it may help to differentiate FTE from OSE derived tumors.

Using previously published microarray data on MOEp53^{R273H} cells, a set of pro-migratory genes including *Cdh6, Pappa, Dcn, Wnt4* and *Ccl2* were chosen to study in oviductal epithelium and OSE. CDH6 was repressed by p53 mutants only in the MOE cells, but it was not expressed or regulated in MOSE cells. Human fallopian tube epithelial cells express CDH6, but CDH6 expression was not detected in human OSE. While gene expression for mutant p53 targets may not be retained throughout all phases of tumor progression, these data suggest that unique mutant p53 targets are present in fallopian tube that may provide clues to distinguish the two cell progenitor populations. This study also identified that p53 mutations are capable of altering a subset of genes identically in fallopian tube and ovarian surface. CDH6 is membrane glycoprotein and a member of the cadherin family that mediates homophilic cell-to-cell adhesion. CDH6 plays a key role in cell morphogenesis and when disrupted, may contribute to cell migration (138,139). CDH6 has been associated with cancer cells in the literature as a target that is repressed by estrogen

signaling in ovarian cancer (127). Cristofaro et al. demonstrated PAX8 can directly bind to CDH6 promoter and induce its expression in an immortalized fallopian tube secretory epithelial cell line (140). Lastly, CDH6 was identified as a downstream target for p53 and Pax2 co-operative regulation during kidney development and nephrogenesis (141).

MOE cells stably transfected with $p53^{R248W}$ migrated more than control cells, but this was lower than $p53^{R273H}$ cells, consistent with previous reports suggesting that R273H increases tumor invasion (48,137). R273H and R248W may have distinct regulation on certain pro-migratory targets, for example SLUG and FOXM1 were only highly regulated by R273H. However, this study cannot fully explain the longer survival times in patients with R273 compared to R248 (137), which may be a reflection of the chemoresistance often seen in tumors with R248 (48,137).

In HGSOC, p53 signatures (p53 protein stabilization in FTE) are the proposed early precursor lesions (39). Intriguingly, $Pax8^{cre/+}p53^{R270H/+}$ oviducts lacked p53 staining by IHC, which is consistent with published data that mutation in p53 alone did not result in p53 stabilization in murine models (2,50). In other models with constitutive mutant p53 expression, the stabilization of the protein is seen in tumors, but not in the adjacent normal cells with p53 mutation (142). Terzian et al. found mice lacking *Mdm2* or $p16^{Ink4a}$ stabilized mutant p53 when crossed with p53 homozygous mutant mice suggesting that loss of heterozygosity, loss of MDM2, or loss of p16 are necessary to mediate p53 stabilization (61). The $Pax8^{cre/+}p53^{R270H/+}$ animals demonstrated no signs of tumor formation up to 12 months whereas our previous results using stable cells lines derived from oviductal cells with stable PTEN knockdown alone demonstrated p53 stabilization (38). These data suggest that mutation alone may not generate the p53 signature, but may be a prerequisite for p53 stabilization.

High mutant p53 occupancy compared to the $p53^{WT}$ on the *Cdh6* promoter was

demonstrated by ChIP analysis in MOE cells. SLUG knockdown restored CDH6 repression in MOE cells with $p53^{R273H}$ mutation. SLUG, a p53 transcriptional target, was enhanced by $p53^{R273H}$ and increased migration (2). SLUG can bind to E-box motifs to repress cadherin expression (143). The TCGA reports amplification of *SNAI2* (encodes for SLUG) in 12% HGSOC. Together, the data suggests that p53 independently and coupled with SLUG can regulate CDH6 expression. CDH6 levels were significantly reduced when $p53^{R273H}$ and $p53^{R248W}$ were expressed even in the absence of wild-type p53. This supports that CDH6 repression by mutant p53 is independent of $p53^{WT}$ and may be due to GOF activity. Zhu et al. found that p53 GOF mutants, including R273 and R248, in a CHIPseq analyses had proximal peaks on chromatin regulatory genes in breast cancer cell lines (144). The same study also found that $p53^{R273H}$ had enriched peaks on E26 transformation-specific (ETS) motifs that were distinct from $p53^{WT}$ (144). The CDH6 promoter contains an ETS binding motif. This observation supports that CDH6 repression by mutant p53 could be due to GOF activity and this is consistent with mechanisms in the literature that require ETS motifs.

Currently, researchers are trying to identify small molecules to increase the degradation of mutant p53 or revert the mutant confirmation to wild type. A cell-penetrating peptide significantly inhibited p53 aggregation in OVCAR3 cells resulting in reduced tumors *in vivo* (66). NSC59984 is a small molecule that can effectively degrade mutant p53 protein via MDM2 mediated ubiquitination, and is effective against colorectal cancer (65). NSC59984 enhanced CDH6 expression, reduced mutant p53 expression, and inhibited cell migration in $MOEp53^{R273H}$ cells. NSC59984 did not have an effect on p53 or CDH6 protein in OVCAR3 cells harboring the $p53^{R248W}$ mutation. These data indicate that p53 mutants are unique and may require distinct small molecules to inhibit their activity, however more exploration is required to support this finding.

Additionally, future clinical studies using small molecules or peptides that inhibit mutant p53 aggregation or that degrade mutant p53 should therefore be considered along with sequencing HGSOC tumors prior and post treatment. The existence of a p53 DNA contact mutant target, which is regulated in the fallopian tube but not expressed in ovaries, with further validations using human ovarian tumors and HGSOC clinical samples, may add to the existing tools for finding the cell of origin of serous tumors and improve personalized therapies that work better in tumors arising from the fallopian tube.

IV. PROLACTIN SIGNALING DRIVES TUMORIGENESIS IN HUMAN HIGH GRADE SEROUS OVARIAN CANCER CELLS AND IN A SPONTANEOUS FALLOPIAN TUBE DERIVED MODEL

A. INTRODUCTION

Although mice models with targeted genetic alterations in the FTE induced HGSOC (34), few models characterize the spontaneous pathogenesis of HGSOC from the FTE, which is essential to identify novel targets of ovarian tumor formation and to understand the disease etiology. Our lab previously created a spontaneous model of FTE-derived OVCA by serially passaging murine oviductal epithelial cells (MOE^{high}), an equivalent of the human FTE. These cells formed highly proliferative subcutaneous tumors in mice and transcriptomic analysis of the MOE^{high} cells revealed several pathways that were altered similar to HGSOC such as FOXM1, c-myc, and loss of Cdkn2a (3). However, several other transcripts were significantly altered that may play an essential role in tumorigenesis of HGSOC, such as *Prl2c2* and *Wnt7b* (3).

Wnt7b (Wingless – type MMTV integration site family, member 7B), is a secreted morphogen (protein that induces morphogenesis), was enriched ≈ 36-fold in MOE^{high} cells (3). WNT7B expression levels were found to be enriched in human, malignant OVCA and breast cancer compared to benign tissues (105,145). *Prl2c2*, that encodes for proliferin was amplified >100 fold in the spontaneous model (3). Enhanced expression of *Prl2c2* was previously identified to induce malignant transformation of murine fibroblasts and as a critical driver of murine lung adenocarcinoma (146,147). *Prl2c2* is a murine hormone, without a direct human homolog;

however, *Prl2c2* belongs to the prolactin (PRL) superfamily (prolactin family 2 subfamily c member 2 (148).

PRL is secreted by the pituitary gland and is best known to stimulate milk production (104). However, prolactin is produced locally by many tissues, and increasing evidence supports the hypothesis that the local accumulation of PRL can contribute to tumorigenesis of cancers, such as breast, and colorectal (84). PRL was a component of a multiplex immunoassay called Ovasure, to detect OVCA (88). While this product is no longer FDA approved, the role of prolactin as a biomarker suggests it might also play a significant role in disease formation and/or progression. Prolactin receptor (PRL-R) activation by PRL activates several kinase pathways that are well known to stimulate cellular proliferation (104). Chronic exposure of PRL induced the transformation of immortalized OSE cells and resulted in tumors in mice (84). Since most human HGSOC are now thought to originate from the FTE, and not the OSE, exploring the signaling mechanism of PRL in human FTE and FTE-like HGSOC cells would be more useful.

We hypothesized that *Prl2c2*, its human homolog PRL, and WNT7B were critical for enhanced cell proliferation and to induce ovarian tumors. This study found that, while *Wnt7b* and *Prl2c2* were essential for increased cell proliferation of MOE^{high} cells *in vitro*, in *in vivo* only *Prl2c2* suppressed MOE^{high} tumors. To translate these findings into human models, the role of PRL and WNT7B signaling in proliferation and tumorigenesis of human FTE and HGSOC cells was explored. Our findings indicate that although PRL and WNT7B were sufficient to alter cell proliferation, PRL alone was pro-tumorigenic in human FTE and tumors, which could have significant implications for future studies aimed at suppressing PRL levels or using neutralizing antibodies to block PRL-R signaling in HGSOC.

B. RESULTS

A stable *Prl2c2* and *Wnt7b* knockdown in MOE^{high} cells reduces cell proliferation by accumulating the cells in the G2 phase.

MOE^{high} cells are the first reported spontaneous model of OVCA derived from fallopian tube (murine oviductal) cells that were tumorigenic *in vivo* and highly proliferative (3). RNA sequencing of MOE^{high} cells revealed the enhanced expression of the PRL-like gene called *Prl2c2* and *Wnt7b* (3). In order to determine if *Prl2c2* or *Wnt7b* was essential for MOE^{high} cell proliferation or transformation, two cell lines with stable knockdown (> 50%) of each gene were generated and validated (**Fig. 11A - 11F**). MOE^{high}/*Prl2c2*$^{shRNA\#1}$ and MOE^{high}/*Prl2c2*$^{shRNA\#2}$ cells displayed a significant reduction in cell proliferation by 65% as compared to a stable non-target shRNA transfected control cells (MOE^{high}/Non-target^{shRNA}) (**Fig. 12A**). A 2D foci assay measured a significant reduction in the number and the size of foci by 90% in MOE^{high} cells with *Prl2c2* knockdown compared to the control cells (**Fig. 12B and Fig. 13A**). Next, MOE^{high}/*Prl2c2*$^{shRNA\#1}$ and MOE^{high}/*Prl2c2*$^{shRNA\#2}$ cells were tested in an anchorage independent growth assay. *Prl2c2* knockdown clones had significantly fewer colonies, compared to the control cells (**Fig. 12C and 13B**). Similarly, *Wnt7b* knockdown significantly reduced MOE^{high} cell proliferation (about 45%) (**Fig. 12D**), 2D foci counts (70%) (**Fig. 12E and 13A**) and the number of anchorage independent colonies (**Fig. 12F and 13B**). Because *Wnt7b* knockdown did not reduce MOE^{high} proliferation to as great an extent as *Prl2c2* knockdown, *Wnt7b's* effect on proliferation was confirmed by transient transfection of constitutively expressed *WNT7B* in normal MOE cells (**Fig. 14A**). The cell proliferation was significantly increased at day 3 and day 5 of transfection compared to the

vector control (**Fig. 14B**), reiterating the hypothesis that WNT7B enhancement increased the FTE proliferation. These results suggest that *Prl2c2* and *Wnt7b* can individually mediate the high proliferation in MOE^{high} cells. To identify if a cell cycle modification could mediate the reduced cell proliferation in *Prl2c2* and *Wnt7b* knockdown cells, a cell cycle assay was performed. Knockdown of *Prl2c2* and *Wnt7b* had similar effects, with a significant decrease (50% and 25% respectively) in the G1 phase and a corresponding increase in the percentage of cells in the G2 phase compared to MOE^{high} (**Figure. 15A, 15B and 15C**).

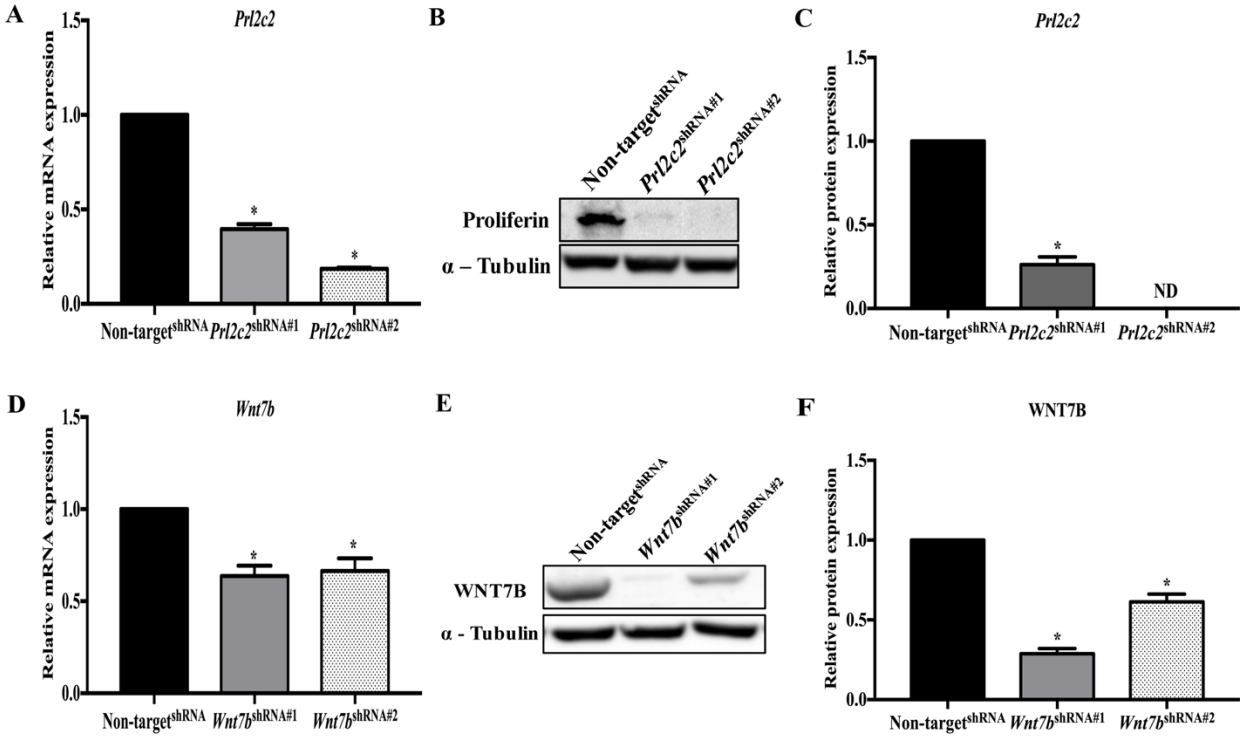

Figure 11 - *Prl2c2* and *Wnt7b* knockdown in MOE^{high} cells.

A&D, Relative levels of *Prl2c2* and *Wnt7b* mRNA quantified by qPCR in MOE^{high} clones. 18srRNA was used as endogenous control. B&E, Representative immunoblot for proliferin and WNT7B levels. α - tubulin was a loading control. C&F, Densitometry analysis of quantified proliferin and WNT7B expression. Data are represented as mean ± SEM (n ≥ 3). *, $p < 0.05$ relative to MOE^{high}/Non-target^{shRNA} cells, ND = not detected.

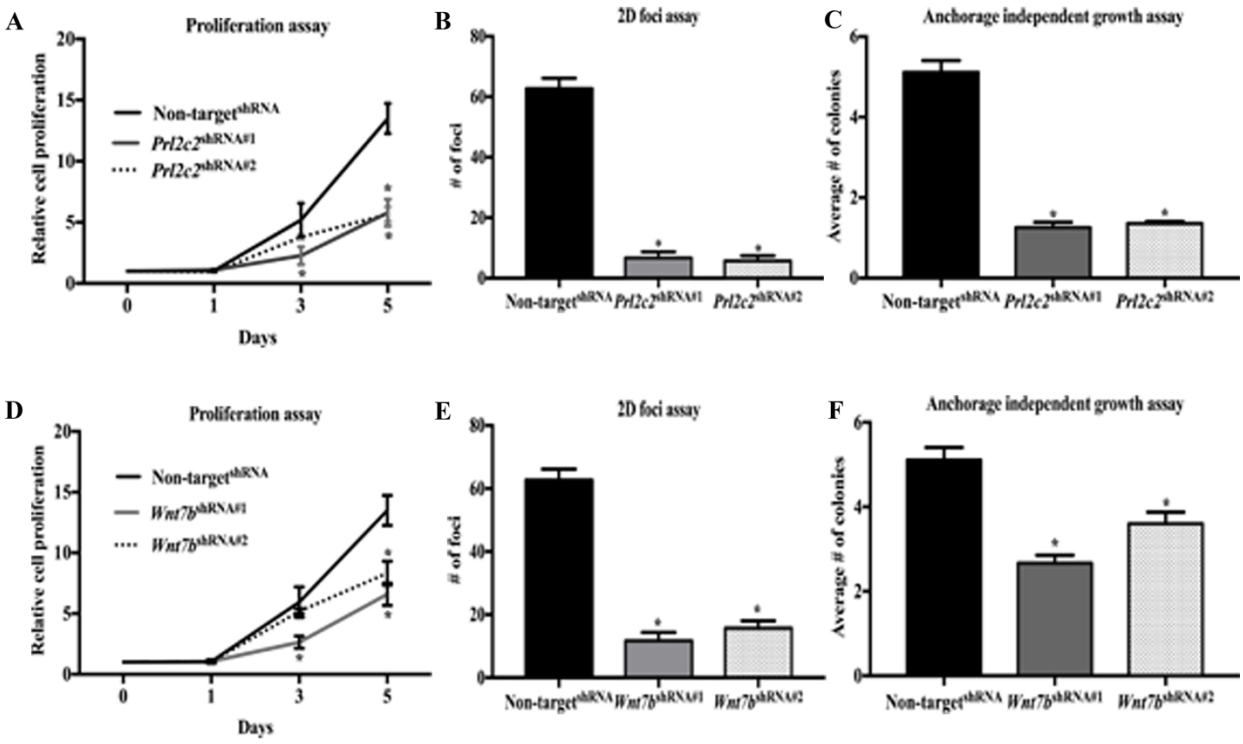

Figure 12 - *Prl2c2* and *Wnt7b* knockdown reduces cell proliferation of MOE^{high} cells.

A & D, SRB assay measured cell proliferation with *Prl2c2* knockdown over days. B & E, 2D foci assay quantified the number of foci on day 7 after plating. C & F, Anchorage independent colonies were quantified using soft agar assay in MOE^{high} clones. Data are represented as mean ± SEM (n ≥ 3). *, $p < 0.05$ relative to MOE^{high}/Non-target^{shRNA} cells.

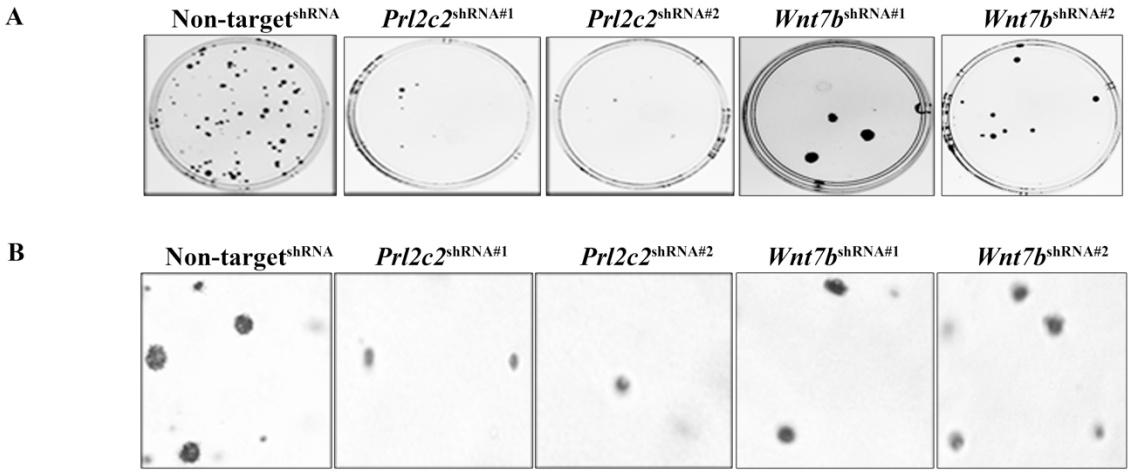

Figure 13 - *In vitro* analysis of *Prl2c2* and *Wnt7b* knockdown in MOE^{high} cells.

A. Representative image of the 2D foci assay performed in MOE^{high} clones. B. Representative image of soft agar assay performed on MOE^{high} clones.

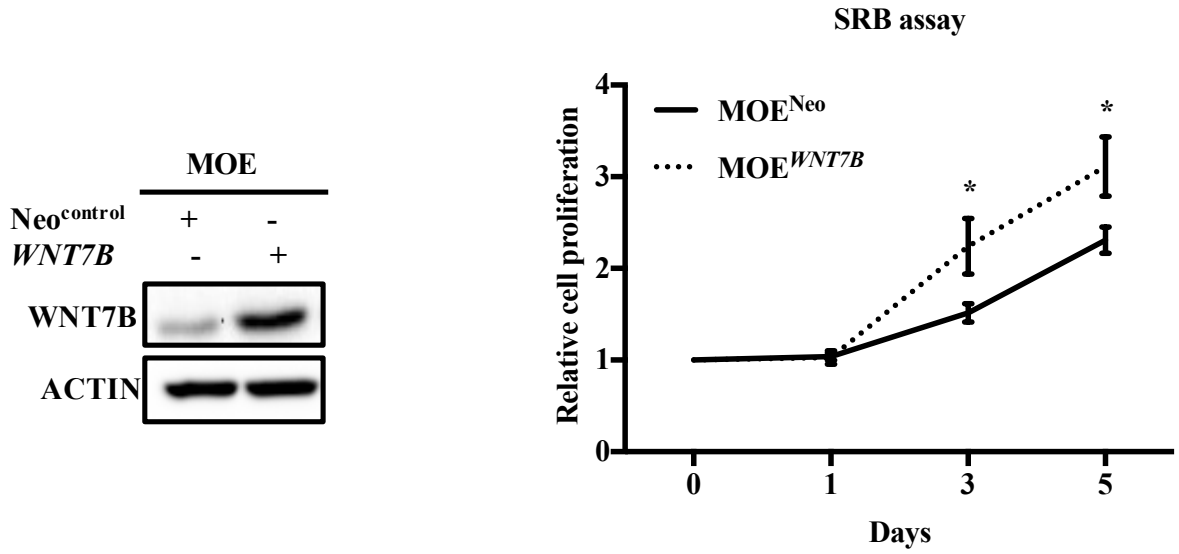

Figure 14 - WNT7B increases MOE cell proliferation.

A. Western blot validating the transient transfection of pCDNA. *WNT7B* in MOE cells. B. SRB assay measured cell proliferation with *WNT7B* transient overexpression. Data are represented as mean ± SEM (n ≥ 3). *, $p < 0.05$ relative to MOE^{Neo} cells.

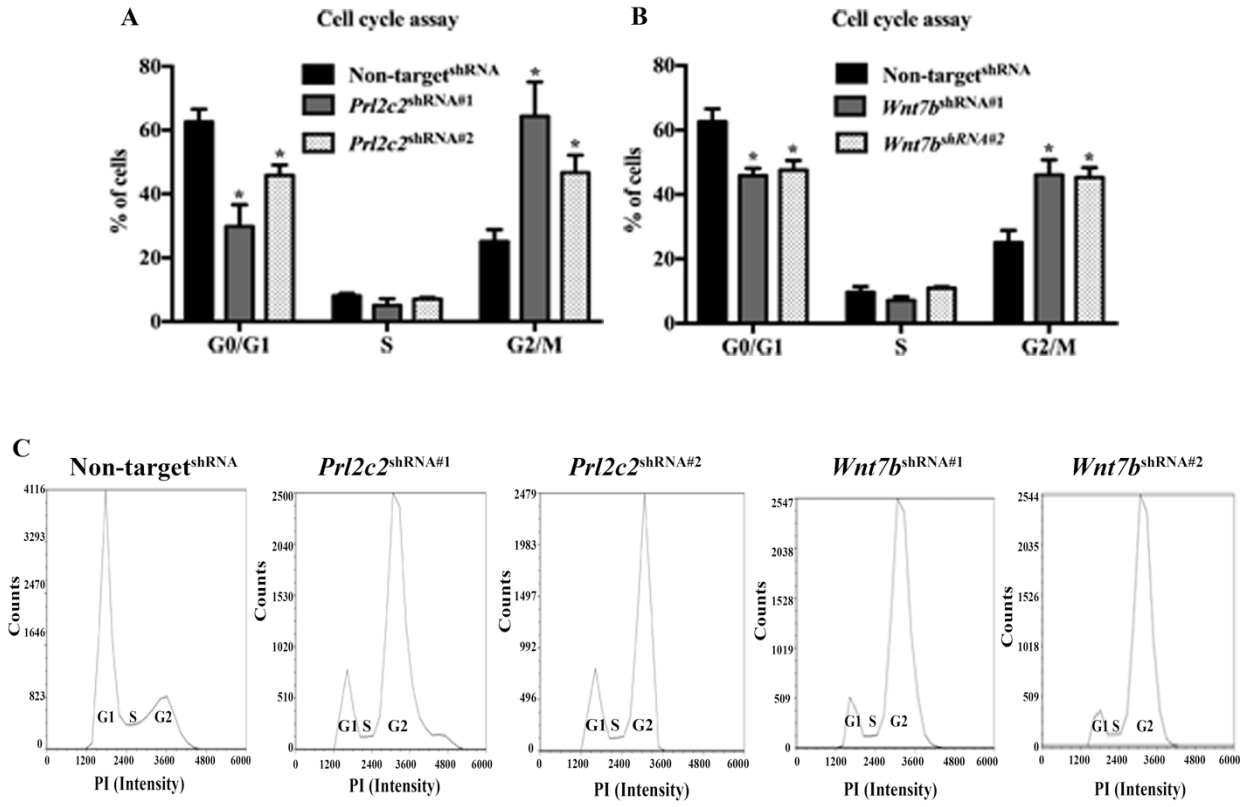

Figure 15 – MOE^{high} cells with *Prl2c2* and *Wnt7b* knockdown had higher accumulation of cells in G2 phase.

A & B, Cell cycle analysis of MOE^{high} cells with *Prl2c2, Wnt7b* knockdown and non-target^{shRNA} control cells. C. Representative image obtained from cell cycle assay. Data are represented as mean ± SEM (n ≥ 3). *, $p < 0.05$ relative to MOE^{high}/Non-target^{shRNA} cells.

In previous studies, MOE^{high} cells demonstrated increased resistance to chemotherapeutic compounds, including cisplatin (3). To determine if *Prl2c2* or *Wnt7b* suppression altered the chemosensitivity, cells were treated with cisplatin in a dose dependent manner followed by cytotoxicity evaluation. No difference was measured between the knockdown and the control cells (**Fig. 16A and 16B**).

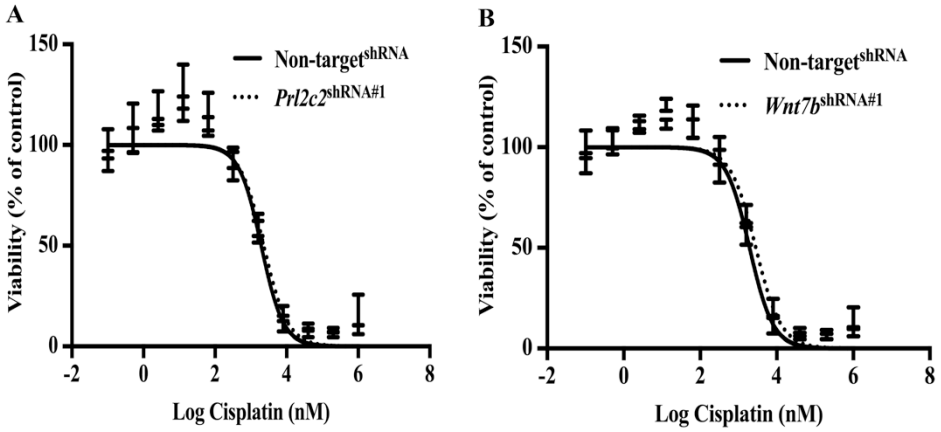

Figure 16 – *Prl2c2* and *Wnt7b* knockdown do not alter MOE^{high} sensitivity to Cisplatin.

A &B, Cisplatin dose response curve on MOE^{high} clones with *Prl2c2* and *Wnt7b* knockdown.

***Prl2c2* reduction in MOE^{high} cells inhibits tumor growth, while *Wnt7b* suppression did not alter MOE^{high} tumor burden.**

MOE^{high} cells formed tumors when injected into the subcutaneous space (3). To identify if *Prl2c2* or *Wnt7b* was a candidate driver of tumorigenesis, MOE^{high}/*Prl2c2*$^{shRNA\#1}$ and MOE^{high}/*Wnt7b*$^{shRNA\#1}$ cells ($1x10^6$ cells/mice) were injected subcutaneously into female athymic nude mice. The same number of MOE^{high} and MOE^{high}/Non-target^{shRNA} cells were injected as control groups. All of the mice (n=3) in the two control groups and *Wnt7b* knockdown (N=5) formed subcutaneous tumors with no significant difference in the tumor volume (**Fig. 17A & 17B**). Interestingly, MOE^{high}/*Prl2c2*$^{shRNA\#1}$ injected mice (n=5) had no detectable tumors (Fig. 17A and 17B). At humane endpoints for controls (115±3 days), mice were sacrificed and IHC analysis was performed on the tumors. Tumors from *Wnt7b* knockdown cells were confirmed to have reduced WNT7B expression compared to tumors from control mice (**Fig. 18**). H&E staining identified similar spindle-like morphology with same level of intensity of proliferative marker Ki67 and negative CK8 staining as seen in control tumors as previously reported (**Fig. 18**) (3). Overall, *Prl2c2* alone, not *Wnt7b* was identified as an essential protein for the tumorigenesis of MOE^{high}.

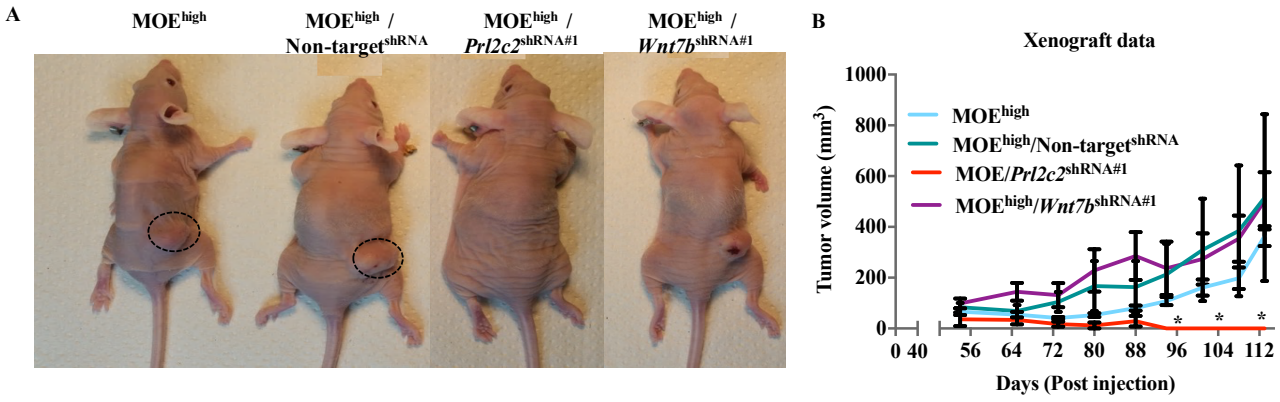

Figure 17 - *Prl2c2* knockdown blocks tumor formation in MOE^{high} cells.

A. Picture of athymic nude mice bearing tumors after xenograft with MOE^{high} clones. Red circles indicate the subcutaneous tumor. B. Tumor volume measured with calipers of MOE^{high} clones over time. Data are represented as mean ± SEM (n ≥ 3). *, $p < 0.05$ relative to MOE^{high}/Non-target^{shRNA} cells.

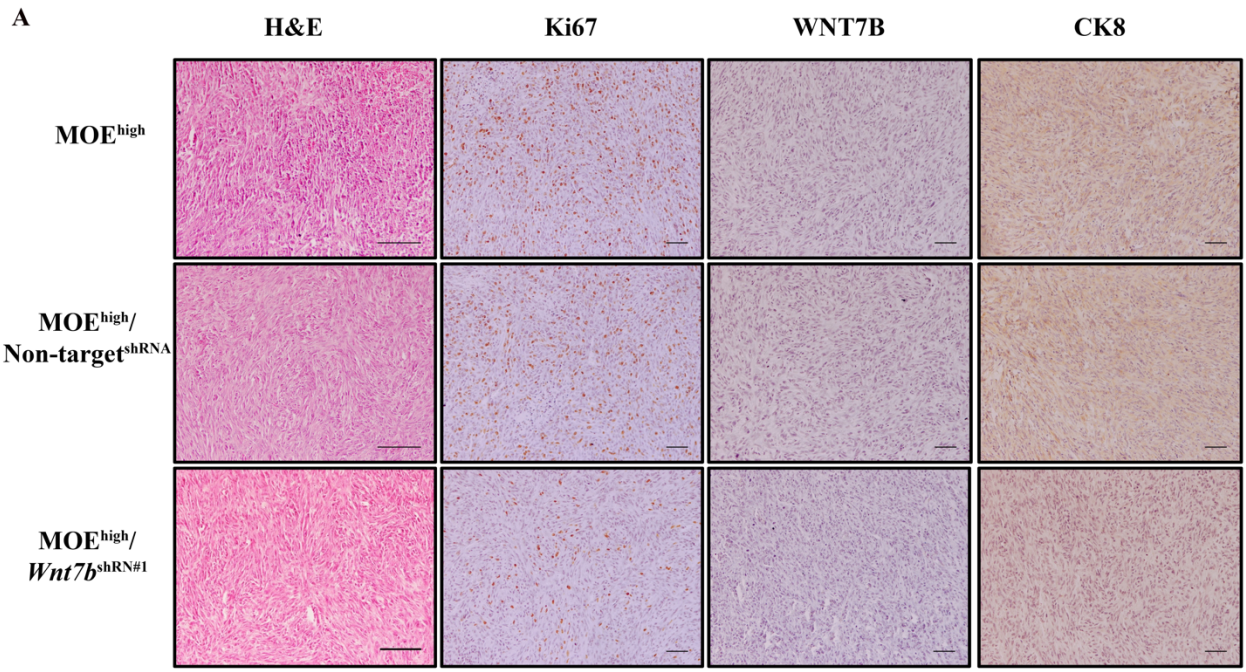

Figure 18 - WNT7B knockdown in MOE^{high} cells.

A. IHC analysis on tumors from MOE^{high}, MOE^{high}/ Non-target^{shRNA} control and MOE^{high}/*Wnt7b*$^{shRNA\#1}$ tumors**.**

WNT7B deletion in human HGSOC cells, exhibited no effect on tumor growth.

To verify if *WNT7B* deletion would be enough to limit human HGSOC tumors and to compare the effect of shRNA knockdown to deletion a CRISPR/Cas9 strategy was used to create a *WNT7B* knockout (KO) in OVCAR8^{RFP} (human HGSOC cell line) (**Fig. 19A and Table VIII**). A significant decrease in cell proliferation by 50% and >70% reduction in the number of 2D foci was measured in OVCAR8^{RFP}/WNT7B$^{-/-}$ compared to OVCAR8^{RFP} cells (**Fig. 20A and 20B and Fig. 19B**). Next, OVCAR8^{RFP}/WNT7B$^{-/-}$ and OVCAR8^{RFP} cells were injected into the subcutaneous space of the athymic nude mice. As observed previously, OVCAR8^{RFP} cells formed tumors in 35 ± 3 days (N=3) (106). At the same time points, OVCAR8^{RFP}/WNT7B$^{-/-}$ also had tumors (N=5), and there was no significant difference in the tumor burden over time (**Fig. 20C and 20D**). These results confirmed that, although *WNT7B* deletion reduced OVCAR8^{RFP} cell proliferation *in vitro,* it was not sufficient to reduce ovarian tumor burden.

TABLE VIII - SEQUENCING ALIGNMENT OF WNT7B$^{-/-}$ DELETION (UPPER SEQUENCE IS PARENTAL SEQUENCE AND THE BOTTOM SEQUENCE IS FROM GRNA TRANSFECTED CLONE).

Gene/Cell line	Sequence
WNT7B$^{-/-}$ / OVCAR8^{RFP}	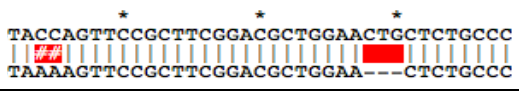

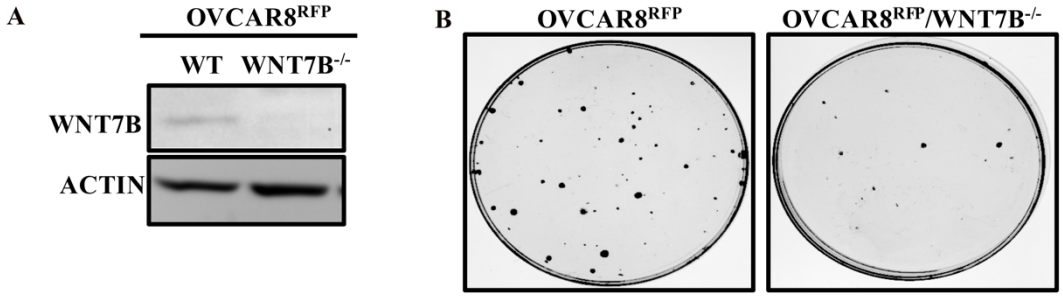

Figure 19 - WNT7B elimination in human HGSOC cells.

A. Western blot confirming the lack of WNT7b expression in OVCAR8 clone. B. Representative image of the 2D foci assay performed in OVCAR8^{RFP} and OVCAR8/*WNT7B*$^{-/-}$ clones.

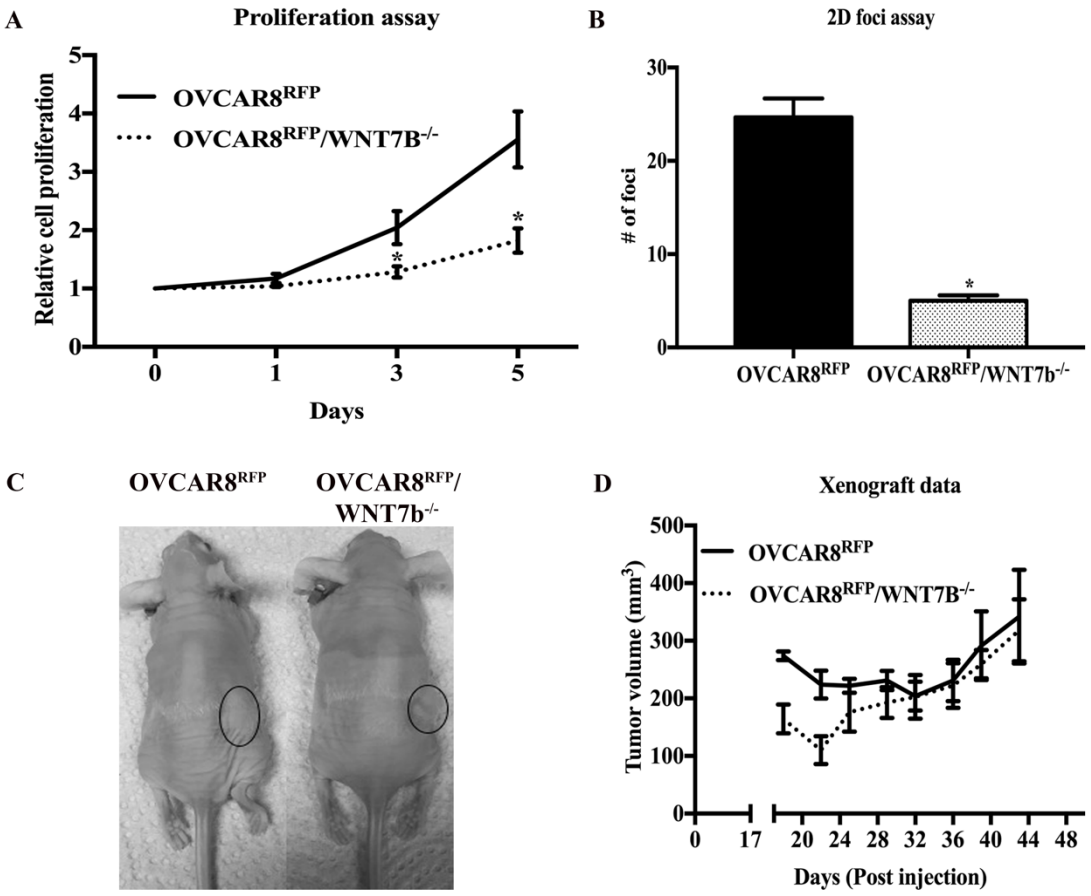

Figure 20 - While *WNT7B* deletion reduced human HGSOC cell proliferation, it does not alter the ovarian tumor burden.

A. SRB assay measured cell proliferation of OVCAR8/*WNT7B*$^{-/-}$. B. 2D foci assay quantified the number of foci. C. Picture with OVCAR8 xenografts. Black circle indicates the tumor growth. D. Tumor volume measured with calipers of OVCAR8^{WT} and OVCAR8/*WNT7B*$^{-/-}$ over time. Data are represented as mean ± SEM (n ≥ 3). *, $p < 0.05$ relative to OVCAR8 cells.

Augmentation of prolactin receptors reduces the overall survival of HGSOC patients.

The closest homolog of murine *Prl2c2* in human is the hormone prolactin (PRL). To translate the observations obtained using the murine *Prl2c2* model to human PRL and HGSOC, ovarian cancer databases were first analyzed to see if alterations in the ligand (PRL) and its receptors (PRL-R) changed the survival of patients with the disease. A transcriptomic microarray analysis from the Cancer Science Institute of Singapore (CSIOVDB) was used that compared 3,431 OVCA samples with normal OSE and FTE. The database identified a significant reduction in the overall survival of the OVCA patients with elevated expression of PRL and PRL-R (**Fig. 21A and 21B**) (149-151). The Cancer Genome Atlas (TCGA) provisional database identified an 11% and 13% amplification of PRL-R and PRL, respectively (Fig. 21C) (138,139). Additionally, high accumulation of PRL (117.6 ng/ml) was reported in the serum samples OVCA patients compared to healthy individuals (PRL – 12.5 ng/ml) (84). A tissue microarray analysis of ovarian tumors contained enriched levels of PRL-R in comparison to normal ovarian epithelial tissue (84). These analyses provided an important clue to the role of PRL and PRL-R in HGSOC.

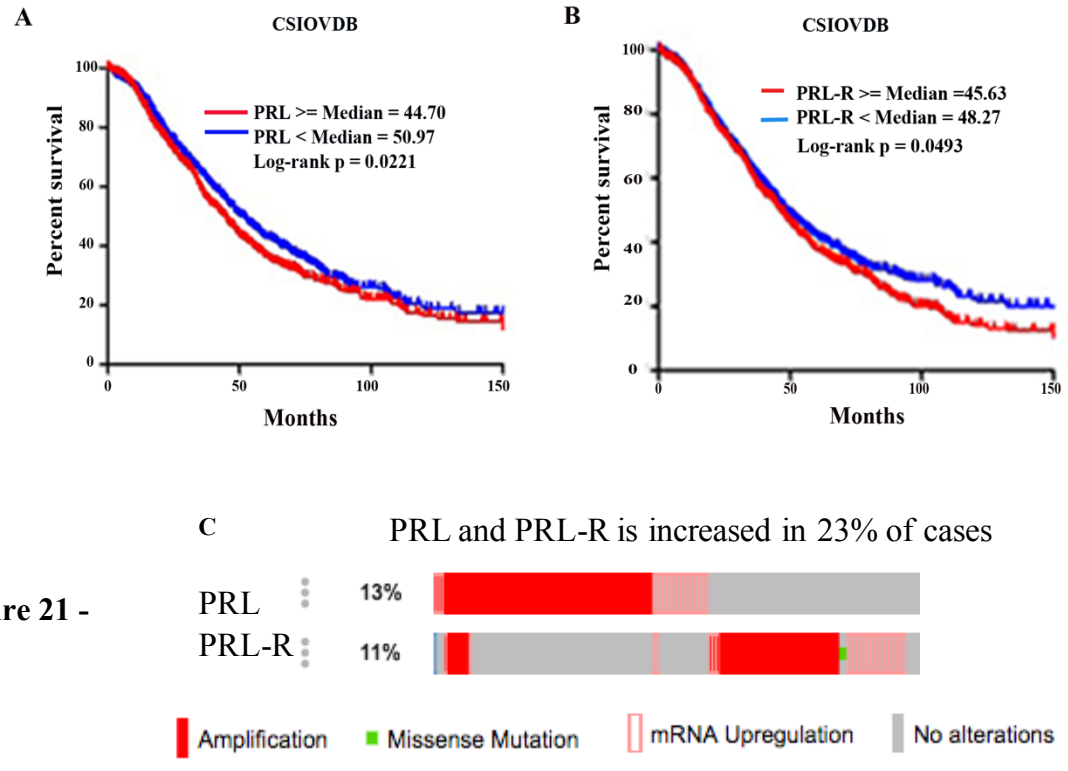

Figure 21 - PRL and PRL-R triggers expression reduced with overall survival of ovarian cancer patients.

A & B. Overall survival from CSIOVDB databases with enhanced expression of PRL and PRL-R. *p* values were obtained for comparison between any two groups, log-rank test. C. Oncoprint from TCGA database.

Chronic PRL exposure increases the cell proliferation of tumorigenic human FTE-myc and OVCA cell lines in a dose dependent manner through PRL-R.

PRL and PRL-R expression levels were first confirmed in FT33-Tag-Myc (human FTE cell line, that has been previously identified to form tumors in immunodeficient mice due to myc) (108), and in human HGSOC cell lines including OVCAR3, OVCAR4 and OVCAR8 (**Fig. 22A**). OVCAR3 and FT33-Tag-Myc strongly expressed PRL-R, while OVCAR4 and OVCAR8 had a weaker expression of PRL-R compared to other cell lines (**Fig. 22A**). By treating these cell lines with recombinant human PRL in a dose dependent manner, cell proliferation was analyzed. OVCAR8 proliferation significantly increased only at higher doses of PRL, whereas OVCAR4 did not respond to PRL exposure (**Fig. 22B**). However, the proliferation of OVCAR3 and FT33-Tag-Myc cells was significantly and dose dependently enriched after 5 days of PRL exposure compared to the vehicle control treated cells and were included in further validation (**Fig. 22B**). Since, PRL has been shown to increase 2D foci counts in OVCAR3 cells previously (84), a similar analysis with FT33-Tag-Myc cells was tested, and it indicated that recombinant PRL increased the number foci up to 200% (in 1ng/ml of PRL), and was saturated at higher doses (**Fig. 22C and 22D**). An siRNA to transiently knockdown PRL-R expression was introduced in FT33-Tag-Myc and OVCAR3 cells to identify if loss of PRL-R can reduce the cell proliferation (**Fig 23A and 23B**). Both FT33-Tag-Myc cells and OVCAR3 had a significant increase in cell proliferation by 5-fold and 2.5-fold respectively, with PRL treatment as observed before (**Fig. 23C and 23D**) and PRL-R knockdown inhibited the PRL induced cell proliferation to the extent as seen in control treatment (**Fig. 23C and 23D**). These results suggest that PRL can induce cell proliferation through its receptor in FTE-derived human HGSOC cells and HGSOC cell lines.

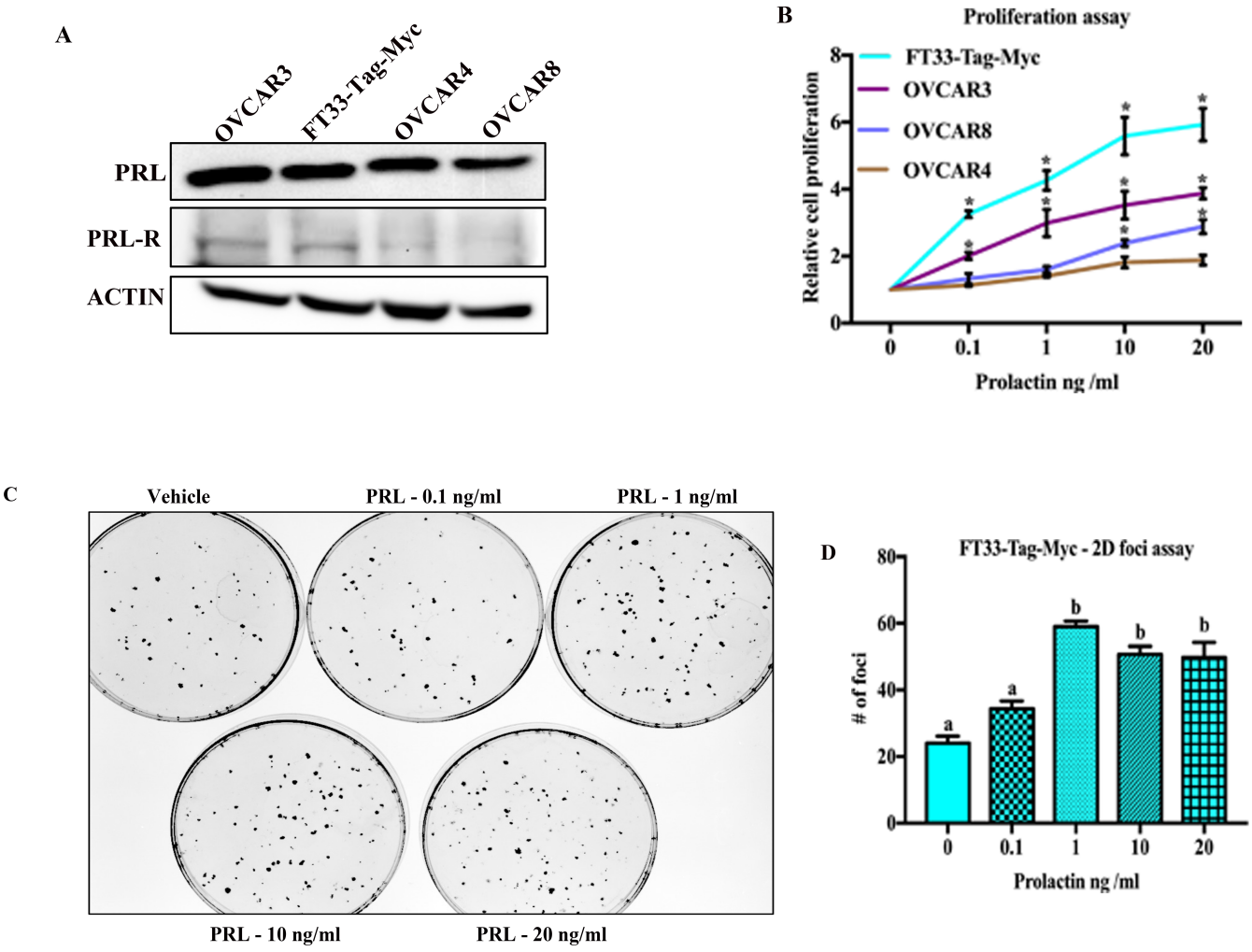

Figure 22 - PRL treatment triggers cell proliferation in human FTE and HGSOC cells.

A. Western blot image indicating the presence of PRL, PRL-R in human FTE and HGSOC cell lines. B. Cell proliferation data obtained by SRB assay on day 5 of PRL treatment. C. Representative 2D foci image. D. 2D foci of FT33-Tag-Myc cells on day 15 of PRL exposure. Data are represented as mean ± SEM (n ≥ 3). *, $p < 0.05$ and bars without common superscript are significantly different ($p < 0.05$) relative to vehicle control treatment.

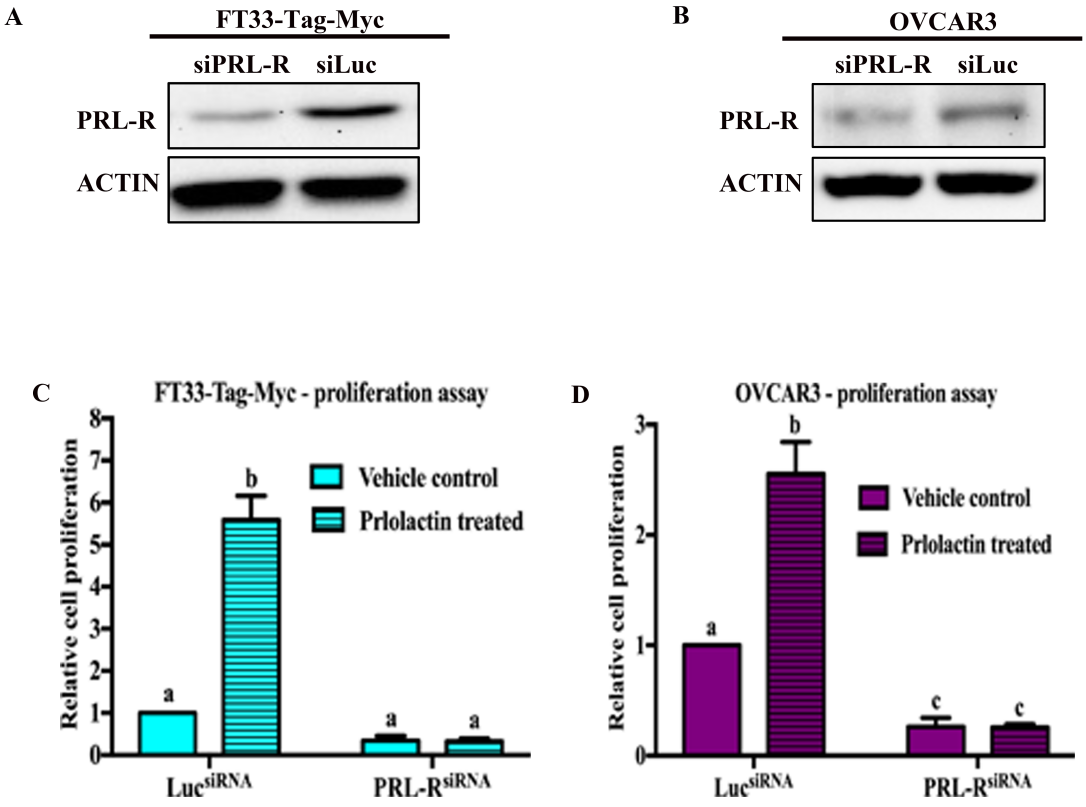

Figure 23 – PRL-R transient knockdown reduced PRL mediated cell proliferation.

PRLR expression was transiently reduced using siRNA. Western blot was performed to confirm the knockdown of PRL-R after 24 hours of siRNA transfection. A &B. Representative image of FT33-Tag-Myc cells and OVCAR3 cells with $PRLR^{siRNA}$ and Luc^{siRNA}. Actin was used as western blot loading controls. After 24 hours of transfection, PRL was added at a concentration of 10 ng/ml and SRB assay was performed after 3 days with FT33-Tag-Myc cells (C) or OVCAR3 cells (D). Data are represented as mean ± SEM ($n \geq 3$). *, $p < 0.05$ and bars without common superscript are significantly different ($p < 0.05$) relative to Luc^{siRNA} transfection.

CRISPR/Cas9-mediated PRL-R knockout blocks FTE cell proliferation, while constitutive activation stimulates FTE proliferation.

To identify if changes in the PRL-R levels will affect the human FTE proliferation rate, a plasmid containing constitutively active PRL-R (PRL-R_{CA}) that was previously reported to activate PRL signaling in cellular models (152,153), and an empty vector construct (control) was stably transfected into FT33-Tag-Myc cells (**Fig. 24A**). A 30% increase in cell proliferation and 2D foci was detected in the FT33-Tag-Myc/PRL-R_{CA} clone compared to FT33-Tag-Myc/$Neo^{control}$ cells (**Fig. 25A, 25B and 24B**). As further validation, a CRISPR/Cas9-mediated PRL-R KO was made in FT33-Tag-Myc cells (**Fig. 24C and Table IX**). A significant reduction in cell proliferation by 50% and number of 2D foci (40%) in the FT33-Tag-Myc/PRL-$R^{-/-}$ clone was measured as compared to control cells (**Fig. 25C, 25D and 24D**). PRL-R signaling can augments proliferation and its inactivation blocks prolactin-stimulated cell growth in human FTE tumor cells.

TABLE IX - SEQUENCING ALIGNMENT OF PRL-R DELETIONS (UPPER SEQUENCE IS PARENTAL SEQUENCE AND THE BOTTOM SEQUENCE IS FROM THE GRNA TRANSFECTED CLONE).

Gene/Cell line	Sequence
PRL-$R^{-/-}$/ FT33-Tag-Myc	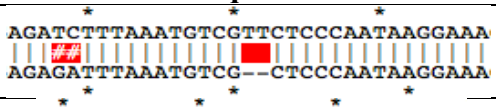
PRL-$R^{-/-\#1}$/ OVCAR3	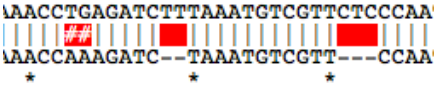
PRL-$R^{-/-\#2}$ / OVCAR3	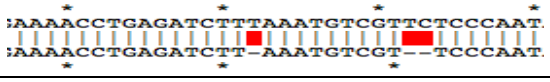

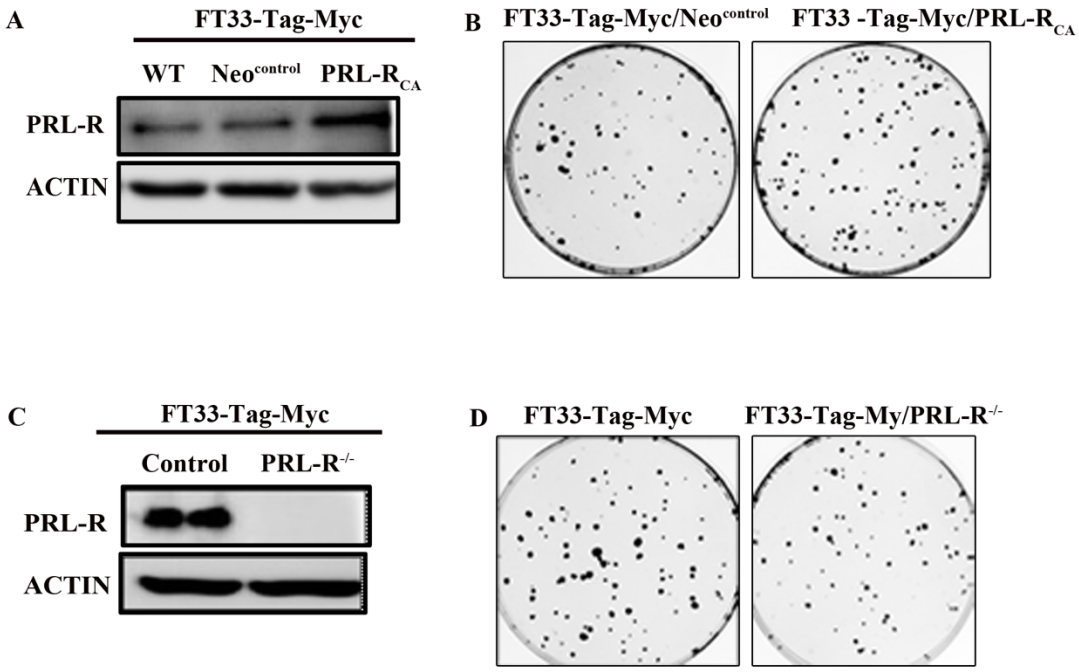

Figure 24 - PRL-R_{CA} and PRL-$R^{-/-}$ validation in FT33-Tag-Myc cells.

A. Western blot image indicating the levels of PRL-R in FT33-Tag-Myc control and PRL-R_{CA} clone. B. Representative image of the 2D foci assay performed on FT33-Tag-Myc plasmid control and PRL-R_{CA} (constitutively active) clone. C. Western blot image of PRL-R in FT-33-Tag-Myc cells control and PRL-$R^{-/-}$ clone. D. Representative image of the 2D foci assay performed on FT33-Tag-Myc control and PRL-$R^{-/-}$ clone. Actin was used as western blot loading controls.

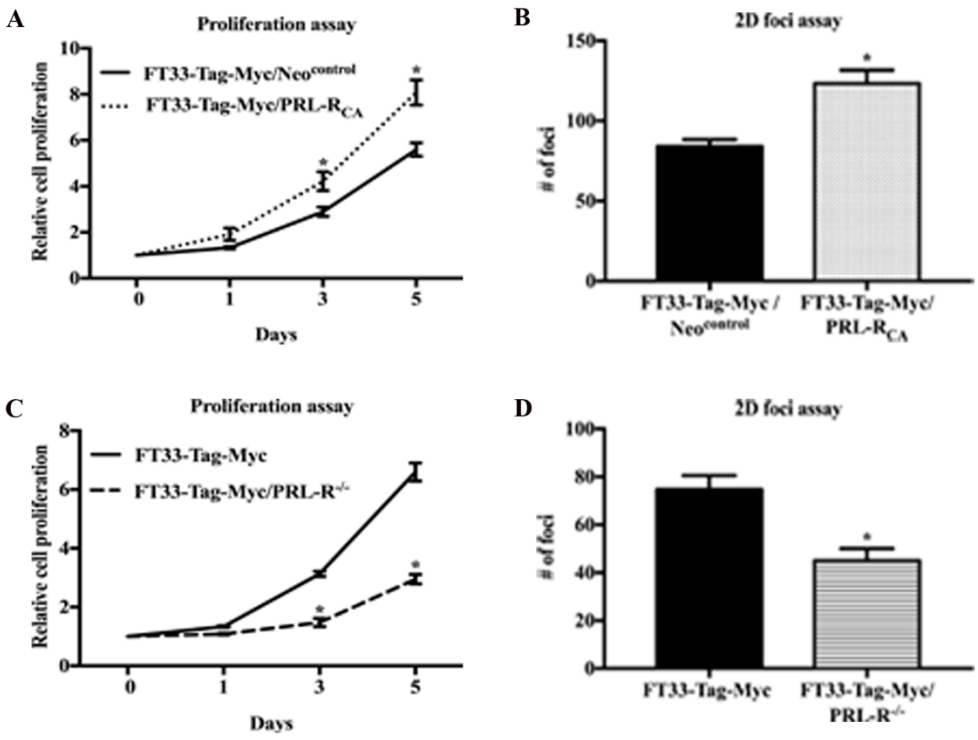

Figure 25 - CRISPR/Cas9 mediated PRL-R$^{-/-}$ blocks cell proliferation in human FTE cells.

A. SRB assay measured the cell proliferation over time. B. 2D foci assay graph with quantified number of foci in FT33-Tag-Myc/PRL-R$_{CA}$ (constitutively active) clone and vector control. C. Relative cell proliferation was measured by SRB assay on FT-33-Tag-Myc and FT33-Tag-Myc/PRL-R$^{-/-}$ clone over days. D. 2D foci assay graph with quantified number of foci in FT33-Tag-Myc/PRL-R$^{-/-}$ clone and control. Data are represented as mean ± SEM (n ≥ 3). *, $p < 0.05$ relative to control cells.

PRL-R deletion blocks the tumor formation in OVCAR3 cells.

Next, to uncover the critical role of PRL-R in HGSOC tumorigenesis, a CRISPR/Cas9-guided PRL-R KO was made in OVCAR3 cells (**26A and Table IX**). A significant reduction in cell proliferation and 2D foci in $PRLR^{-/-\#1}$ and $PRLR^{-/-\#2}$ cells by >70% and >50% respectively, was observed compared to its parental cells (**Fig. 27A, 27B and 26B**). OVCAR3 cells were previously identified to form subcutaneous tumors in mice (106). To evaluate if PRL-R deletion, could reduce tumor burden in OVCAR3 cells, OVCAR3/$PRL\text{-}R^{-/-\#1}$ and OVCAR3/$PRL\text{-}R^{-/-\#2}$ cells were injected subcutaneously in athymic nude mice ($1x10^6$ cells/mice, N=5). Similar amount of OVCAR3 cells were injected as control groups, (N=5). All the mice in control groups formed tumors, but no tumors were detected in mice models injected with $PRL\text{-}R^{-/-}$ clones (**Fig. 27C**). At humane endpoints for controls (35±5 days) mice were sacrificed. These findings indicate that PRL-R deletion can significantly inhibit the tumor formation in HGSOC models.

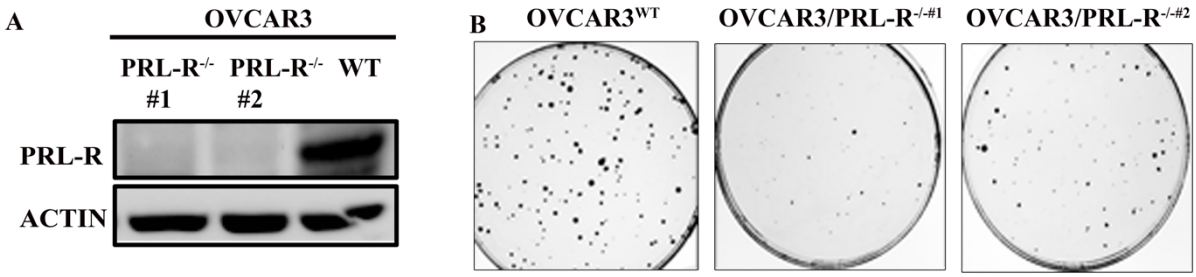

Figure 26 - $PRL\text{-}R^{-/-}$ reduces cell proliferation in OVCAR3 cells.

A. Western blot confirming the lack of PRL-R protein in OVCAR3/$PRLR^{-/-}$ clones. B. Representative image of the 2D foci assay performed on OVCAR3 control & $PRL\text{-}R^{-/-}$ clones. Actin was used as western blot loading controls.

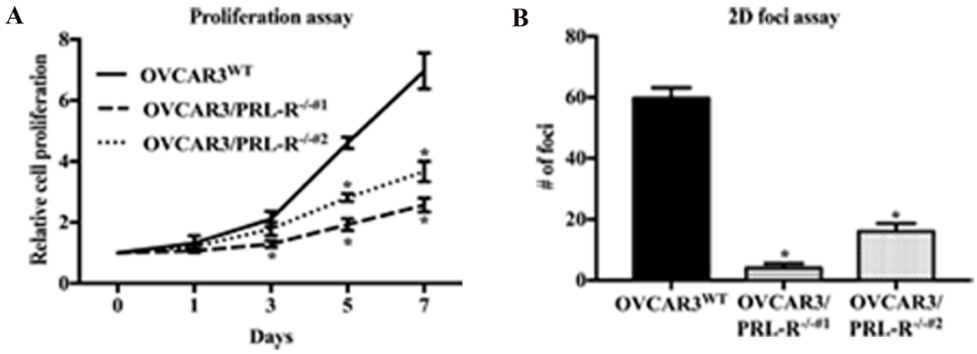

C OVCAR3 xenograft

S.No	Cell line	Tumor take
1	OVCAR3^{WT}	4/5
2	OVCAR3/PRLR$^{-/-\#1}$	0/5
3	OVCAR3/PRLR$^{-/-\#2}$	0/5

Figure 27 - PRL-R$^{-/-}$ blocks tumor formation in OVCAR3 cells.

A. Cell proliferation data of OVCAR3 cells control and PRL-R$^{-/-}$ clones. B. 2D foci assay after 15 days. C. Table indicating the tumor take rate in OVCAR3 xenografts models. Data are represented as mean ± SEM (n ≥ 3). *, $p < 0.05$ relative to control cells.

PRL-induced proliferation is mediated by increased phosphorylation of ERK, AKT, STAT5 and mTOR.

Although increased PRL exposure has been previously shown to activate proteins and kinases, such as STAT5 and MAPK, in cancer (104,154), its effect in FTE-derived human HGSOC is underexplored. Hence, OVCAR3 cells were treated with recombinant prolactin, and phosphorylation of kinases was analyzed using a phosphokinase array. Several proteins including MSK1/2, AKT, TOR, STAT5, p70S6, WNK1 and GSK-3a/b was phosphorylated at critical Ser/Thr/Tyr residues in PRL treated cells compared to the control treatment (**Fig. 28A, 28B and 28C**). Additionally, PRL treatment induced the phosphorylation of β-catenin and p53 (**Fig. 28A, 28B and 28C**). A hypothetical signaling mechanism of PRL in inducing HGSOC proliferation was predicted, based on the phosphokinase array results and previously published data (**Fig. 29A**) (104,155). Western blotting confirmed, that PRL phosphorylated ERK, AKT, STAT5 and mTOR in OVCAR3 and FT33-Tag-Myc cells within 30 minutes of exposure (**Fig. 29B and 29C**).

To test the hypothetical PRL signaling in HGSOC, inhibitors for MEK, AKT, STAT5, mTOR, and players in canonical WNT signaling (including β-catenin), were added to OVCAR3 and FT33-Tag-Myc cells with and without PRL, and cell proliferation was assessed. A significant increase in cell proliferation with PRL alone was confirmed compared to the DMSO treated control cells (**Fig. 30A and 30B**). The cell proliferation was suppressed by the inhibitors to the level as seen in the control treatment in the presence and absence of PRL (**Fig. 30A and 30B**). Interestingly, PRL addition increased the cell proliferation by 1.5-fold in the β-catenin inhibitor treated OVCAR3 and FT33-Tag-Myc cells (**Fig. 30A and 30B**). These results found critical clues to PRL signaling, that PRL mainly induced the aberrant cell proliferation by activating AKT, STAT5 ERK and m-TOR signaling in human FTE and HGSOC cells.

A

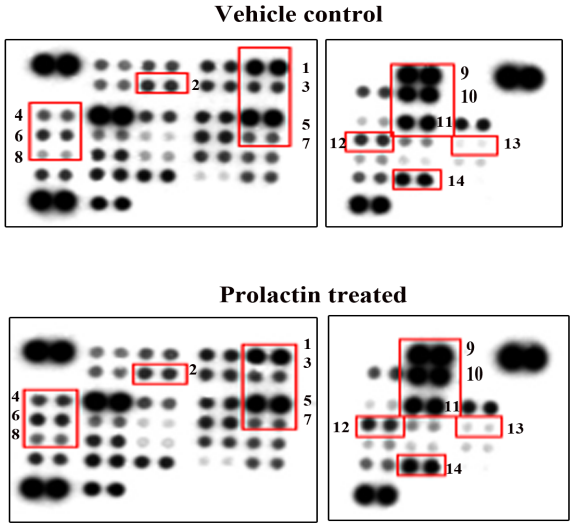

B

Number in the blot	Protein
1	GSK-3a/b (S21/S29)
2	MSK1/2 (S376/S360)
3	AKT1/2/3 (S473)
4	TOR (S2448)
5	B-Cat
6	Src (Y419)
7	Stat5a (Y694)
8	Fyn Y420)
9	p53 (S392)
10	p53 (S46)
11	p53 (S15)
12	p70 S6 kinase (T421/S424)
13	eNOS (S1177)
14	WNK1 (T60)

C

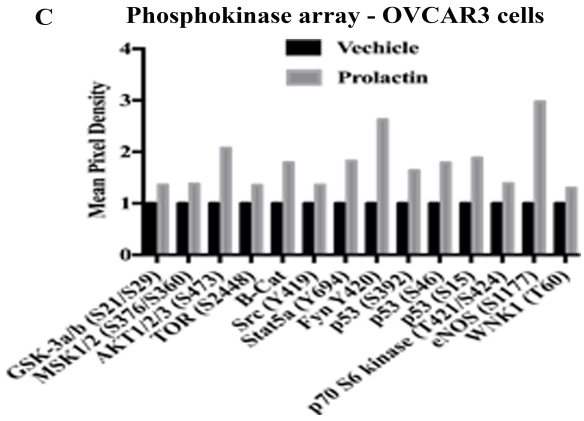

Figure 28 - Human phosphokinase array with PRL treatment in OVCAR3 cells.

A. Dot blot analysis image of OVAR3 cells with vehicle control and PRL treatment for 30 minutes. Red box indicates the duplicate spots of different proteins B. Table indicating the proteins that were phosphorylated with PRL exposure, the number in the table is matched with the number allotted in the blot image in A panel. C. Human phosphokinase array identified phosphorylated proteins in OVCAR3 cells.

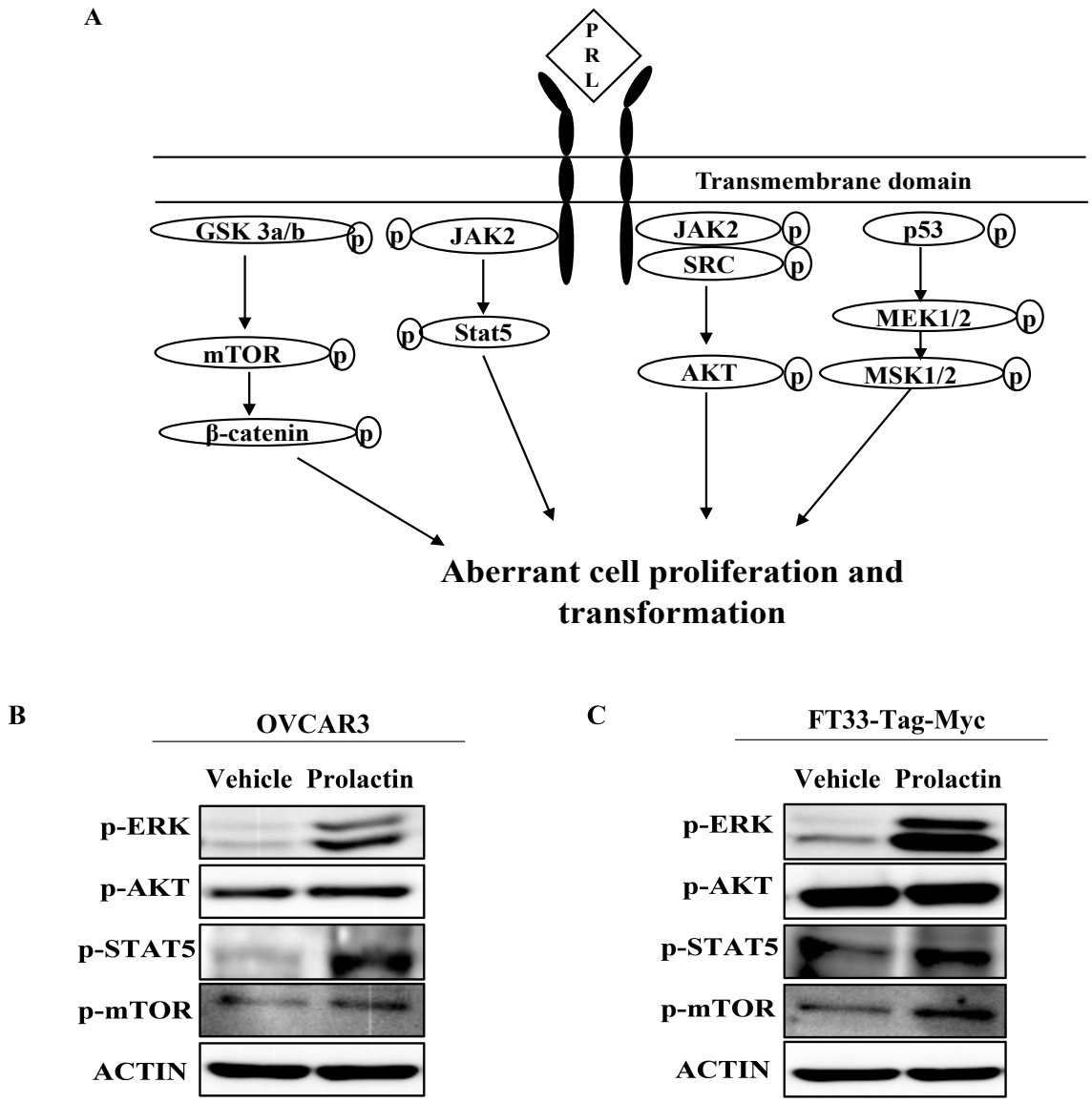

Figure 29 - PRL exposure induces phosphorylation of many growth pathways in human FTE and FTE-derived HGSOC cells.

A. Hypothetical signaling of PRL in ovarian cancer. B&C. Western blotting confirmed the phosphorylated proteins post 30 minutes of PRL treatment. Data are represented as mean ± SEM (n≥3). Actin is used as a loading control.

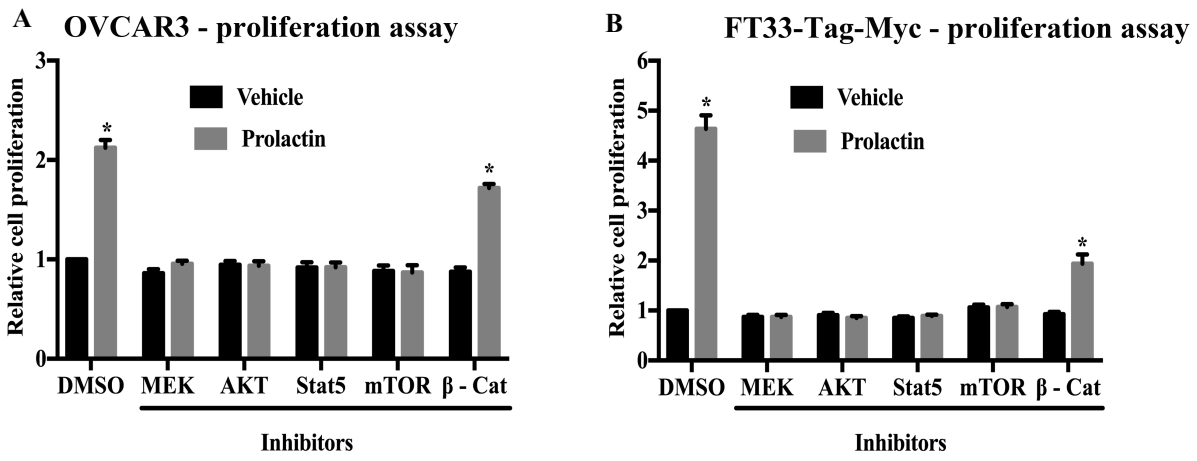

Figure 30 - PRL treatment induces cell proliferation by activating AKT, STAT5 ERK and m-TOR signaling in human FTE and HGSOC cells.

A&B. SRB assay measured cell proliferation changes with PRL and inhibitors. Data are represented as mean ± SEM (n≥3). *, $p < 0.05$ relative to control.

C. DISCUSSION

Overexpression of PRL and its signaling through the PRL-R enhances cell proliferation, colony formation, and tumor formation, while the loss of PRL-R blocks these effects. We identified that PRL primarily signals through activation of AKT, STAT5, m-TOR and MEK and induces abnormal cell proliferation and transformation in FTE cells, which likely give rise to HGSOC, and in HGSOC cells. The enhanced expression of PRL homolog, *Prl2c2*, in a murine spontaneous model of fallopian tube-derived cancer led us to investigate PRL in in human HGSOC (3).

The spontaneous FTE derived model, mimicked ageing related changes that can occur in women and provided many novel targets, that can be investigated in ovarian cancer pathogenesis (3). This study selected to evaluate the role of *Prl2c2* and *Wnt7b*, which were both in the top ten significantly modified transcripts in the RNAseq obtained from the spontaneous model. *Prl2c2* was identified to be a critical regulator of cellular proliferation, malignant transformation and tumor growth. Although *prl2c2* is not expressed in humans, it belongs to the PRL family of proteins that share similar structure and function in human reproduction and cancer (156). Hence, it is important to note that our study relates to human fallopian tube cancer based on PRL, and not *Prl2c2*, which is not in the human genome.

Significant attention has focused on evaluating the role of PRL in cancer. Serum PRL and its receptor levels increase in OVCA, leading to its inclusion as a significant component of a previously-used OVCA screening kit called Ovasure (88). However, the presence of PRL in the serum does not address if this is a biomarker of cancer or a driver or tumorigenesis. Recently, PRL was re-tested along with seven other proteins and found to be an efficient diagnostic marker for screening OVCA with BRCA1 mutation (157). However, the expression of PRL and its regulation

of FTE cells reamins relatively unknown. This study found that human FTE and most HGSOC expressed PRL and PRL-R. Previous studies found that chronic PRL exposure induced malignant transformation of immortalized OSE cells, which is no longer considered the major progenitor of serous ovarian cancers (84). Our study focused on FTE – derived OVCA, and used OVCAR3 cells (predicted to be FTE-like) (158). Although, the protein signature in OVCAR3 cells is similar to FTE cells, it was not completely identical, hence human FTE cells (FT33-Tag-Myc cells) were included (108). Our observations identified that OVCAR3 and FT33-Tag-Myc, proliferated significantly higher in response to PRL. PRL-R elimination completely abrogated OVCAR3 tumor growth in mice models, which supports the design of molecules to antagonize PRL signaling in ovarian cancer.

Previously, PRL exposure had been found to activate STAT3, ERK and RAS in gynecological cancer cells, but there could be tissue specific activation of many kinases after PRL treatment (104). By performing a phosphokinase array with OVCAR3 cells exposed to PRL, phosphorylation of critical proteins including AKT, STAT5, m-TOR, MSK1/2 and β-catenin was identified. Blocking these kinases in both OVCAR3 and FT33-Tag-Myc cells, PRL signaling in stimulating the cellular proliferation and transformation in human fallopian tube derived tumor cells and in HGSOC cells was identified. PRL accumulation can inhibit the tumor suppressive activity of p21 in breast cancer cells by translocating p-STAT5 into the nucleus and by forming an inhibitory complex with BRCA1 (most common mutated tumor suppressor in ovarian cancer) (159). Although this study identified the importance of PRL-mediated STAT5 phosphorylation in cell proliferation, its ability to inhibit p21 activity was not tested.

Local accumulation of PRL-amplifies canonical WNT signaling and triggers the increase in the cancer stem-like progenitors in neu-related lipocalin (NRL) – PRL transgenic breast cancer

mice models (89). While, PRL treated OVAR3 and FT33-Tag-Myc cellular proliferation was induced, in the presence of a canonical WNT inhibitor, PRL direct activation of canonical WNTs was not explored. Importantly, we identified novel serine residues in p53 (S15, S46, and S392), that were phosphorylated post-PRL treatment. These p53 residues had been shown earlier to stabilize the p53 protein levels (early precursors of HGSOC) and to increase resistance against chemotherapeutics (160). It would be interesting to further investigate the biological link between PRL and p53 phosphorylation, which may provide novel targets to increase chemosensitivity of ovarian tumors.

This study also attempted to validate the role of WNT7b in mediating ovarian tumors from the FTE. Our findings revealed that increased WNT7B potentiated cell proliferation *in vitro*; however, both suppression and elimination of WNT7B was not sufficient to block tumor burden in both murine and human ovarian cancer models *in vivo*. All WNTs are secreted proteins and possess high structural similarity (161). Hence, we speculate that in the MOE^{high} model, the knockdown of WNT7B could have been rescued by other functional WNTs, such as WNT7A.

In the human HGSOC model, the murine WNT7B produced *in vivo* could have restored the functional knockout of human WNT7B in the cell line. Another possibility could be that while WNT7B had a critical function in abnormal cell proliferation and was elevated in malignant cancers, its cellular partner WNT7A may have additional unknown mechanism that could trigger tumor formation. Both MOE^{high} and the human HGSOC models used in this study had high levels of WNT7A. In support of this prediction, an earlier study identified that WNT7A knockdown alone resulted in reduced tumor burden using xenografts of ovarian cancer (105). Hence, WNT7B knockdown may have to be combined with other WNTs suppression in order to reduce ovarian tumor burden and this needs further testing.

Until now, PRL was only identified as a diagnostic marker for screening OVCA. However, this study for the first time, report that PRL is expressed and mediates tumors in human FTE. Small molecules were identified to block PRL-R activity and thereby providing a novel strategy, which with further clinical validation can be used to prevent HGSOC tumor formation from fallopian tube.

V. MOLECULAR MECHANISMS CONTRIBUTING TO PERITONEAL SPREAD OF A SPONTANEOUS MURINE MODEL OF FALLOPIAN TUBE DERIVED CANCER

A. INTRODUCTION

HGSOC is a rapidly metastasizing histotype of ovarian cancer and it can originate from the FTE (4). Techniques like transvaginal scan, that measures ovarian size to screen for ovarian cancer, are ineffective for screening HGSOC histotype, since the disease has typically spread to pelvic sites when ovarian enlargement is found (4). The ACS reports that the survival rate of ovarian cancer patients is >70% if tumors can be detected before metastasis (162). Hence, identifying novel targets that induces HGSOC peritoneal dissemination would be very significant to prevent or reverse HGSOC metastases.

A spontaneous model of FTE derived ovarian cancer was developed by serially passaging the oviductal epithelial cells from outbred CD1 mice (MOE^{high}) (3). The MOE^{high} cells were highly proliferative compared to the parental cells (MOE^{low}) (3). However, MOE^{high} cell migration was not altered and did not form metastatic tumors in athymic nude mice. MOE^{high} cells expressed a significantly modified transcriptome compared to control cells that was concordant with ovarian cancer. Importantly, three characteristics that were unlike HGSOC were the lack of a p53 DNA binding mutation, abundant PAX2 expression and enhanced $p19^{ARF}$, all of which may block metastasis and explain the lack of peritoneal disease from this model (3). Instead, MOE^{high} cells contained a splice variant of p53, that lacked the last 23 amino acids, which are critical for MDM2 mediated ubiquitination; therefore, MOE^{high} cells had stable p53 protein by western blotting. The splice variant of p53 displayed mutant p53 functions by inducing FOXM1 (usually repressed by

$p53^{WT}$), repressed p21 and THBS1 (both are positively regulated by $p53^{WT}$). Additionally, p53 splice variant also exhibited $p53^{WT}$ function by inducing IGFBP3 levels, indicating a mixed role of p53 splice variant as $p53^{WT}$ and mutant p53 (3).

96% of HGSOC contain a mutation in the DNA binding domain of p53 (1). The R273H mutation in p53 is the most common mutation observed in human ovarian cancer samples (48). The R273H mutation in mouse models increased tumor invasion of Li-Fraumeni disease (50). Although, a tissue specific transgenic mice model with $p53^{R273H}$ did not lead to ovarian tumors, it increased the FTE migration (2). R273H mutation primarily induced SLUG and FOXM1 which are identified as key drivers of tumor progression in many cancers (2). Therefore, p53 mutation alone is not sufficient to form tumors but, it is critical for cell migration. Transcriptome profiling of MOE cells with $p53^{R273H}$ mutation revealed pro-migratory pathways as a significantly altered pathway compared to the control cells (2). The objective was to test the hypothesis that stable expression of a p53 DNA binding mutation (R273H) in MOE^{high} cells would stimulate cell migration and thereby permit intraperitoneal metastases.

PAX2 is a transcription factor, belongs to the paired homeobox domain protein family, and is regulated by p53 mutations (163). A SCOUT (secretory cell outgrowth) is predicted to be the earliest change in HGSOC progression from FTE, which is defined as the loss of PAX2 expression. When SCOUTS acquire a p53 mutation, they progress into to serous tubal intraepithelial carcinoma (STICs) (164). PAX2 is not present in most of HGSOC tissues (164). A stable knockdown of PTEN, a tumor suppressor gene, in MOE cells formed serous intraperitoneal ovarian cancer in mice models (38). However, PAX2 re-expression reduced PTEN deletion mediated tumor burden (163). These findings indicated that PAX2 in has a tumor suppressor like function in HGSOC metastases. MOE^{high} cells had a surprising high expression of PAX2, which

is not typically associated with FTE-derived HGSOC. Therefore, we predicted that deletion of PAX2 in MOE^{high} cells could increase the metastatic behavior of the cell model.

FOXM1 belongs to a large family of forkhead box (FOX) transcription actors. FOXM1 expression is induced in many proliferative tumors including, breast, lung and ovary, due to a mutation in p53 or loss of wild type p53 function (133). FOXM1 signaling is amplified in >80% of ovarian cancer (165). Overexpression of FOXM1 in various tumors indicates a strong dependence on FOXM1, and that is explained partly by its role in cell proliferation (166). The alternative reading frame ($p19^{ARF}$) tumor protein is induced in response to oncogenic stimuli and prevents abnormal cell proliferation through a p53-dependent cell-cycle arrest by increasing the stability of p53 through nucleolar targeting of the p53 ubiquitin ligase protein MDM2 (167). Loss of ARF increases FOXM1and thereby tumor invasion. A synthetic ARF peptide blocked FOXM1 function, causing apoptosis of liver cancer cells, and inducing angiogenesis (168). ARF peptide was sufficient to sequester FOXM1 to the nucleolus and subsequently inhibit its transcriptional activity (168). MOE^{high} cells showed increased expression of $p19^{ARF}$ and FOXM1 in absence of p53 mutation compared to MOE^{low} cells (3). We predicted that $p19^{ARF}$ was sequestering FOXM1 resulting in loss the of FOXM1 transcriptional activity, which therefore hindered metastases in the MOE^{high} cells.

B. RESULTS

$p53^{R273H}$ mutation increases cell migration of MOE^{high} cells.

MOE^{high} cells were highly proliferative, with no change in migration and formed non-metastatic tumors. RNA sequencing detected a lack of p53 DNA contact mutant, like R273H,

which was previously proven to increase FTE migration and is thought to be critical to disease formation (2,3). To test the hypothesis that $p53^{R273H}$ mutation is critical for MOE^{high} cell migration and to form intraperitoneal tumors, a stable transfection of a construct encoding $p53^{R273H}$ was made in MOE^{high} cells ($MOE^{high}/p53^{R273H}$). Western blotting measured stabilized human p53 protein and induction in key pro-migratory targets including SLUG and DCN in $MOE^{high}/p53^{R273H}$ compared to the stable vector control transfected cells ($MOE^{high}/Neo^{control}$) that lacked SLUG and DCN expression (**Fig. 31A**). Confirming, the protein data, qPCR measured decreased MDM2, increased SLUG and DCN mRNA (**Fig. 31B**).

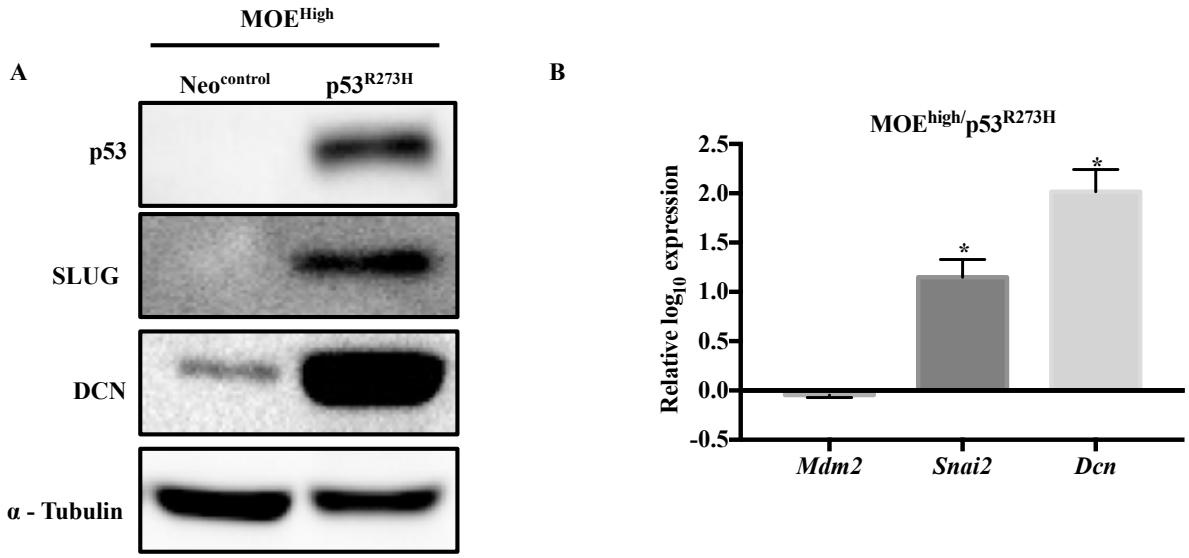

Figure 31 – Stable $p53^{R273H}$ induces the expression of pro-migratory genes in MOE high cells.

A. Western blot with induced SLUG, DCN and p53 expression. α - Tubulin is a loading control. B. qPCR measured reduced *Mdm2* and confirmed increased *Snai2* and *Dcn* mRNA levels. Data are represented as mean ± SEM (n≥3). *, $p < 0.05$ relative to control.

Scratch assays confirmed a >40% significant increase in $MOE^{high}/p53^{R273H}$ cell migration compared to the control cells (**Fig. 32A**). To confirm the increased cell migration using another assay, the automated xCELLigence assay (a real time cell assay that uses gold microelectrodes embedded in the bottom of the microtiter to non-invasively monitor cell status including cell migration) was performed. $MOE^{high}/p53^{R273H}$ significantly migrated 1.5-fold higher after 24 hours compared to the $MOE^{high}/Neo^{control}$ cells (**Fig. 32B**). Cell proliferation was analyzed in $MOE^{high}/p53^{R273H}$ cells in order to test changes in the proliferation rate by $p53^{R273H}$ expression. SRB assay that monitors cell proliferation, measured no significant change in proliferation and by 2D assay, no alteration in foci formation was observed in $MOE^{high}/p53^{R273H}$ compared to its control cells (**Fig. 33A and 33B**). Further validation would need to evaluate if $MOE^{high}/p53^{R273H}$ cells form intraperitoneal tumors in female athymic nude mice by xenografting $1*10^7$ cells into the intraperitoneal space. Small molecules that degrade $p53^{R273H}$ could be administered in MOE^{high} cells to confirm if it could reverse the cell migration. These studies could also be performed using HGSOC models, for example OVCAR5 (a $p53^{null}$ human HGSOC cell line). These results would collectively reveal the critical role of p53 mutation alone in the migration of malignantly transformed FTE cells to ovary and to the intraperitoneal cavity.

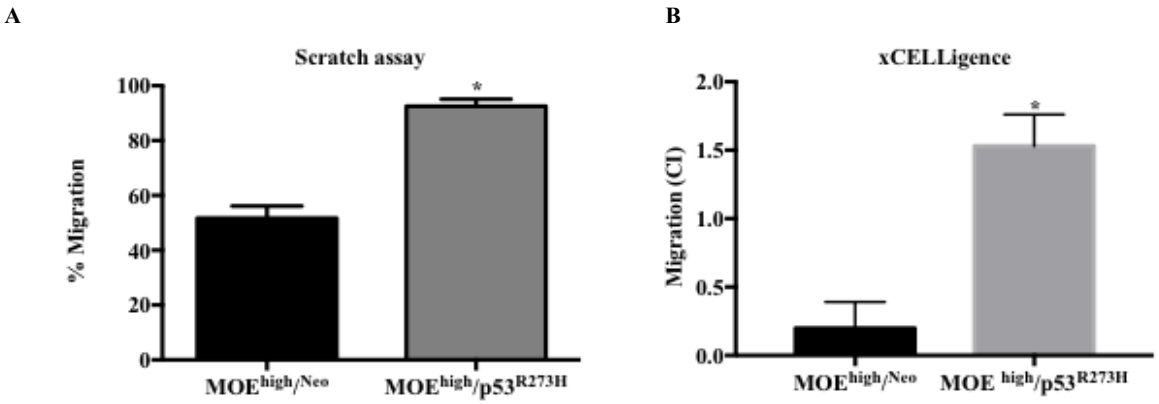

Figure 32 – p53^{R273H} stimulates cell migration in MOE high cells.

A. Scratch assay B. Migration measured using automated xCELLigenece. Data are represented as mean ± SEM (n≥3). *, $p < 0.05$ relative to control.

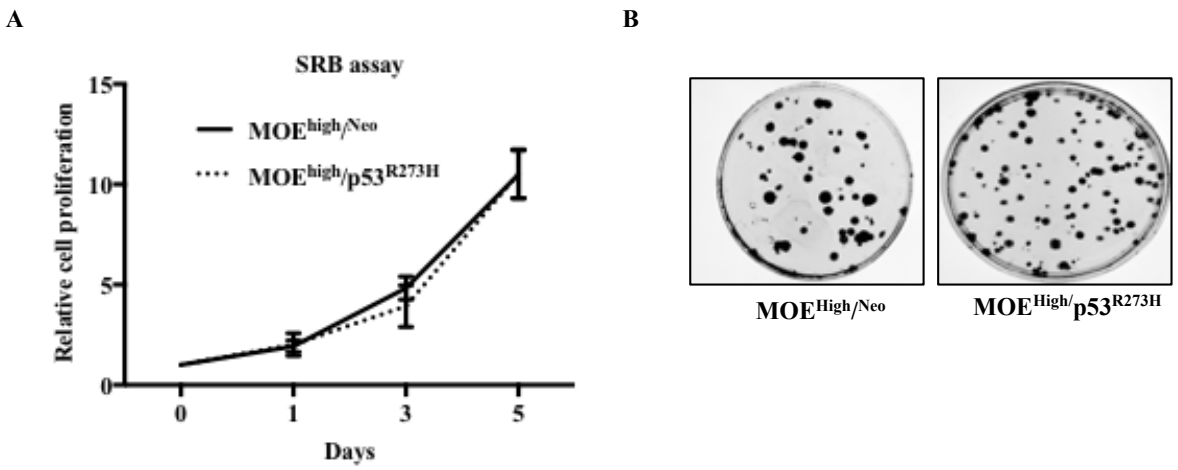

Figure 33 – p53^{R273H} did not alter MOE high proliferation.

A. SRB assay B. 2D foci image. Data are represented as mean ± SEM (n≥3).

p19^{ARF} suppression moderately increases cell migration of MOE^{high} cells.

MOE^{high} cells contained enriched levels of p19^{ARF} compared to MOE^{low} cells (3). In order to test the prediction that p19^{ARF} was blocking FOXM1 activity to block MOE^{high} tumor metastasis, shRNA was used to mediate p19^{ARF} knockdown in MOE^{high} cells (MOE^{high}/p19^{ARFshRNA}). Western blot confirmed more than 50% significant reduction of the p19^{ARF} protein in the MOE^{high}/p19^{ARFshRNA} stable clones compared to empty vector control transfected cells (MOE^{high}/puro^{control}) (**Fig. 34A**). Scratch assays identified only a slight increase (≈10%) in MOE^{high}/p19^{ARFshRNA} cell migration compared to the control cells (**Fig. 34B**). To observe for changes in cell proliferative phenotype, SRB and 2D foci assay was performed on MOE^{high}/p19^{ARFshRNA} cells. There was no significant change in cell proliferation and 2D foci formation was detected in MOE^{high}/p19^{ARFshRNA} cells compared to the control cells (**Fig. 34C and 34D**). These findings indicated that although, p19^{ARF} is suppressed, a p53 mutation might be required to induce FOXM1 mediated migration in ovarian tumor metastasis.

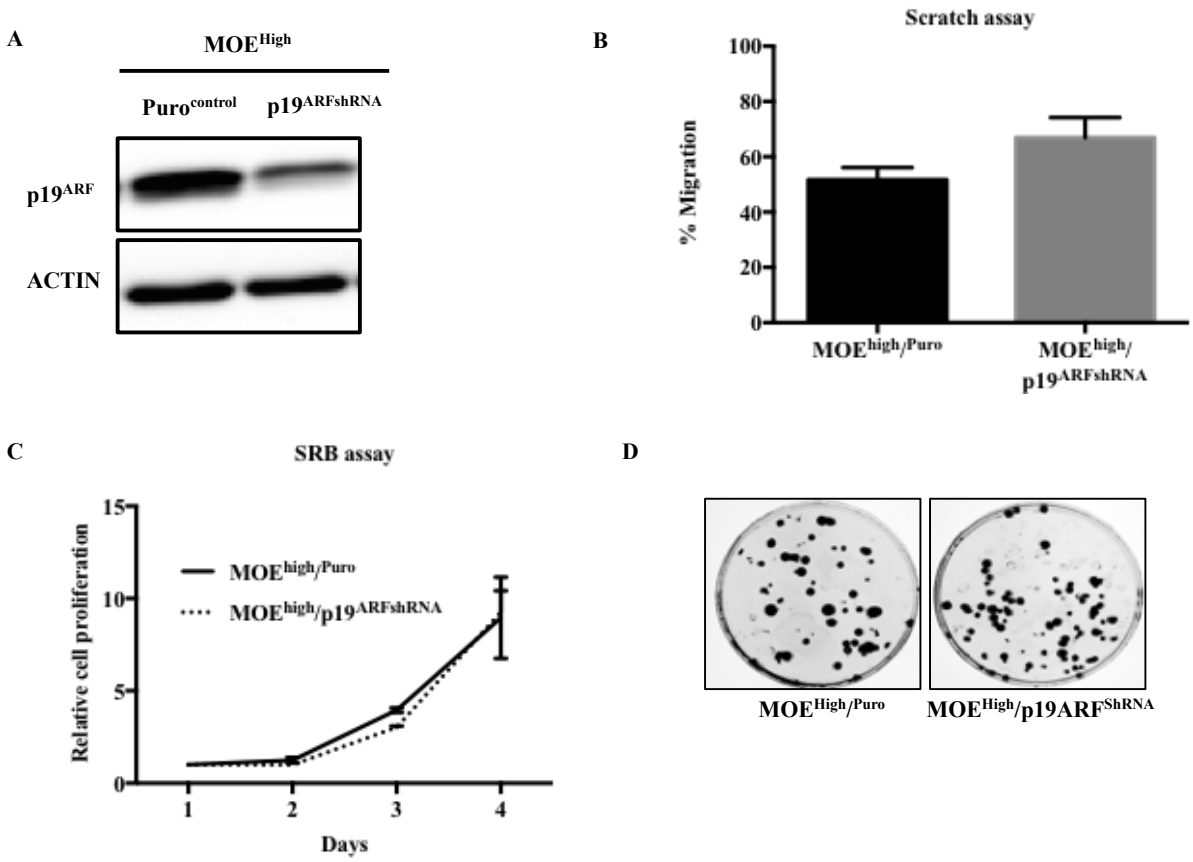

Figure 34 – p19^{ARF} knockdown moderately increased MOE high migration.

A. Western blot image measuring ARF knockdown. B. Cell migration by scratch assay. C. Cell proliferation by SRB assay B. 2D foci image. Data are represented as mean ± SEM (n≥3).

PAX2 deletion in MOE^{high} cells.

PAX2, a transcription factor, is lost in HGSOC, and it's loss has been hypothesized to increase cell migration and tumor invasion (163). MOE^{high} cells had enhanced levels of PAX2 compared to MOE^{low} cells, which was unexpected (**Fig. 35A**). In order to verify if PAX2 deletion could stimulate MOE^{high} cell migration and tumor progression to other pelvic sites, CRISPR/Cas9 mediated genetic deletion of PAX2 was introduced into MOE^{high} cells (MOE^{high}/PAX2$^{-/-}$). Homozygous elimination of PAX2 was verified by sequencing (**Table X**). Western blot confirmed lack of PAX2 protein in MOE^{high}/PAX2$^{-/-}$ stable clones compared to control cells (**Fig. 35B**). Further testing to ultimately test the role of PAX2 would include scratch assays and automated xCELLigence assays to measure an increased pro-migratory phenotype in PAX2 deleted MOE^{high} clones. Based on the cell migration results, the PAX2 deleted MOE^{high} clones ($1*10^7$ cells/mice) would then be injected into female athymic nude mice. The results from this section, will recapitulate and confirm the necessity of PAX2 loss to trigger HGSOC tumor metastasis from the fallopian tube.

TABLE X - SEQUENCING ALIGNMENT OF PAX2 DELETIONS IN MOE^{high} CELLS (UPPER SEQUENCE IS PARENTAL SEQUENCE AND THE BOTTOM SEQUENCE IS FROM THE GRNA TRANSFECTED CLONE).

Gene/Exon	Sequence
PAX2$^{-/-}$/ Exon2	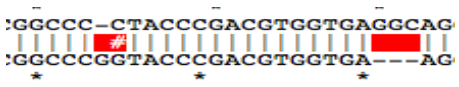
PAX2$^{-/-\ \#1}$/ Exon3	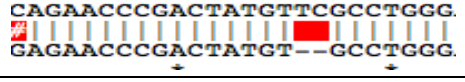

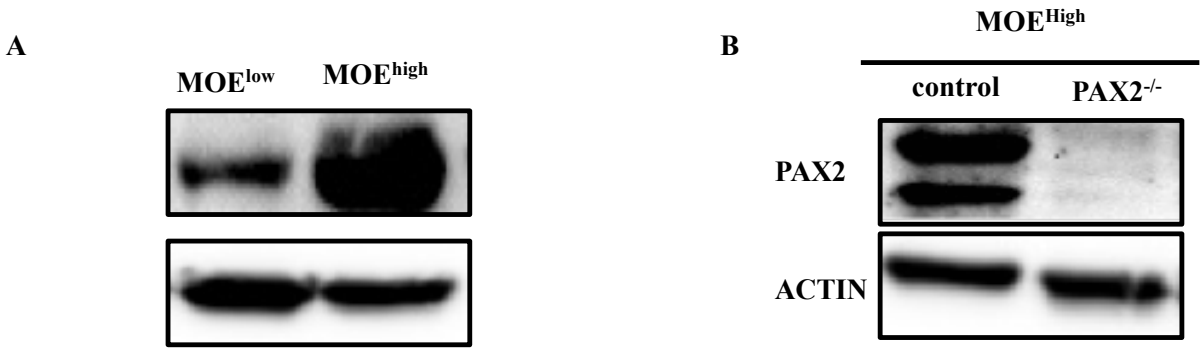

Figure 35 – PAX2 deletions in MOE^{high} cells.

A. Western blot image indicating the PAX2 levels. B. Western blot image indicating the lack of PAX2 protein in MOE^{high} cells.

C. DISCUSSION

This part of the study attempted to identify critical mechanisms in ovarian tumor metastases. Our findings so far indicate that p53 mutation is critical for the cell migration of the spontaneous model of FTE derived ovarian cancer. A stable expression of $p53^{R273H}$ alone in MOE^{high} increased cell motility by inducing SLUG and DCN, indicating the possibility that it might trigger tumor metastasis. Confirming this observation, $p19^{ARF}$ knockdown did not alter MOE^{high} cell migration to the level that p53 mutation did, reiterating the requirement of p53 DNA contact mutant for motility. ARF peptides that blocked FOXM1 activity in liver cancer cells (168), may be applied with a p53 modulator for ovarian tumor cells that contain p53 mutation.

PAX2 suppression combined with p53 mutation increased the FTE migration. Previously, luteolin induced PAX2 protein in MOE cells (163). With further validations, this study may elucidate the role of PAX2 alone as an anti-metastatic factor or its heightened expression in MOE^{high} cells may be random and not a critical part of their phenotype. Small molecule inhibitors for degrading or reversing mutant p53 functions have been tested in many cancer cell lines including ovarian cancer cells (65). A p53 drug candidate (Kevetrin) that degraded the mutant p53 in human HGSOC cells (OVCAR3), is currently under phase 2 clinical trial. The observations from this study will illuminate the drug discovery field for p53 inhibitors to block or reverse HGSOC progression from the fallopian tube epithelium.

VI. DISCUSSION AND FUTURE DIRECTIONS

Overall, the first project helped to i) identify a tissue specific marker of mutant p53, that can be potentially tested and used to discern FTE derived from OSE derived ovarian tumors, ii) determined that p53 DNA mutations are not sufficient to drive HGSOC formation from the FTE. The second project in this thesis utilized the first spontaneously FTE derived ovarian cancer model to attempt to identify new drivers of tumor formation and identified a novel role of prolactin in ovarian tumor proliferation. This suggests that small molecules that block prolactin receptor signaling might be used as therapeutic intervention. Lastly, this work began to characterize pathways in the MOE^{high} cells that blocked or inhibited peritoneal metastasis, which included investigating p53 mutations, $p19^{ARF}$ and loss of PAX2 in ovarian tumor progression.

Implication of the findings and scope of study

A. Why do we care about the cell of origin and ovarian cancer prevention strategy?

It was thought that all HGSOC originated from the OSE; however, increasing multi-disciplinary evidence including pathologic, genetic, and proteomic studies indicate that most HGSOC tumors comes from the FTE (4). Being able to differentiate between OSE- and FTE-derived tumors may be important clinically, because patients with FTE-derived ovarian tumors experienced a reduced overall survival compared to OSE derived (36). Salpingectomy was associated with a reduced the risk of ovarian cancer by 45% in women with benign indication (169). Most HGSOCs (>96%) contain a mutation in p53 and p53 stabilization is an early precursor lesion to HGSOC from FTE (39). We found that $p53^{R273H}$ mutation alone neither formed ovarian

tumors in mice models nor stabilized the p53 protein. This raised a question to the role of p53 mutation in HGSOC. To address this point, $p53^{R273H}$ mutation (most common mutation), was stably expressed in MOE cells, the mouse equivalent to human FTE. MOE$p53^{R273H}$ cells migrated faster compared to control cells; however, the same mutation did not change MOSE cell migration (2). Transcriptome profiling identified more than 2000 genes that were altered due to $p53^{R273H}$ mutation. Pro-migratory genes including SLUG, DCN, FOXM1 were significantly enriched by $p53^{R273H}$ mutation alone, supporting the increased cell migration (2). This observation suggests that there are critical migratory steps in the FTE, that can be studied to identify novel p53 targets to differentiate the FTE derived tumors from OSE derived.

A unique focus of our study was using MOE cells, the mouse equivalent to human FTE with stable expression of the $p53^{R273H}$ mutation, to identify FTE specific mutant p53 targets. Our data found Cadherin-6 (K- Cadherins, CDH6), a membrane glycoprotein, to be expressed in FTE and repressed by $p53^{R273H}$ but not expressed in OSE cells. Suppression of CDH6 expression by p53 mutation, may induce cell migration and tumor metastasis. Additionally, DCN (decorin), a secreted proteoglycan, was enhanced by $p53^{R273H}$ mutation in MOE cells, while the control cells lacked DCN expression by western blotting. In MOSE cells, the same mutation did not alter DCN expression.

In future, CDH6 potential to decipher FTE derived from OSE derived ovarian cancer, will be validated using human tumor and tissue samples. CDH6 levels will be assessed in ovarian tumors extracted from primary debulking, in fallopian tubes and ovaries that are removed for prophylactic reasons. The levels of CDH6 will also be correlated by sequencing the tissues for p53 status. Hypothetically, CDH6 expression will be lower in FTE derived tumors compared to normal fallopian tube, and tumors that are negative for CDH6 may be OSE derived. Predicted FTE derived

tumors will also be confirmed by comparing their gene profiling with normal fallopian tube and ovarian tissues. A similar analysis can be done by measuring DCN levels. DCN was enriched by $p53^{R273H}$ in MOE cells, and not in MOSE cells. Enriched DCN levels are reported in ovarian cancer and can significantly mediate tumor cell migration from FTE. The advantage of using DCN is that, it is a secreted protein, enriched compared to suppression as seen with CDH6 expression, and can also be measured by collecting circulating fluids and performing an ELISA technique. If CDH6 and DCN levels, correlate with and FTE derived tumors, then CDH6 can be carried to further trials.

These analyses can provide reasonable approach to decipher FTE derived tumors from OSE derived. That may facilitate clinical oncologists to decide on preventative therapy like removing one or both the fallopian tubes along with ovaries. A better specific tissue based therapy can also be derived, because FTE derived ovarian tumors are more aggressive than OSE derived and each tissue respond to p53 mutations differently.

B. How to monitor efficacy of mutant p53 inhibitors?

Many small molecules are currently being tested to degrade mutant p53 protein or to restore $p53^{WT}$ activity (65). Kevetrin, is a small molecule that activates $p53^{WT}$ protein in cancer cells, and it was found to be effective in human ovarian cancer cell models. Recently, Kevetrin was moved to phase 2 clinical trial, indicating the possibility that molecules targeting p53 might be a promising treatment for inhibiting ovarian cancer metastasis and increase the sensitivity of tumors. (https://globenewswire.com/news-release/2017/03/03/931526/0/en/Cellceutix-Provides-Update-on-Developing-p53-Drug-Candidate-Kevetrin-as-an-Oral-Anti-Cancer-Agent.html). A small molecule (chetomin) caused a potential conformational change of $p53^{R175H}$ to $p53^{WT}$ in human cancer cells (170). However, $p53^{WT}$ is constantly degraded by MDM2, which makes it challenging

to monitor the efficacy of p53 modulators. An interesting approach to circumvent this challenge would be to have a mutant p53 marker. Our findings, showed that degradation of mutant p53 protein rescued CDH6 expression in cellular models, indicating the potential use of CDH6 to monitor the efficacy of drugs targeting mutant p53.

In order to support this observation, it would be ideal to examine CDH6 and/or DCN levels in women with HGSOC, on the day of diagnosis, before and after beginning treatment with mutant p53 modulators. A correlation of CDH6 and DCN levels, should be monitored with other treatment progress, such as reduction in tumor volume. Another approach could be using microfluidics system. Our lab has recently obtained a microfluidic device, which is a culturing device that can be used to mimic the flow of fluids and provide *ex vivo* microenvironment for the growth of ovarian tumors similar to as seen in human physiology (171). Tumors obtained from ovarian cancer patients, will be grown in the microfluidics chamber, and treated with mutant p53 modulators. ELISA technique could be used to measure DCN levels, and tumor cell migration or adhesion from one can be measured for CDH6 phenotype. $p53^{R273H}$ also induced SLUG, reduced WNT4, PAPPA and integrins in MOE cells. WNT4 and PAPPA were secreted proteins. Hence, more p53 targets can also be measured using this device approach. This experiment can help to obtain a significantly usable approach to monitor the ovarian cancer treatment with mutant p53 modulators.

C. Different p53 mutations exhibit different functions.

The vast majority of HGSOCs contain a mutation in p53. R273H and R248W are the most frequently mutated sites in the p53 gene in HGSOCs (48). Previous studies found that R273H increased tumor invasion and R248W induced the expression of multi drug resistance gene and increased the chemoresistance (48). Since both are DNA contact mutants, it was believed that

their signaling targets and regulatory pattern would very similar or identical and that small molecules would work for multiple p53 DNA contact mutants. However, this work found that different p53 mutations possess different functions. Our data illustrates that $p53^{R273H}$ induced key pro-migratory targets, SLUG, DCN and FOXM1, that resulted in increased FTE migration. $p53^{R248W}$ did not induce SLUG, moderately induced DCN and FOXM1 and the efficiency of inducing cell migration was lesser compared to R273H. A small molecule that degraded R273H did not have any effect on R248W protein, indicating different small molecules are required for degrading different mutant p53 protein and SLUG inhibitors may not be effective in tumors with R248W mutation.

In the future, it would be useful to perform transcriptome profiling in MOE cells with stable $p53^{R248W}$ expression to identify its downstream targets in the FTE. It may provide novel targets that contribute to aberrant proliferation or increased chemoresistance. Since $p53^{R248W}$ has a weaker effect on cell migration than $p53^{R273H}$, its effect on cell proliferation, 2D foci formation should also be assessed. $p53^{R273H}$ alone did not form tumors, however it will be useful to test if $p53^{R248W}$ will form ovarian tumors in athymic nude mice. The small molecule library from NCI or the Prestwick library will be used to identify molecules that can degrade $p53^{R248W}$ in human HGSOC cells. The results can be measured by testing CDH6 and WNT4 levels (both R248W and R273H repressed CDH6 and WNT4) or other downstream target identified from transcriptome profiling of $p53^{R248W}$ cells. This will identify novel signaling mechanism of $p53^{R248W}$ and a small molecule inhibitor to block its activity in ovarian cancer.

D. Novel targets to block HGSOC tumorigenesis.

Using the first made spontaneous model of FTE derived ovarian cancer (MOE^{high}) and transcriptome profiling, we identified a close human homolog of prolactin (PRL), called *Prl2c2* that when silenced completely blocked MOE^{high} tumor formation (3). PRL was used as a component of an ovarian cancer screening kit Ovasure, indicating PRL is a marker of ovarian cancer (88). Although, amplification of PRL and prolactin receptors (PRL-R) reduced the overall survival of ovarian cancer patients, its role in ovarian tumor growth from FTE was understudied (149-151). Our findings identified that PRL to be a critical mediator of tumor growth in human HGSOC cells. By blocking PRL-R alone, in human HGSOC cells (OVCAR3), subcutaneous tumor formation was prevented. PRL downstream signaling was identified and small molecules were evaluated to block PRL induced proliferation in OVCAR3 and FTE cells.

Since this study intended to study the role of PRL in fallopian tube derived tumors, immortalized human FTE cells were used, which was identified previously to form tumors in SCID mice models (108). We found that PRL-R elimination reduced the cellular proliferation, while a constitutive activation stimulated FTE proliferation. However, it will be useful to study the role of PRL alone in normal human FTE cells. In future, by using an immortalized FTE cells that do not form tumors, PRL mechanism and its role in aberrant proliferation will be tested. This will identify the role of PRL alone in transforming the normal human fallopian tube epithelium.

PRL had been reported to induce angiogenesis in many cancer types including ovarian and breast cancer. However, this thesis, so for did not identify the contribution of PRL in tumor metastasis. Although, elimination of PRL-R blocked tumor growth, subcutaneous tumor models may not indicate the importance of PRL in ovarian tumor metastasis, because HGSOC spreads rapidly to the peritoneal space (4). In the future, OVCAR3 parental cells (previously identified to induce intraperitoneal tumors in mice) (106), and OVCAR3 cells with PRL-R knockout (KO), will

be stably transfected to express red fluorescence protein. Both the control and PRL-R KO cell lines will be injected into the intraperitoneal space of athymic nude mice, and IVIS imaging will be performed to monitor disease progression. Our prediction is that, since PRL-R deletion inhibited the subcutaneous tumor growth for more than 35 days, it might block disease progression to the peritoneal space. This experiment will confirm the significance of PRL in HGSOC angiogenesis and will encourage pharmaceutical team to identify drugs to block PRL signaling, treat ovarian tumors and inhibit HGSOC progression from the fallopian tube.

In order to translate the preliminary screen of small molecules against AKT, STAT5, MEK and m-TOR, that blocked PRL signaling, into therapeutic level, human HGSOC tumors and respective patient's serum samples will be obtained. After evaluating the levels of PRL, the tumors will be maintained using microfluidic device. Different doses of previously tested compounds will be added and tumor size and cell death will be measured. This will identify small molecules to inhibit PRL-R activity that can potentially be used to treat ovarian cancer. Most small molecules exhibit toxicity to normal cells making the patient susceptible to other infections. Recently, nanoparticles are being widely applied to overcome this issue. A study recently identified that >98% of ovarian cancer express PRL-R and developed a new molecular imaging strategy to detect ovarian cancer. The human placental lactogen, which is a specific PRL-R ligand, was fused to a magnetic resonance imaging agent and found that the fused molecule underwent selective intenralizaton into ovarian cancer cells facilitating ovarian cancer diagnosis (172). This suggests that synthetic fusions may be effective in antagonizing PRL-R activity in ovarian cancer. Our lab previously has also identified that a nanoparticle specifically targeted follicle stimulating hormone receptor that are only ovarian tumor cells (173). By collaborating with chemistry lab at UIC, nanoparticles will be designed that can tag the small molecule inhibitor that antagonize PRL-R

signaling to mediate targeted inhibition of PRL-R activity in tumors, which can be a useful therapy for HGSOC.

E. PRL induced p53 phosphorylation and chemoresistance.

Although, platinum drugs are currently being used to treat ovarian cancer, >60% of patients report remission, suggesting requirement of novel therapeutic strategies to overcome this problem(174). Human phosphokinase array identified that p53 was phosphorylated at critical serine residues (15,46 and 392) in human HGSOC cells, with 30 minutes of PRL exposure. Phosphorylation of these residues are reported to stabilize $p53^{WT}$ protein, resulting in active DNA repair and chemoresistance in many cancers (160).

In future, OVCAR3 control and PRL-$R^{-/-}$ cells will be treated with PRL for 30 minutes, and exposed to platinum drugs like cisplatin. Cytotoxicity assay will be performed to identify the dose response curve and cell lethality; western blotting can be implied to test p53 phosphorylation in PRL-$R^{-/-}$ cells. This experiment will provide preliminary validation if blocking PRL-R prevented p53 phosphorylation and sensitize the HGSOC tumor cells to platinum drugs. In order to identify the exact serine residue from the three residues (S15, S46 and S392), that might encode chemoresistance, specific p53 phosphomimetic will be procured and expressed in OVCAR3 parental and PRL-R KO cells. Platinum drugs will be added to the cells that expressing different p53 phosphomimetics, and cytotoxicity assay will be performed. This may reveal the p53 residue, that is critical for chemoresistance in HGSOC. This may be translated using human tumor samples, which with further testing, can be used as a combined therapeutic approach of blocking p53 phosphorylation aggregates and PRL-R signaling.

F. p53 mutation and PAX2 loss role in HGSOC metastasis.

HGSOC is a rapid spreading histotype of ovarian cancer. Druggable targets to block HGSOC metastasis from fallopian tube are required. p53 DNA binding mutations increase FTE migration (2). Although, our spontaneous MOE^{high} tumor model possessed concordant gene signatures as seen in human HGSOC, it lacked a p53 DNA binding mutation and failed to form intraperitoneal disease (3). A stable expression of $p53^{R273H}$ increased MOE^{high} migration. By injecting MOE^{high} cells with stable expression of $p53^{R273H}$ into the intraperitoneal space, the efficiency of p53 DNA contact mutation in ovarian tumor metastasis will be evaluated. MOE^{high} cells also expressed enriched PAX2 levels. PAX2 loss had been hypothesized to induce cell migration (163,175). CRISPR/Cas9 mediated PAX2 deletions were made in MOE^{high} cells. Migration efficiency will be tested using scratch and xCELLigence assays in PAX2 deleted and control cells. Further, PAX2 deleted cells will be injected into the intraperitoneal space of athymic nude mice. Since HGSOC comes from the fallopian tube, the results from these experiments will recapitulate and support the requirement of p53 mutation and PAX2 loss alone and in combination for stimulating ovarian tumor metastasis. Finally, it may add valuable targets for designing therapies to inhibit or reverse HGSOC metastasis.

G. Integrins role in ovarian tumor metastases.

Integrins are cell adhesion proteins, that are crucial for cell migration and tumor progression. Loss of Integrin expression is reported in many cancer tissues (176). Integrins can bind to the extracellular matrix (ECM) and stimulate cell motility and invasion by remodeling the ECM and increasing VEGF signaling (177). Many studies have identified the contribution of integrins in tumor progression that made them appealing for cancer therapy. ITGB2 (Integrin beta

subunit 2) belongs to the integrin family of proteins and may possess a critical role in tumor metastasis. The MOE^{high} model had enriched levels of ITGB2 by RNA sequencing, while $p53^{R273H}$ mutation significantly reduced ITGB2 levels in MOE cells (2,3). We predict, enhanced ITGB2 signaling may block MOE^{high} metastasis.

Using, CRISPR/Cas9, ITGB2 can be deleted in MOE^{high} cells. The cell migration can be assessed using scratch and xCELLigence assay. The cells can further be injected into mice models to observe for MOE^{high} metastasis. These observations can also be translated using human HGSOC cells, such as OVCAR3 or OVCAR8. The cell lines will be screened first for the expression of ITGB2. Previously, agonists like cilengitide, for integrins such as $\alpha v\beta 3$ and $\alpha v\beta 5$, had been shown to have promising results in Phase II clinical trials (176). Hence, our identifications using the spontaneous FTE tumor model, may add valuable biological targets to the existing therapy, that can be used to block the lethal HGSOC metastasis.

HGSOC is a complex, heterogenic and deadly disease, with multiple diversities in their cellular and molecular features. There is a dire need to discover biological targets that are druggable to prevent and treat serous tumor initiation and progression. Significant efforts had been made to improve early diagnosis, prevention, treatment and increasing the progression free survival of HGSOC. Every finding of this study, will significantly increase the cognizance of ovarian cancer pathogenesis, prevention and treatment.

APPENDICES

APPENDIX A

Permission for reprinting Chapter I

Oncotarget
ONLINE ISSN: 1949-2553

For Authors

Papers cannot be withdrawn after publishing in the public domain, online. There are no refunds available.

II. EDITORIAL POLICIES

The general instructions below apply to all journals published by Impact Journals, LLC. Before you submit a manuscript for publication, please be sure to read and follow them. **Submission of a manuscript to any of our journal implies that its author(s) understand and accept the policies of the journal and have complied with the Instructions for Authors.**

COPYRIGHT AND LICENSE POLICIES

Open-Access License

No Permission Required

Oncotarget applies the **Creative Commons Attribution 3.0 License** (CC BY 3.0) to all works we publish (read the **human-readable summary** or the **full license legal code**). Under the CC BY, authors retain ownership of the copyright for their article, but authors allow anyone to download, reuse, reprint, modify, distribute, and/or copy articles in *Oncotarget*, so long as the original authors and source are cited.

No permission is required from the authors or the publishers.

In most cases, appropriate attribution can be provided by simply citing the original article. If the item you plan to reuse is not part of a published article (e.g., a featured issue image), then please indicate the originator of the work, and the volume, issue, and date of the journal in which the item appeared. For any reuse or redistribution of a work, you must also make clear the license terms under which the work was published. This broad license was developed to facilitate open access to, and free use of, original works of all types. Applying this standard license to your own work will ensure your right to make your work freely and openly available.

For queries about the license, please contact us at forms@oncotarget.com

APPENDIX B

UIC UNIVERSITY OF ILLINOIS AT CHICAGO

Office of Animal Care and
Institutional Biosafety Committees (MC 672)
Office of the Vice Chancellor for Research
206 Administrative Office Building
1737 West Polk Street
Chicago, Illinois 60612-7227

November 2, 2017

Joanna Burdette
Medicinal Chemistry & Pharmacognosy
M/C 781

Dear Dr. Burdette:

The protocol indicated below was reviewed at a convened ACC meeting in accordance with the Animal Care Policies of the University of Illinois at Chicago on **10/17/2017**. *The protocol was not initiated until final clarifications were reviewed and approved on* **11/2/2017**. *The protocol is approved for a period of* ***3*** years with annual continuation.

Title of Application: Akt transformation of ovarian surface and oviductal cells

ACC Number: 17-174

Initial Approval Period: 11/2/2017 to 10/17/2018

Current Funding: ***Portions of this protocol are supported by the funding sources indicated in the table below.***
Number of funding sources: 2

Funding Agency	**Funding Title**			**Portion of Proposal Matched**
Ovarian Cancer Research Fund Alliance (OCRFA)	*The Ovarian Microenvironment in Metastasis of Fallopian Tube Derived Cancer (Institutional # 00369145)*			*Other* *Studies also linked to 17-174*
Funding Number	**Current Status**	**UIC PAF NO.**	**Performance Site**	**Funding PI**
	Funded		*UIC*	*Matthew Dean*
Funding Agency	**Funding Title**			**Portion of Proposal Matched**
NIH	*Pax2 Loss in Fallopian Tube Lesions and Strategies for Restoration in Serous Cancer*			*All matched*
Funding Number	**Current Status**	**UIC PAF NO.**	**Performance Site**	**Funding PI**
1 R21CA208610-01	*Funded*	*201602399*	*UIC*	*Joanna Burdette*

APPENDIX B (Continued)

UIC UNIVERSITY OF ILLINOIS AT CHICAGO

Office of Animal Care and Institutional
Biosafety Committee (OACIB) (M/C 672)
Office of the Vice Chancellor for Research
206 Administrative Office Building
1737 West Polk Street
Chicago, Illinois 60612

11/18/2016

Joanna Burdette
Medicinal Chemistry & Pharmacognosy
M/C 781

Dear Dr. Burdette:

The protocol indicated below was reviewed in accordance with the Animal Care Policies and Procedures of the University of Illinois at Chicago and **renewed on 11/18/2016.**

Title of Application: Akt Transformation of Ovarian Surface and Oviductal Cells
ACC NO: 14-180
Original Protocol Approval: 1/12/2015 **(3 year approval with annual continuation required).**
Current Approval Period: 11/18/2016 **to** 11/18/2017

Funding: ***Portions of this protocol are supported by the funding sources indicated in the table below.***
Number of funding sources: 2

Funding Agency	**Funding Title**			**Portion of Funding Matched**
ACS- American Cancer Society	*AKT Transformation of Ovarian and Fallopian Cells*			*Protocol is linked to form G 14-181*
Funding Number	**Current Status**	**UIC PAF NO.**	**Performance Site**	**Funding PI**
RSG-12-230-01-TBG	*Funded*	*2012-01837*	*UIC*	*Joanna Burdette*
Funding Agency	**Funding Title**			**Portion of Funding Matched**
NIH/NCI- National Cancer Institute	*Pax2 Loss in Fallopian Tube Lesions and Strategies for Restoration in Serous Cancer*			*All matched*
Funding Number	**Current Status**	**UIC PAF NO.**	**Performance Site**	**Funding PI**
1R21CA208610-01	*Pending*	*2016-02399*	*UIC*	*Joanna Burdette*

This institution has Animal Welfare Assurance Number A3460.01 on file with the Office of Laboratory Animal Welfare, NIH. **This letter may only be provided as proof of IACUC approval for those specific funding sources listed above in which all portions of the grant are matched to this ACC protocol.**

Thank you for complying with the Animal Care Policies and Procedures of the UIC.

Sincerely,

John P. O'Bryan, PhD
Chair, Animal Care Committee
JPO/*kg*
cc: BRL, ACC File, Daniel Lantvit

Phone (312) 996-1972 • Fax (312) 996-9088

APPENDIX B (Continued)

UIC UNIVERSITY OF ILLINOIS AT CHICAGO

Office of Animal Care and Institutional
Biosafety Committee (OACIB) (M/C 672)
Office of the Vice Chancellor for Research
206 Administrative Office Building
1737 West Polk Street
Chicago, Illinois 60612

11/18/2015

Joanna Burdette
Medicinal Chemistry & Pharmacognosy
M/C 781

Dear Dr. Burdette:

The protocol indicated below was reviewed in accordance with the Animal Care Policies and Procedures of the University of Illinois at Chicago and **renewed on 11/18/2015.**

Title of Application: **Akt Transformation of Ovarian Surface and Oviductal Cells**
ACC NO: **14-180**
Original Protocol Approval: **1/12/2015 (3 year approval with annual continuation required).**
Current Approval Period: **11/18/2015 to 11/18/2016**

Funding: ***Portions of this protocol are supported by the funding sources indicated in the table below.***
Number of funding sources: 1

Funding Agency	**Funding Title**			**Portion of Funding Matched**
ACS- American Cancer Society	*AKT Transformation of Ovarian and Fallopian Cells*			*Protocol is linked to form G 14-181*
Funding Number	**Current Status**	**UIC PAF NO.**	**Performance Site**	**Funding PI**
RSG-12-230-01-TBG	*Funded*	*2012-01837*	*UIC*	*Joanna Burdette*

This institution has Animal Welfare Assurance Number A3460.01 on file with the Office of Laboratory Animal Welfare, NIH. **This letter may only be provided as proof of IACUC approval for those specific funding sources listed above in which all portions of the grant are matched to this ACC protocol.**

Thank you for complying with the Animal Care Policies and Procedures of the UIC.

Sincerely,

John P. O'Bryan, PhD
Chair, Animal Care Committee
JPO/*kg*
cc: BRL, ACC File, Daniel Lantvit

Phone (312) 996-1972 • Fax (312) 996-9088

CITED REFERENCES

1. Karthikeyan S, Lantvit DD, Chae DH, Burdette JE. Cadherin-6 type 2, K-cadherin (CDH6) is regulated by mutant p53 in the fallopian tube but is not expressed in the ovarian surface. Oncotarget **2016**;7:69871-82

2. Quartuccio SM, Karthikeyan S, Eddie SL, Lantvit DD, E Oh, Modi DA*, et al.* Mutant p53 expression in fallopian tube epithelium drives cell migration. International journal of cancer Journal international du cancer **2015**;137:1528-38

3. Endsley MP, Moyle-Heyrman G, Karthikeyan S, Lantvit DD, Davis DA, Wei JJ*, et al.* Spontaneous Transformation of Murine Oviductal Epithelial Cells: A Model System to Investigate the Onset of Fallopian-Derived Tumors. Front Oncol **2015**;5:154

4. Karst AM, Drapkin R. Ovarian cancer pathogenesis: a model in evolution. Journal of oncology **2010**;2010:932371

5. Chen VW, Ruiz B, Killeen JL, Cote TR, Wu XC, Correa CN. Pathology and classification of ovarian tumors. Cancer **2003**;97:2631-42

6. Benedet JL, Bender H, Jones H, 3rd, Ngan HY, Pecorelli S. FIGO staging classifications and clinical practice guidelines in the management of gynecologic cancers. FIGO Committee on Gynecologic Oncology. Int J Gynaecol Obstet **2000**;70:209-62

7. Dubeau L. The cell of origin of ovarian epithelial tumors and the ovarian surface epithelium dogma: does the emperor have no clothes? Gynecologic oncology **1999**;72:437-42

8. Seidman JD, Horkayne-Szakaly I, Haiba M, Boice CR, Kurman RJ, Ronnett BM. The histologic type and stage distribution of ovarian carcinomas of surface epithelial origin. International journal of gynecological pathology : official journal of the International Society of Gynecological Pathologists **2004**;23:41-4

9. Malpica A. Grading of ovarian cancer: a histotype-specific approach. International journal of gynecological pathology : official journal of the International Society of Gynecological Pathologists **2008**;27:175-81

10. Shimizu Y, Kamoi S, Amada S, Hasumi K, Akiyama F, Silverberg SG. Toward the development of a universal grading system for ovarian epithelial carcinoma. I. Prognostic significance of histopathologic features--problems involved in the architectural grading system. Gynecologic oncology **1998**;70:2-12

11. Jones PM, Drapkin R. Modeling High-Grade Serous Carcinoma: How Converging Insights into Pathogenesis and Genetics are Driving Better Experimental Platforms. Front Oncol **2013**;3:217

12. Silverberg SG. Histopathologic grading of ovarian carcinoma: a review and proposal. International journal of gynecological pathology : official journal of the International Society of Gynecological Pathologists **2000**;19:7-15

13. Landen CN, Jr., Birrer MJ, Sood AK. Early events in the pathogenesis of epithelial ovarian cancer. J Clin Oncol **2008**;26:995-1005

14. Shih Ie M, Kurman RJ. Ovarian tumorigenesis: a proposed model based on morphological and molecular genetic analysis. Am J Pathol **2004**;164:1511-8

15. Singer G, Oldt R, 3rd, Cohen Y, Wang BG, Sidransky D, Kurman RJ*, et al.* Mutations in BRAF and KRAS characterize the development of low-grade ovarian serous carcinoma. J Natl Cancer Inst **2003**;95:484-6

16. Mok SC, Bell DA, Knapp RC, Fishbaugh PM, Welch WR, Muto MG*, et al.* Mutation of K-ras protooncogene in human ovarian epithelial tumors of borderline malignancy. Cancer research **1993**;53:1489-92

17. Mayr D, Hirschmann A, Lohrs U, Diebold J. KRAS and BRAF mutations in ovarian tumors: a comprehensive study of invasive carcinomas, borderline tumors and extraovarian implants. Gynecologic oncology **2006**;103:883-7

18. Wang SE, Narasanna A, Perez-Torres M, Xiang B, Wu FY, Yang S*, et al.* HER2 kinase domain mutation results in constitutive phosphorylation and activation of HER2 and EGFR and resistance to EGFR tyrosine kinase inhibitors. Cancer cell **2006**;10:25-38

19. Nakayama K, Nakayama N, Kurman RJ, Cope L, Pohl G, Samuels Y*, et al.* Sequence mutations and amplification of PIK3CA and AKT2 genes in purified ovarian serous neoplasms. Cancer Biol Ther **2006**;5:779-85

20. Ho CL, Kurman RJ, Dehari R, Wang TL, Shih Ie M. Mutations of BRAF and KRAS precede the development of ovarian serous borderline tumors. Cancer research **2004**;64:6915-8

21. May T, Virtanen C, Sharma M, Milea A, Begley H, Rosen B*, et al.* Low malignant potential tumors with micropapillary features are molecularly similar to low-grade serous carcinoma of the ovary. Gynecologic oncology **2010**;117:9-17

22. Dehari R, Kurman RJ, Logani S, Shih Ie M. The development of high-grade serous carcinoma from atypical proliferative (borderline) serous tumors and low-grade micropapillary serous carcinoma: a morphologic and molecular genetic analysis. Am J Surg Pathol **2007**;31:1007-12

23. Senturk E, Cohen S, Dottino PR, Martignetti JA. A critical re-appraisal of BRCA1 methylation studies in ovarian cancer. Gynecologic oncology **2010**;119:376-83

24. Nakayama K, Nakayama N, Jinawath N, Salani R, Kurman RJ, Shih Ie M*, et al.* Amplicon profiles in ovarian serous carcinomas. International journal of cancer Journal international du cancer **2007**;120:2613-7

25. Cancer Genome Atlas Research N. Integrated genomic analyses of ovarian carcinoma. Nature **2011**;474:609-15

26. Shih Ie M, Chen L, Wang CC, Gu J, Davidson B, Cope L*, et al.* Distinct DNA methylation profiles in ovarian serous neoplasms and their implications in ovarian carcinogenesis. Am J Obstet Gynecol **2010**;203:584 e1-22

27. Auersperg N, Maines-Bandiera SL, Dyck HG, Kruk PA. Characterization of cultured human ovarian surface epithelial cells: phenotypic plasticity and premalignant changes. Lab Invest **1994**;71:510-8

28. Murdoch WJ, Martinchick JF. Oxidative damage to DNA of ovarian surface epithelial cells affected by ovulation: carcinogenic implication and chemoprevention. Exp Biol Med (Maywood) **2004**;229:546-52

29. Dubeau L. The cell of origin of ovarian epithelial tumours. Lancet Oncol **2008**;9:1191-7

30. Wong AS, Leung PC. Role of endocrine and growth factors on the ovarian surface epithelium. J Obstet Gynaecol Res **2007**;33:3-16

31. Piek JM, van Diest PJ, Zweemer RP, Jansen JW, Poort-Keesom RJ, Menko FH*, et al.* Dysplastic changes in prophylactically removed Fallopian tubes of women predisposed to developing ovarian cancer. The Journal of pathology **2001**;195:451-6

32. Medeiros F, Muto MG, Lee Y, Elvin JA, Callahan MJ, Feltmate C*, et al.* The tubal fimbria is a preferred site for early adenocarcinoma in women with familial ovarian cancer syndrome. American Journal of Surgical Pathology **2006**;30:230-6

33. Kindelberger DW, Lee Y, Miron A, Hirsch MS, Feltmate C, Medeiros F*, et al.* Intraepithelial carcinoma of the fimbria and pelvic serous carcinoma: Evidence for a causal relationship. Am J Surg Pathol **2007**;31:161-9

34. Perets R, Wyant GA, Muto KW, Bijron JG, Poole BB, Chin KT*, et al.* Transformation of the fallopian tube secretory epithelium leads to high-grade serous ovarian cancer in Brca;Tp53;Pten models. Cancer cell **2013**;24:751-65

35. Marquez RT, Baggerly KA, Patterson AP, Liu J, Broaddus R, Frumovitz M*, et al.* Patterns of gene expression in different histotypes of epithelial ovarian cancer correlate with those in normal fallopian tube, endometrium, and colon. Clinical cancer research : an official journal of the American Association for Cancer Research **2005**;11:6116-26

36. Merritt MA, Bentink S, Schwede M, Iwanicki MP, Quackenbush J, Woo T*, et al.* Gene expression signature of normal cell-of-origin predicts ovarian tumor outcomes. PloS one **2013**;8:e80314

37. Klinkebiel D, Zhang W, Akers SN, Odunsi K, Karpf AR. DNA Methylome Analyses Implicate Fallopian Tube Epithelia as the Origin for High-Grade Serous Ovarian Cancer. Molecular cancer research : MCR **2016**;14:787-94

38. Eddie SL, Quartuccio SM, E Oh, Moyle-Heyrman G, Lantvit DD, Wei JJ*, et al.* Tumorigenesis and peritoneal colonization from fallopian tube epithelium. Oncotarget **2015**;6:20500-12

39. Levanon K, Crum C, Drapkin R. New Insights Into the Pathogenesis of Serous Ovarian Cancer and Its Clinical Impact. J Clin Oncol **2008**;26:5284-93

40. Folkins AK, Jarboe EA, Roh MH, Crum CP. Precursors to pelvic serous carcinoma and their clinical implications. Gynecologic oncology **2009**;113:391-6

41. Pradeep S, Kim SW, Wu S, Masato N, Miyake T, Hyun-Jin C*, et al.* Hematogenous metastasis of ovarian cancer: Re-thinking mode of spread. Cancer research **2014**;74

42. Yokoi A, Yoshioka Y, Yamamoto Y, Ishikawa M, Ikeda SI, Kato T*, et al.* Malignant extracellular vesicles carrying MMP1 mRNA facilitate peritoneal dissemination in ovarian cancer. Nat Commun **2017**;8:14470

43. Eckert MA, Pan S, Hernandez KM, Loth RM, Andrade J, Volchenboum SL*, et al.* Genomics of Ovarian Cancer Progression Reveals Diverse Metastatic Trajectories Including Intraepithelial Metastasis to the Fallopian Tube. Cancer Discov **2016**;6:1342-51

44. Vousden KH, Lu X. Live or let die: the cell's response to p53. Nat Rev Cancer **2002**;2:594-604

45. Laptenko O, Prives C. Transcriptional regulation by p53: one protein, many possibilities. Cell Death Differ **2006**;13:951-61

46. Moll UM, Petrenko O. The MDM2-p53 interaction. Molecular cancer research : MCR **2003**;1:1001-8

47. Freed-Pastor WA, Prives C. Mutant p53: one name, many proteins. Genes & development **2012**;26:1268-86

48. Brachova P, Thiel KW, Leslie KK. The consequence of oncomorphic TP53 mutations in ovarian cancer. International journal of molecular sciences **2013**;14:19257-75

49. Wong AS, Maines-Bandiera SL, Rosen B, Wheelock MJ, Johnson KR, Leung PC*, et al.* Constitutive and conditional cadherin expression in cultured human ovarian surface epithelium: influence of family history of ovarian cancer. International journal of cancer Journal international du cancer **1999**;81:180-8

50. Olive KP, Tuveson DA, Ruhe ZC, Yin B, Willis NA, Bronson RT*, et al.* Mutant p53 gain of function in two mouse models of Li-Fraumeni syndrome. Cell **2004**;119:847-60

51. Blandino G, Levine AJ, Oren M. Mutant p53 gain of function: differential effects of different p53 mutants on resistance of cultured cells to chemotherapy. Oncogene **1999**;18:477-85

52. Liu K, Ling SY, Lin WC. TopBP1 Mediates Mutant p53 Gain of Function through NF-Y and p63/p73. Molecular and Cellular Biology **2011**;31:4464-81

53. Adorno M, Cordenonsi M, Montagner M, Dupont S, Wong C, Hann B*, et al.* A Mutant-p53/Smad complex opposes p63 to empower TGFbeta-induced metastasis. Cell **2009**;137:87-98

54. Stambolsky P, Tabach Y, Fontemaggi G, Weisz L, Maor-Aloni R, Siegfried Z*, et al.* Modulation of the vitamin D3 response by cancer-associated mutant p53. Cancer cell **2010**;17:273-85

55. Wong KB, DeDecker BS, Freund SM, Proctor MR, Bycroft M, Fersht AR. Hot-spot mutants of p53 core domain evince characteristic local structural changes. Proc Natl Acad Sci U S A **1999**;96:8438-42

56. Chan KT, Lung ML. Mutant p53 expression enhances drug resistance in a hepatocellular carcinoma cell line. Cancer Chemother Pharmacol **2004**;53:519-26

57. Song H, Hollstein M, Xu Y. p53 gain-of-function cancer mutants induce genetic instability by inactivating ATM. Nature cell biology **2007**;9:573-80

58. Weisz L, Zalcenstein A, Stambolsky P, Cohen Y, Goldfinger N, Oren M*, et al.* Transactivation of the EGR1 gene contributes to mutant p53 gain of function. Cancer research **2004**;64:8318-27

59. Di Agostino S, Cortese G, Monti O, Dell'Orso S, Sacchi A, Eisenstein M*, et al.* The disruption of the protein complex mutantp53/p73 increases selectively the response of tumor cells to anticancer drugs. Cell Cycle **2008**;7:3440-7

60. Meng X, Laidler LL, Kosmacek EA, Yang S, Xiong Z, Zhu D*, et al.* Induction of mitotic cell death by overriding G2/M checkpoint in endometrial cancer cells with non-functional p53. Gynecologic oncology **2013**;128:461-9

61. Terzian T, Suh YA, Iwakuma T, Post SM, Neumann M, Lang GA*, et al.* The inherent instability of mutant p53 is alleviated by Mdm2 or p16INK4a loss. Genes & development **2008**;22:1337-44

62. Kang HJ, Chun SM, Kim KR, Sohn I, Sung CO. Clinical relevance of gain-of-function mutations of p53 in high-grade serous ovarian carcinoma. PloS one **2013**;8:e72609

63. Yu X, Vazquez A, Levine AJ, Carpizo DR. Allele-specific p53 mutant reactivation. Cancer cell **2012**;21:614-25

64. Lunghi P, Costanzo A, Mazzera L, Rizzoli V, Levrero M, Bonati A. The p53 family protein p73 provides new insights into cancer chemosensitivity and targeting. Clinical cancer research : an official journal of the American Association for Cancer Research **2009**;15:6495-502

65. Zhang S, Zhou L, Hong B, van den Heuvel AP, Prabhu VV, Warfel NA*, et al.* Small-Molecule NSC59984 Restores p53 Pathway Signaling and Antitumor Effects against Colorectal Cancer via p73 Activation and Degradation of Mutant p53. Cancer research **2015**;75:3842-52

66. Soragni A, Janzen DM, Johnson LM, Lindgren AG, Thai-Quynh Nguyen A, Tiourin E*, et al.* A Designed Inhibitor of p53 Aggregation Rescues p53 Tumor Suppression in Ovarian Carcinomas. Cancer cell **2016**;29:90-103

67. Twombly R. Cancer killer may be "Silent" no more. J Natl Cancer I **2007**;99:1359-61

68. Bankhead CR, Collins C, Stokes-Lampard H, Rose P, Wilson S, Clements A*, et al.* Identifying symptoms of ovarian cancer: a qualitative and quantitative study. BJOG **2008**;115:1008-14

69. Goff BA, Mandel L, Muntz HG, Melancon CH. Ovarian carcinoma diagnosis. Cancer **2000**;89:2068-75

70. Bourne TH, Campbell S, Reynolds KM, Whitehead MI, Hampson J, Royston P*, et al.* Screening for early familial ovarian cancer with transvaginal ultrasonography and colour blood flow imaging. BMJ **1993**;306:1025-9

71. Sato S, Yokoyama Y, Sakamoto T, Futagami M, Saito Y. Usefulness of mass screening for ovarian carcinoma using transvaginal ultrasonography. Cancer **2000**;89:582-8

72. Lerner JP, Timor-Tritsch IE, Federman A, Abramovich G. Transvaginal ultrasonographic characterization of ovarian masses with an improved, weighted scoring system. Am J Obstet Gynecol **1994**;170:81-5

73. van Nagell JR, Jr., DePriest PD, Reedy MB, Gallion HH, Ueland FR, Pavlik EJ*, et al.* The efficacy of transvaginal sonographic screening in asymptomatic women at risk for ovarian cancer. Gynecologic oncology **2000**;77:350-6

74. Valentin L, Skoog L, Epstein E. Frequency and type of adnexal lesions in autopsy material from postmenopausal women: ultrasound study with histological correlation. Ultrasound in obstetrics & gynecology : the official journal of the International Society of Ultrasound in Obstetrics and Gynecology **2003**;22:284-9

75. Murta EF, Nomelini RS. Early diagnosis and predictors of malignancy of adnexal masses. Curr Opin Obstet Gynecol **2006**;18:14-9

76. Menon U, Gentry-Maharaj A, Hallett R, Ryan A, Burnell M, Sharma A*, et al.* Sensitivity and specificity of multimodal and ultrasound screening for ovarian cancer, and stage distribution of detected cancers: results of the prevalence screen of the UK Collaborative Trial of Ovarian Cancer Screening (UKCTOCS). Lancet Oncol **2009**;10:327-40

77. Jacobs IJ, Skates SJ, MacDonald N, Menon U, Rosenthal AN, Davies AP*, et al.* Screening for ovarian cancer: a pilot randomised controlled trial. Lancet **1999**;353:1207-10

78. Jacobs I, Bast RC, Jr. The CA 125 tumour-associated antigen: a review of the literature. Hum Reprod **1989**;4:1-12

79. Kenemans P, van Kamp GJ, Oehr P, Verstraeten RA. Heterologous double-determinant immunoradiometric assay CA 125 II: reliable second-generation immunoassay for determining CA 125 in serum. Clin Chem **1993**;39:2509-13

80. Nustad K, Bast RC, Jr., Brien TJ, Nilsson O, Seguin P, Suresh MR*, et al.* Specificity and affinity of 26 monoclonal antibodies against the CA 125 antigen: first report from the

ISOBM TD-1 workshop. International Society for Oncodevelopmental Biology and Medicine. Tumour Biol **1996**;17:196-219

81. Zurawski VR, Jr., Orjaseter H, Andersen A, Jellum E. Elevated serum CA 125 levels prior to diagnosis of ovarian neoplasia: relevance for early detection of ovarian cancer. International journal of cancer Journal international du cancer **1988**;42:677-80

82. Gadducci A, Zola P, Landoni F, Maggino T, Sartori E, Bergamino T*, et al.* Serum half-life of CA 125 during early chemotherapy as an independent prognostic variable for patients with advanced epithelial ovarian cancer: results of a multicentric Italian study. Gynecologic oncology **1995**;58:42-7

83. Yuan Q, Song J, Yang W, Wang H, Huo Q, Yang J*, et al.* The effect of CA125 on metastasis of ovarian cancer: old marker new function. Oncotarget **2017**;8:50015-22

84. Levina VV, Nolen B, Su Y, Godwin AK, Fishman D, Liu J*, et al.* Biological significance of prolactin in gynecologic cancers. Cancer research **2009**;69:5226-33

85. Drapkin R, von Horsten HH, Lin Y, Mok SC, Crum CP, Welch WR*, et al.* Human epididymis protein 4 (HE4) is a secreted glycoprotein that is overexpressed by serous and endometrioid ovarian carcinomas. Cancer research **2005**;65:2162-9

86. Huhtinen K, Suvitie P, Hiissa J, Junnila J, Huvila J, Kujari H*, et al.* Serum HE4 concentration differentiates malignant ovarian tumours from ovarian endometriotic cysts. Br J Cancer **2009**;100:1315-9

87. Van Gorp T, Cadron I, Despierre E, Daemen A, Leunen K, Amant F*, et al.* HE4 and CA125 as a diagnostic test in ovarian cancer: prospective validation of the Risk of Ovarian Malignancy Algorithm. Brit J Cancer **2011**;104:863-70

88. Buchen L. Cancer: Missing the mark. Nature **2011**;471:428-32

89. O'Leary KA, Shea MP, Salituro S, Blohm CE, Schuler LA. Prolactin Alters the Mammary Epithelial Hierarchy, Increasing Progenitors and Facilitating Ovarian Steroid Action. Stem Cell Reports **2017**;9:1167-79

90. Dutta D, Ghosh S, Pandit K, Mukhopadhyay P, Chowdhury S. Leptin and cancer: Pathogenesis and modulation. Indian J Endocrinol Metab **2012**;16:S596-600

91. Giede KC, Kieser K, Dodge J, Rosen B. Who should operate on patients with ovarian cancer? An evidence-based review. Gynecologic oncology **2005**;99:447-61

92. Katsumata N, Yasuda M, Takahashi F, Isonishi S, Jobo T, Aoki D*, et al.* Dose-dense paclitaxel once a week in combination with carboplatin every 3 weeks for advanced ovarian cancer: a phase 3, open-label, randomised controlled trial. Lancet **2009**;374:1331-8

93. Carmeliet P. VEGF as a key mediator of angiogenesis in cancer. Oncology-Basel **2005**;69:4-10

94. Schmid BC, Oehler MK. New perspectives in ovarian cancer treatment. Maturitas **2014**;77:128-36

95. Mukhopadhyay A, Curtin N, Plummer R, Edmondson RJ. PARP inhibitors and epithelial ovarian cancer: an approach to targeted chemotherapy and personalised medicine. Bjog-Int J Obstet Gy **2011**;118:429-32

96. Schreiber V, Dantzer F, Ame JC, de Murcia G. Poly(ADP-ribose): novel functions for an old molecule. Nat Rev Mol Cell Biol **2006**;7:517-28

97. Ledermann J, Harter P, Gourley C, Friedlander M, Vergote I, Rustin G*, et al.* Olaparib maintenance therapy in patients with platinum-sensitive relapsed serous ovarian cancer: a preplanned retrospective analysis of outcomes by BRCA status in a randomised phase 2 trial. Lancet Oncol **2014**;15:852-61

98. Flesken-Nikitin A, Choi KC, Eng JP, Shmidt EN, Nikitin AY. Induction of carcinogenesis by concurrent inactivation of p53 and Rb1 in the mouse ovarian surface epithelium. Cancer research **2003**;63:3459-63

99. Kim J, Coffey DM, Ma L, Matzuk MM. The ovary is an alternative site of origin for high-grade serous ovarian cancer in mice. Clinical Cancer Research **2015**;21

100. Testa JR, Getts LA, Salazar H, Liu Z, Handel LM, Godwin AK*, et al.* Spontaneous transformation of rat ovarian surface epithelial cells results in well to poorly differentiated tumors with a parallel range of cytogenetic complexity. Cancer research **1994**;54:2778-84

101. Johnson PA, Giles JR. The hen as a model of ovarian cancer. Nat Rev Cancer **2013**;13:432-6

102. Roby KF, Taylor CC, Sweetwood JP, Cheng Y, Pace JL, Tawfik O*, et al.* Development of a syngeneic mouse model for events related to ovarian cancer. Carcinogenesis **2000**;21:585-91

103. McCloskey CW, Goldberg RL, Carter LE, Gamwell LF, Al-Hujaily EM, Collins O*, et al.* A new spontaneously transformed syngeneic model of high-grade serous ovarian cancer with a tumor-initiating cell population. Front Oncol **2014**;4:53

104. Bernard V, Young J, Chanson P, Binart N. New insights in prolactin: pathological implications. Nat Rev Endocrinol **2015**;11:265-75

105. Yoshioka S, King ML, Ran S, Okuda H, MacLean JA, 2nd, McAsey ME*, et al.* WNT7A regulates tumor growth and progression in ovarian cancer through the WNT/beta-catenin pathway. Molecular cancer research : MCR **2012**;10:469-82

106. Mitra AK, Davis DA, Tomar S, Roy L, Gurler H, Xie J*, et al.* In vivo tumor growth of high-grade serous ovarian cancer cell lines. Gynecologic oncology **2015**;138:372-7

107. O' hAinmhire E, Quartuccio SM, Cheng W, Ahmed RA, King SM, Burdette JE. Mutation or loss of p53 differentially modifies TGFβ action in ovarian cancer. PloS one **2014**;9:e89553

108. Karst AM, Levanon K, Drapkin R. Modeling high-grade serous ovarian carcinogenesis from the fallopian tube. Proc Natl Acad Sci U S A **2011**;108:7547-52

109. Baker SJ, Markowitz S, Fearon ER, Willson JK, Vogelstein B. Suppression of human colorectal carcinoma cell growth by wild-type p53. Science **1990**;249:912-5

110. Najdi R, Proffitt K, Sprowl S, Kaur S, Yu J, Covey TM*, et al.* A uniform human Wnt expression library reveals a shared secretory pathway and unique signaling activities. Differentiation **2012**;84:203-13

111. Tan Y, Raychaudhuri P, Costa RH. Chk2 mediates stabilization of the FoxM1 transcription factor to stimulate expression of DNA repair genes. Mol Cell Biol **2007**;27:1007-16

112. Haeussler M, Schonig K, Eckert H, Eschstruth A, Mianne J, Renaud JB*, et al.* Evaluation of off-target and on-target scoring algorithms and integration into the guide RNA selection tool CRISPOR. Genome Biol **2016**;17:148

113. Cong L, Ran FA, Cox D, Lin SL, Barretto R, Habib N*, et al.* Multiplex Genome Engineering Using CRISPR/Cas Systems. Science **2013**;339:819-23

114. Tucker KL, Beard C, Dausman T, JacksonGrusby L, Laird PW, Lei H*, et al.* Germ-line passage is required for establishment of methylation and expression patterns of imprinted but not of nonimprinted genes. Genes & development **1996**;10:1008-20

115. Bouchard M, Souabni A, Busslinger M. Tissue-specific expression of cre recombinase from the Pax8 locus. Genesis **2004**;38:105-9

116. King SM, Hilliard TS, Wu LY, Jaffe RC, Fazleabas AT, Burdette JE. The impact of ovulation on fallopian tube epithelial cells: evaluating three hypotheses connecting ovulation and serous ovarian cancer. Endocrine-related cancer **2011**;18:627-42

117. Vasudevan D, Hickok JR, Bovee RC, Pham V, Mantell LL, Bahroos N*, et al.* Nitric oxide regulates gene expression in cancers by controlling histone posttranslational modifications. Cancer research **2015**;75:5299-308

118. Dean M, Davis DA, Burdette JE. Activin A stimulates migration of the fallopian tube epithelium, an origin of high-grade serous ovarian cancer, through non-canonical signaling. Cancer Lett **2017**;391:114-24

119. Hickok JR, Sahni S, Mikhed Y, Bonini MG, Thomas DD. Nitric oxide suppresses tumor cell migration through N-Myc downstream-regulated gene-1 (NDRG1) expression: role of chelatable iron. J Biol Chem **2011**;286:41413-24

120. Karst AM, Drapkin R. The new face of ovarian cancer modeling: better prospects for detection and treatment. F1000 medicine reports **2011**;3:22

121. Vang R, Shih IM, Kurman RJ. Fallopian tube precursors of ovarian low- and high-grade serous neoplasms. Histopathology **2013**;62:44-58

122. Jones PM, Drapkin R. Modeling high-grade serous carcinoma: how converging insights into pathogenesis and genetics are driving better experimental platforms. Frontiers in oncology **2013**;3

123. Seagle BL, Yang CP, Eng KH, Dandapani M, Odunsi-Akanji O, Goldberg GL*, et al.* TP53 hot spot mutations in ovarian cancer: selective resistance to microtubule stabilizers in vitro and differential survival outcomes from The Cancer Genome Atlas. Gynecologic oncology **2015**;138:159-64

124. Fenouille N, Tichet M, Dufies M, Pottier A, Mogha A, Soo JK*, et al.* The epithelial-mesenchymal transition (EMT) regulatory factor SLUG (SNAI2) is a downstream target of SPARC and AKT in promoting melanoma cell invasion. PloS one **2012**;7:e40378

125. Ribeiro RC, Sandrini F, Figueiredo B, Zambetti GP, Michalkiewicz E, Lafferty AR*, et al.* An inherited p53 mutation that contributes in a tissue-specific manner to pediatric adrenal cortical carcinoma. Proceedings of the National Academy of Sciences **2001**;98:9330-5

126. Soussi T. p53 alterations in human cancer: more questions than answers. Oncogene **2007**;26:2145-56

127. Walker G, MacLeod K, Williams AR, Cameron DA, Smyth JF, Langdon SP. Estrogen-regulated gene expression predicts response to endocrine therapy in patients with ovarian cancer. Gynecologic oncology **2007**;106:461-8

128. Hess AP, Talbi S, Hamilton AE, Baston-Buest DM, Nyegaard M, Irwin JC*, et al.* The human oviduct transcriptome reveals an anti-inflammatory, anti-angiogenic, secretory and matrix-stable environment during embryo transit. Reproductive biomedicine online **2013**;27:423-35

129. Becker MA, Haluska P, Jr., Bale LK, Oxvig C, Conover CA. A novel neutralizing antibody targeting pregnancy-associated plasma protein-a inhibits ovarian cancer growth and

ascites accumulation in patient mouse tumorgrafts. Molecular cancer therapeutics **2015**;14:973-81

130. Kuchenbaecker KB, Ramus SJ, Tyrer J, Lee A, Shen HC, Beesley J*, et al.* Identification of six new susceptibility loci for invasive epithelial ovarian cancer. Nature genetics **2015**;47:164-71

131. Zhang Y, Wang Y, Du Z, Wang Q, Wu M, Wang X*, et al.* Recombinant human decorin suppresses liver HepG2 carcinoma cells by p21 upregulation. OncoTargets and therapy **2012**;5:143-52

132. Hacke K, Rincon-Orozco B, Buchwalter G, Siehler SY, Wasylyk B, Wiesmuller L*, et al.* Regulation of MCP-1 chemokine transcription by p53. Molecular cancer **2010**;9:82

133. Raychaudhuri P, Park HJ. FoxM1: a master regulator of tumor metastasis. Cancer research **2011**;71:4329-33

134. Garritano S, Inga A, Gemignani F, Landi S. More targets, more pathways and more clues for mutant p53. Oncogenesis **2013**;2:e54

135. Alves CC, Carneiro F, Hoefler H, Becker KF. Role of the epithelial-mesenchymal transition regulator Slug in primary human cancers. Frontiers in bioscience **2009**;14:3035-50

136. Anglesio MS, Wiegand KC, Melnyk N, Chow C, Salamanca C, Prentice LM*, et al.* Type-specific cell line models for type-specific ovarian cancer research. PloS one **2013**;8:e72162

137. Seagle BL, Eng KH, Dandapani M, Yeh JY, Odunsi K, Shahabi S. Survival of patients with structurally-grouped TP53 mutations in ovarian and breast cancers. Oncotarget **2015**;6:18641-52

138. Gao J, Aksoy BA, Dogrusoz U, Dresdner G, Gross B, Sumer SO*, et al.* Integrative analysis of complex cancer genomics and clinical profiles using the cBioPortal. Sci Signal **2013**;6:pl1

139. Cerami E, Gao J, Dogrusoz U, Gross BE, Sumer SO, Aksoy BA*, et al.* The cBio cancer genomics portal: an open platform for exploring multidimensional cancer genomics data. Cancer Discov **2012**;2:401-4

140. de Cristofaro T, Di Palma T, Soriano AA, Monticelli A, Affinito O, Cocozza S*, et al.* Candidate genes and pathways downstream of PAX8 involved in ovarian high-grade serous carcinoma. Oncotarget **2016**

141. Saifudeen Z, Liu J, Dipp S, Yao X, Li Y, McLaughlin N*, et al.* A p53-Pax2 pathway in kidney development: implications for nephrogenesis. PloS one **2012**;7:e44869

142. Lang GA, Iwakuma T, Suh YA, Liu G, Rao VA, Parant JM*, et al.* Gain of function of a p53 hot spot mutation in a mouse model of Li-Fraumeni syndrome. Cell **2004**;119:861-72

143. Hotz B, Arndt M, Dullat S, Bhargava S, Buhr HJ, Hotz HG. Epithelial to mesenchymal transition: expression of the regulators snail, slug, and twist in pancreatic cancer. Clinical cancer research : an official journal of the American Association for Cancer Research **2007**;13:4769-76

144. Zhu J, Sammons MA, Donahue G, Dou Z, Vedadi M, Getlik M*, et al.* Gain-of-function p53 mutants co-opt chromatin pathways to drive cancer growth. Nature **2015**;525:206-11

145. Huguet EL, McMahon JA, McMahon AP, Bicknell R, Harris AL. Differential expression of human Wnt genes 2, 3, 4, and 7B in human breast cell lines and normal and disease states of human breast tissue. Cancer research **1994**;54:2615-21

146. Parfett CL. Induction of proliferin gene expression by diverse chemical agents that promote morphological transformation in C3H/10T1/2 cultures. Cancer Lett **1992**;64:1-9

147. Kanellakis NI, Giannou A, Pepe M, Agalioti T, Zazara D, Vreka M*, et al.* Mouse Lung Adenocarcinoma Cell Lines Reveal Prl2c2 as a Novel Lung Tumour Promoter. Thorax **2016**;71:A7-A

148. Missan DS, Chittur SV, DiPersio CM. Regulation of fibulin-2 gene expression by integrin alpha3beta1 contributes to the invasive phenotype of transformed keratinocytes. J Invest Dermatol **2014**;134:2418-27

149. Tan TZ, Yang H, Ye J, Low J, Choolani M, Tan DS*, et al.* CSIOVDB: a microarray gene expression database of epithelial ovarian cancer subtype. Oncotarget **2015**;6:43843-52

150. Tan TZ, Miow QH, Huang RY, Wong MK, Ye J, Lau JA*, et al.* Functional genomics identifies five distinct molecular subtypes with clinical relevance and pathways for growth control in epithelial ovarian cancer. EMBO Mol Med **2013**;5:1051-66

151. Tan TZ, Miow QH, Miki Y, Noda T, Mori S, Huang RY*, et al.* Epithelial-mesenchymal transition spectrum quantification and its efficacy in deciphering survival and drug responses of cancer patients. EMBO Mol Med **2014**;6:1279-93

152. Frasor J, Barkai U, Zhong L, Fazleabas AT, Gibori G. PRL-induced ERalpha gene expression is mediated by Janus kinase 2 (Jak2) while signal transducer and activator of transcription 5b (Stat5b) phosphorylation involves Jak2 and a second tyrosine kinase. Mol Endocrinol **2001**;15:1941-52

153. Stocco C, Djiane J, Gibori G. Prostaglandin F(2alpha) (PGF(2alpha)) and prolactin signaling: PGF(2alpha)-mediated inhibition of prolactin receptor expression in the Corpus luteum. Endocrinology **2003**;144:3301-5

154. Goffin V. Prolactin receptor targeting in breast and prostate cancers: New insights into an old challenge. Pharmacol Ther **2017**;179:111-26

155. Liu H, Remedi MS, Pappan KL, Kwon G, Rohatgi N, Marshall CA*, et al.* Glycogen synthase kinase-3 and mammalian target of rapamycin pathways contribute to DNA synthesis, cell cycle progression, and proliferation in human islets. Diabetes **2009**;58:663-72

156. Lopez Vicchi F, Becu-Villalobos D. Prolactin: The Bright and the Dark Side. Endocrinology **2017**;158:1556-9

157. Gschwantler-Kaulich D, Weingartshofer S, Rappaport-Furhauser C, Zeilinger R, Pils D, Muhr D*, et al.* Diagnostic markers for the detection of ovarian cancer in BRCA1 mutation carriers. PloS one **2017**;12:e0189641

158. Coscia F, Watters KM, Curtis M, Eckert MA, Chiang CY, Tyanova S*, et al.* Integrative proteomic profiling of ovarian cancer cell lines reveals precursor cell associated proteins and functional status. Nat Commun **2016**;7:12645

159. Chen KE, Walker AM. Prolactin inhibits a major tumor-suppressive function of wild type BRCA1. Cancer Lett **2016**;375:293-302

160. Thompson T, Tovar C, Yang H, Carvajal D, Vu BT, Xu Q*, et al.* Phosphorylation of p53 on key serines is dispensable for transcriptional activation and apoptosis. J Biol Chem **2004**;279:53015-22

161. Nusse R, Clevers H. Wnt/beta-Catenin Signaling, Disease, and Emerging Therapeutic Modalities. Cell **2017**;169:985-99

162. Siegel RL, Miller KD, Jemal A. Cancer statistics, 2018. CA: a cancer journal for clinicians **2018**

163. Modi DA, Tagare RD, Karthikeyan S, Russo A, Dean M, Davis DA*, et al.* PAX2 function, regulation and targeting in fallopian tube-derived high-grade serous ovarian cancer. Oncogene **2016**

164. Ning G, Bijron JG, Yamamoto Y, Wang X, Howitt BE, Herfs M*, et al.* The PAX2-null immunophenotype defines multiple lineages with common expression signatures in benign and neoplastic oviductal epithelium. The Journal of pathology **2014**;234:478-87

165. Pilarsky C, Wenzig M, Specht T, Saeger HD, Grutzmann R. Identification and validation of commonly overexpressed genes in solid tumors by comparison of microarray data. Neoplasia **2004**;6:744-50

166. Wen N, Wang Y, Wen L, Zhao SH, Ai ZH, Wang Y*, et al.* Overexpression of FOXM1 predicts poor prognosis and promotes cancer cell proliferation, migration and invasion in epithelial ovarian cancer. J Transl Med **2014**;12:134

167. Forys JT, Kuzmicki CE, Saporita AJ, Winkeler CL, Maggi LB, Jr., Weber JD. ARF and p53 coordinate tumor suppression of an oncogenic IFN-beta-STAT1-ISG15 signaling axis. Cell Rep **2014**;7:514-26

168. Gusarova GA, Wang IC, Major ML, Kalinichenko VV, Ackerson T, Petrovic V*, et al.* A cell-penetrating ARF peptide inhibitor of FoxM1 in mouse hepatocellular carcinoma treatment. J Clin Invest **2007**;117:99-111

169. Falconer H, Yin L, Gronberg H, Altman D. Ovarian cancer risk after salpingectomy: a nationwide population-based study. J Natl Cancer Inst **2015**;107

170. Hiraki M, Hwang SY, Cao S, Ramadhar TR, Byun S, Yoon KW*, et al.* Small-Molecule Reactivation of Mutant p53 to Wild-Type-like p53 through the p53-Hsp40 Regulatory Axis. Chem Biol **2015**;22:1206-16

171. Young AN, Moyle-Heyrman G, Kim JJ, Burdette JE. Microphysiologic systems in female reproductive biology. Exp Biol Med (Maywood) **2017**;242:1690-700

172. Sundaram KM, Zhang Y, Mitra AK, Kouadio JK, Gwin K, Kossiakoff AA*, et al.* Prolactin Receptor-Mediated Internalization of Imaging Agents Detects Epithelial Ovarian Cancer with Enhanced Sensitivity and Specificity. Cancer research **2017**;77:1684-96

173. Modi DA, Sunoqrot S, Bugno J, Lantvit DD, Hong S, Burdette JE. Targeting of follicle stimulating hormone peptide-conjugated dendrimers to ovarian cancer cells. Nanoscale **2014**;6:2812-20

174. Korkmaz T, Seber S, Basaran G. Review of the current role of targeted therapies as maintenance therapies in first and second line treatment of epithelial ovarian cancer; In the light of completed trials. Crit Rev Oncol Hemat **2016**;98:180-8

175. Li CG, Eccles MR. PAX Genes in Cancer; Friends or Foes? Front Genet **2012**;3:6

176. Desgrosellier JS, Cheresh DA. Integrins in cancer: biological implications and therapeutic opportunities. Nat Rev Cancer **2010**;10:9-22

177. Assoian RK, Klein EA. Growth control by intracellular tension and extracellular stiffness. Trends Cell Biol **2008**;18:347-52

VITA

SUMMARY

- Six years of qualitative research & development experience in pharmaceutical industry, India.
- Detail oriented with an analytical bent of mind with flexible and positive attitude.
- Team player with strong communication and interpersonal skills.

GOALS

To perform academic research in multidisciplinary team environment that advances and translates to identifying targets for drug discovery, early diagnostic markers leading to preventive care and pain management.

EDUCATION

- **PhD in cancer biology –** University of Illinois at Chicago 2013 to present.
- **Master's in biotechnology**- University of Madras 2002 - 2004.
- **Bachelor's in microbiology** - University of Madras 1999- 2002.

PROFESSIONAL EXPERIENCE

May 2015 – current: **Graduate research assistant**, center for Biomolecular Sciences, college of pharmacy, UIC, Chicago, IL. Mentor: Dr. Joanna E. Burdette.

Contributions

- Currently investigating the signaling mechanism and transcriptional targets of mutant p53 involved in tumorigenesis and metastasis of High-grade serous ovarian cancer from fallopian tube epithelium.
- Identified mutant p53 fallopian tube specific marker using murine models.
- Contributed to identify the phenotypic effects of dominant negative $p53^{R273H}$ mutation in fallopian tube epithelium.
- Helped to validate spontaneously transformed murine model system to investigate the onset of fallopian tube derived tumors.
- Developed CRISPR/Cas9 deletion models of ovarian cancer.

July 2012- July 2013: **Deputy manager** in "Discovery biology" department at Anthem Biosciences, Bangalore, India.
January 2010- July 2012: **Senior scientist** in "Discovery biology" department at Anthem Biosciences, Bangalore, India.

Major project contributions:

- BIRAP grant for 3 years "Generation of an E. coli strain for extracellular production of Industrial enzymes" and "Ketoreductases– Whole cell Biotransformation for chiral chemistry".
- Cloning and gene expression of maltogenic amylase, Insulin, phytase in E. coli & Yeast.

- Genotoxicity & mitotoxicity testing of new compounds on engineered mammalian cell lines.
- Chimerism analysis using a spectrum of biomarkers on Bone marrow transplantation clinical samples.
- Generation of single cell clones with stable gene knock out in CHO cells using ZFN technology.

Apr 2006 - Oct 2009: **Junior Scientific officer** in "Molecular medicine" department at Apollo hospitals & cancer research institute, Chennai, India.

Job Responsibilities:
HLA typing, DNA sequencing, immunofluorescence, chimerism analysis, gene copy number analysis, Preparing Standard operating procedures, technical module, for JCIA, NABL, ISO and CII accreditations.

January 2005 – April 2006: **Research assistant** in "Plant biotechnology" department at International institute of biotechnology and toxicology, Chennai, India. Performed DNA and RNA extractions, PCR, cloning, preparing lab buffers, media etc.,

Jan 2004 – Jun 2004: **Intern.** Worked in a project titled - "Cloning and gene expression of catalase gene from A. niger into E. coli", towards partial fulfillment for Master's degree at Orchid Chemicals & Pharmaceuticals**,** Chennai.

PUBLICATIONS & PATENTS

1. **Karthikeyan S**, Russo A, Dean M, Lantvit D, Endsley M and Burdette JE. Prolactin signaling drives tumorigenesis in human high grade serous ovarian cancer cells and in a spontaneous fallopian tube derived model (In preparation for **Cancer Research**, 2018).

2. Meyden S, Klepacki D, **Karthikeyan S**, Margus T, Thomas P, Jones JE, Khan Y, Briggs J, Dinman JD, Vazquez-Laslop N and Mankin AS. Programmed ribosomal frameshifting generates a copper transporter and a copper chaperone from the same gene. **Molecular cell**. 2017 January 19; DOI: 10.1016/j.molcel.2016.12.008.

3. Haq SF, Shanbhag AP, D, **Karthikeyan S**, Hassan I, Thanukrishnan K, Ashok A, Sukumaran S, Ramaswamy S, Bharatham N, Datta S, Samant S, and Katagihallimath N. Prediction and synthesis of pharmaceutically relevant (S) -specific chiral alcohols by ketoreductases. **Journal of industrial microbiology and biotechnology**. (under review).

4. Modi DA, Tagare RD, **Karthikeyan S**, Russo A, Dean M, Davis DA, Lantvit DD and Burdette JE. PAX2 function, regulation and targetin in fallopian tube derived high-grade serous ovarian cancer. **Oncogene**. 2016 December 19; DOI: 10.1038/onc.2016.455.

5. **Karthikeyan S**, Lantvit DD, Chae DM and Burdette JE. Cadherin - 6 type 2, K- cadherin (CDH6) is regulated by mutant p53 in the fallopian tube but is not expressed in the ovarian surface. **Oncotarget**. 2016 August 22; DOI: 10.18632/oncotarget.11499.

6. Endsley MP, Moyle-Heyrman G, **Karthikeyan S**, Lantvit DD, Davis DA, Wei JJ and Burdette JE. Spontaneous transformation of murine oviductal epithelial cells: a model system to investigate the onset of fallopian – derived tumors. **Frontiers in oncology**. 2015 July 17; DOI: 10.3389/fonc.2015.00154.

7. Quartuccio SM, **Karthikeyan S**, Eddie SL, Lantvit DD, Ó hAinmhire E, Modi DA, Wei JJ and Burdette JE. Mutant p53 expression in fallopian tube epithelium drives migration. **International journal of cancer**. 2015 Apr11; DOI: 10.1002/ijc.29528.

8. Samant S, Gupta G, **Karthikeyan S**, Haq SF, Nair A, Sambasivam G and Sukumaran S. Effect of codon optimized E. coli signal peptides on recombinant Bacillus stearothermophilus maltogenic amylase periplasmic localization yield and activity. **Journal of industrial microbiology and biotechnology**. 2014 July 7;41(9). DOI: 10.1007/s10295-014-1482-8.

9. International patent - "Generation of a high throughput invitro genotoxicity screen for use in mammalian cells" **US patent no: US 20140148360**, **European patent no: EP2694687A1**, **PCT/IB2012/051729**, publication no: WO/2012/137186, date of filing: APR 2012. Nair A, Subbiah M, Gupta G, Rajakrishna L, **Karthikeyan S**, Raghavendra PS, Unni SK and Sambasivam G. Anthem biosciences, Bangalore, India.

10. Indian patent - "A combination of primers, methods & kit for chimerism analysis" patent no: **2653/CHE/2011** date of filing: Feb 2011. Sukumaran S, **Karthikeyan S**, Sadagopan S, and Sambasivam G. Anthem biosciences, Bangalore, India.

AWARDS AND HONORS

- Dean's Scholar Fellowship, UIC, 2017 to 2018.
- Best poster award from the center for clinical and translational science in College of Pharmacy research day, UIC – 2017.
- First prize poster award under cancer targets and therapeutics category from Cancer center research forum – 2016.
- Second place poster award in Women's health research day – 2016.
- Larry Ewing travel award, Society for the study of reproduction – 2016 and 2017.
- Graduate college student travel award, UIC – 2016 and 2017.
- Graduate college presenter travel award, UIC – 2016 and 2017.
- W.E. Van doren Scholar award COP research day, UIC - 2016.
- Chancellor's graduate research fellowship for multi-disciplinary research, UIC - 2015.
- Young scientist award given by south Indian pharmaceutical industry association – 2011.
- ICMR's Young contributing scientist award – 2006.
- "Young achievers award - 2012" from Pharmaceutical Industry association, South India for developing chimerism analysis kit to assess the therapy response in bone marrow transplantation patients.
- ICMR's best contributing scientist award for developing TMA based detection kit for monitoring tuberculosis therapy response – 2007.
- Secured second prize in national student paper presentation competition on Genomics, 2003.

TEACHING EXPERIENCE

Jan 2014 – May 2015: Graduate teaching assistant, college of pharmacy, UIC, Chicago, IL.

- Courses - Fundamentals of drug action II (PHAR 332), Principles of drug action and therapeutics VI (PHAR 406), Experiential 1 - IPPE (PHAR 342).
  Duties – Class management and podium set up, assisting and clarifying student's queries through regular office hours, proctoring and grading exams, assisting the faculty in getting printouts and distributing in class, recording attendance, preparing and posting quizzes.
- Mentored 2 undergraduate and 2 PhD rotation students, Burdette Lab, UIC (Advisor: Dr. Joanna E. Burdette).

ORAL PRESENTATIONS

- **Karthikeyan S**, Lantvit DD, Chae DH and Burdette JE. Cadherin - 6 type 2, K- cadherin (CDH6) is regulated by mutant p53 in the fallopian tube but is not expressed in the ovarian surface.
  1. Society for the Study of Reproduction conference, July 2016.
  2. MidWest Ovarian Cancer Coalition conference, May 2016.
  3. Center for Biomolecular Sciences seminar series, UIC, October 2016.

POSTER PRESENTATIONS

- **Karthikeyan S**, Lantvit DD, Dean MD and Burdette JE. Signaling pathways contributing to tumorigenesis and peritoneal spread in spontaneous model of fallopian tube derived cancer.
  1. Society for the Study of Reproduction, July 2017.
  2. University of Illinois College of Pharmacy research day, February 2018.
  3. University of Illinois College of Pharmacy research day, February 2017.
  4. Cancer center research forum UIC, October 2016.

- **Karthikeyan S**, Lantvit DD, Chae DH and Burdette JE. Cadherin - 6 type 2, K- cadherin (CDH6) is regulated by mutant p53 in the fallopian tube but is not expressed in the ovarian surface.
  1. University of Illinois College of Pharmacy research day, February 2016.
  2. Women's health research day. April 2016.
  3. Illinois symposium for reproductive sciences, October 2015.

- Meyden S, Klepacki D, **Karthikeyan S**, Margus T, Thomas P, Jones JE, Khan Y, Briggs J, Dinman JD, Vazquez-Laslop N and Mankin AS. Programmed ribosomal frameshifting generates a copper transporter and a copper chaperone from the same gene.
  1. University of Illinois College of Pharmacy research day, February 2016.

- Nair A, **Karthikeyan S**, Sukumaran S, Kates M and Brian R. "A versatile human cell based in vitro high throughput genotoxicity screen".
  1. The new paradigm for drug discovery, Baltimore convention center, Johns Hopkins Medicine-Brain Science Institute, Baltimore, Maryland, USA, October 18, 2011.

LEADERSHIP EXPERIENCE

- Deputy manager in "Discovery biology" department at Anthem Biosciences, Bangalore, India. Managed a team of 5 scientists.

- UIC student chapter secretary for American Association for Pharmaceutical Scientists 2015 to current.

- Workshop coordinator and committee member for Expanding Your Horizons at Chicago 2015 to current.

- Volunteered and served as a secretary for Indian Red Cross society in blood donor association from 1999- 2003.

- Served as youth association president of south Indian refugee camp from 2005 to 2010.

ACTIVE PROFESSIONAL MEMBERSHIPS

- American Association for Pharmaceutical Scientist
- Society for the Study of Reproduction
- Endocrine Society